Spring 5-29-2020

A Numerical Survey of Multi-Planet Systems' Inclination Excitation and Survival Under the Influence of an Oblate, Tilted Star

Kathleen M T Schultz
University of Maine, tickertapeship@gmail.com

A NUMERICAL SURVEY OF MULTI-PLANET SYSTEMS' INCLINATION

EXCITATION AND SURVIVAL UNDER THE INFLUENCE

OF AN OBLATE, TILTED STAR

By

Kathleen Margaret Thornton Schultz

B.A. University of Maine at Farmington, 2015

A THESIS

Submitted in Partial Fulfillment of the

Requirements for the Degree of

Master of Science

(in Physics & Astronomy)

The Graduate School

The University of Maine

May 2020

Advisory Committee:

    Neil Comins, Ph.D., Professor of Physics, University of Maine, Advisor

    Christopher Spalding, Ph.D. Postdoctoral Researcher, Yale University

        and Princeton University, Co-Advisor

    Robert Meulenberg, Ph.D., Associate Professor of Physics, University of Maine

    Thomas Stone, Ph.D., Associate Professor of Mathematics and Physics,

        Husson University; Adjunct Graduate Faculty, University of Maine

© 2020 Kathleen Schultz

All Rights Reserved

A NUMERICAL SURVEY OF MULTI-PLANET SYSTEMS' INCLINATION

EXCITATION AND SURVIVAL UNDER THE INFLUENCE

OF AN OBLATE, TILTED STAR

By Kathleen Margaret Thornton Schultz

Thesis Advisor: Dr. Neil Comins

An Abstract of the Thesis Presented
in Partial Fulfillment of the Requirements for the
Degree of Master of Science
(in Physics & Astronomy)
May 2020

Among the many exciting and thought-provoking discoveries facilitated by the *Kepler* telescope, one of the most puzzling is the very large proportion of systems with only a single transiting planet in them, relative to the number of systems with multiple transiting planets. Given that most of these multis are close together and have low mutual inclinations, and that planetary systems tend to form in such a configuration, the next logical step is to guess that at least some of the singles are part of multi-planet systems with large mutual inclinations between planets, excited by some other object's gravitational perturbations. A number of such mechanisms have been put forth as explanations for the excess of singles, but our currently limited knowledge of planetary systems prevents any one mechanism from being identified as the most probable cause. One mechanism involves a young, tilted, oblate star that forces its closest-in planets to precess about its spin axis, rotating them out of alignment with each other as its oblateness decays. Still relatively new territory in planetary science, the stellar oblateness mechanism has only been explored thus far for specific Kepler systems; its effects on generic systems as different planetary variables are tuned is not well understood. In addition, while it has been put forth as a possible

source for the abundance of single-transit systems, we do not know whether the stellar oblateness mechanism creates singles from multis frequently enough to reproduce that high single/multi ratio. To address this issue, I perform a suite of N-body simulations on Kepler-like systems, evolved under the influence of a star with different tilts and spin periods. I observe the final average mutual inclinations of the surviving systems, as well as the conditions under which they go unstable, and the maximum number of transiting planets observable at the end of evolution. Recent data analysis has shown that the closest-in exoplanet pairs are also the most highly mutually inclined; I demonstrate that this is a natural outcome of evolution around an oblate, tilted star. I have further found that multi-planet systems in this scenario most often come out of it with all of their planets on fairly coplanar orbits, or with very few of their planets remaining, dynamically excited to the point where only one of the few surviving planets can be observed to transit at a time. Thus, I conclude that Kepler singles are almost always truly single, sometimes with one or two hidden neighbors, very rarely more. In addition, truly single post-instability planets tend to "relax" onto lower-inclination orbits, somewhat erasing their star's initial obliquity. This implies that modern measurements of misalignment in Kepler singles likely underrepresent the true distribution of initial stellar obliquities in the universe.

DEDICATION

For my dad, who listens, asks questions, reads big books, and takes it easy.

I love you the most.

ACKNOWLEDGEMENTS

TABLE OF CONTENTS

Chapter

LIST OF FIGURES

LIST OF DEFINITIONS AND SYMBOLS

semimajor axis a	The average distance between planet and star. For a circular orbit, this is simply the distance between the two. (Figure 0)
eccentricity e	The measure of an orbit's deviation away from circular; spans between 0 (circular) and 1 (a line). (Figure 0)
orbital inclination i	The angle between a planet's orbital plane and the dominant plane in the system, usually the star's equatorial plane. (Figure 0)
viewing inclination θ	The angle between a planet's orbital plane and a viewer's line of sight
mean anomaly	An approximation of a planet's angular position along its own orbit (see true anomaly, Figure 0).
ascending node	The point at which a planet's orbital plane intersects with the dominant plane in the system. (Figure 0)
longitude of ascending node	The position of the ascending node, measured from some fixed axis of reference. (Figure 0)
pericenter/periapsis	The point on a planet's orbit that lies closest to the host star.
argument of pericenter/periapsis	The angle between ascending node and pericenter/periapsis. (Figure 0)
tranet	A "transiting planet"; a planet detectable by the transit method.
transit timing variation (TTV)	Variations in the span of time it takes a planet to transit.

radial velocity (RV)	Detection method by which a planet exerts a strong enough gravitational force on a star to induce wobble, and therefore changes in the star's observed spectrum.
β_* / stellar obliquity	The angle between a star's spin axis and the average planetary plane; may also be the angle between star and a single planet.
J_2 / stellar oblateness	A measure of the deformation of a rapidly rotating spherical body.
quadrupole	In this context, shorthand for "gravity that is strongest near the equator and weakest toward the poles of a star".
$J_{2,0}$	The initial oblateness of a star that is spinning down.
Δi	The mutual inclination between a planet pair, defined as a combination of each planet's orbital inclinations and longitudes of ascending node.
a_1	The semimajor axis of the innermost planet in a system of planets
R_*	The radius of a host star.
$R_\oplus, M_\oplus$	The radius and mass of Earth.
$R_\odot, M_\odot$	The radius and mass of the Sun.
N	Generally, the number of planets in a system to start out with. Can be replaced with the more specific N_i.
$\Delta\sigma$	The time-averaged mean mutual inclination of planets in a system with N>2.

N_i	The initial number of planets in a system.
N_f	The final number of planets in a system.
N_T	The maximum number of planets that can be seen to transit from an observer's fixed perspective.
AU	Astronomical Unit; the distance between Earth and the Sun.
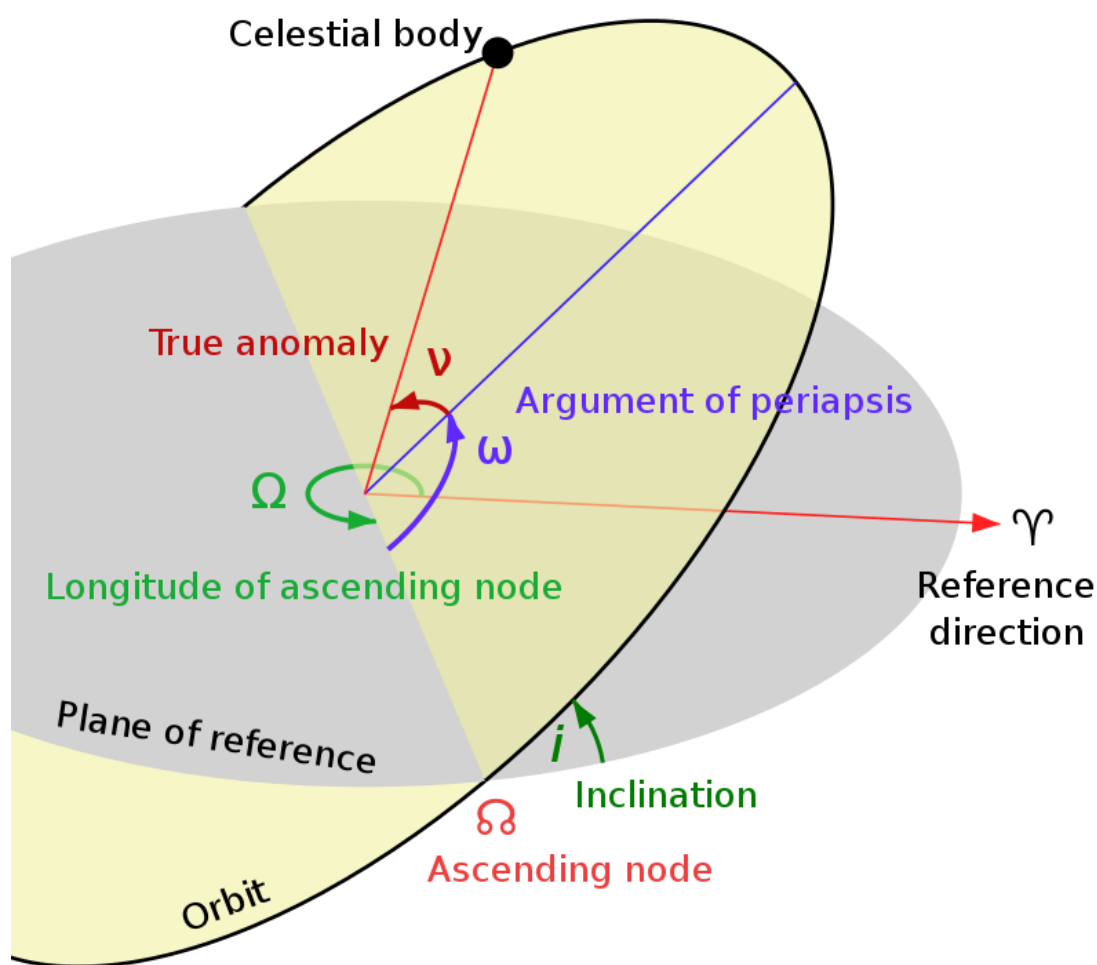
Figure 0. The traditional elements of a Keplerian orbit. Credit to Lasunncty at the English Wikipedia, CC BY-SA 3.0, https://commons.wikimedia.org/w/index.php?curid=8971052

LIST OF EQUATIONS

CHAPTER 1

INTRODUCTION AND BACKGROUND

1.1 Introduction

When we imagine the types of planets that exist around stars other than the Sun, we do so through the lens of a Solar System inhabitant. We name whole classes of extrasolar planets after our own neighbors – hot Jupiters, super-Earths, sub-Neptunes – and elevate the discovery of planets with the potential to bear the thing that is most familiar to us in the universe, that provides meaning for many to the hunt for exoplanetary systems: life. Indeed, when the Kepler space telescope began observations in 2009, its primary purpose was to search ~250,000 stars for potentially life-hosting planets (Borucki et al. 2009). In addition, the data it gathered over the course of its operation provided invaluable insights into the architectures of these alien systems, characterizing planets' orbital periods, radii, and semimajor axes, as well as the number of observable planets extant in a given system. This data set has revealed much about planetary systems that, while perhaps only of partial interest to exobiologists, provides ample opportunity for astrophysicists and planetary scientists to study real systems and model the processes that form and sculpt them.

The detection method employed by Kepler was, however, limited in its planet-finding abilities. The Kepler telescope was designed to look for minute variations in light intensity coming from target stars, caused by planets in orbit around those stars. If the viewing geometry is just right, a planet passes between the observer and the host star along the observer's line of sight, briefly and periodically reducing the amount of light the observer receives from the host star. This is the "transit method" for detecting extrasolar planets, and its implementation has led to the majority of exoplanet discoveries (thanks in no small part to the fruitfulness of the Kepler

1

and K2 missions: a project intended to last for 4 years was extended multiple times, despite partial failure of the telescope's directional controls, for a total of 9.5 years of data gathering[1].

The transit method is inherently biased toward systems that are oriented close to line of sight. For a star with radius R_* and a planet with semimajor axis a (see List of Definitions and Symbols) orbiting in a plane inclined at angle θ relative to the viewer's line of sight, the following inequality must generally be satisfied in order for the planet to transit:

$$\sin(\theta) \lesssim \frac{R_*}{a} \tag{1}$$

For a planet pair with semimajor axes a_1 and a_2, angles θ_1 and θ_2 relative to an observer's line of sight, and mutual inclination $\Delta i = \theta_1 + \theta_2$, the spherical law of cosines relates all angles:

$$\sin(\Delta i) = \sin\theta_1\cos\theta_2 + \sin\theta_2\cos\theta_1 \tag{2}$$

When θ_1 and θ_2 are very small, $\cos\theta_1 \approx \cos\theta_2 \approx 1$. Using the substitution $\sin\theta_p = R_*/a_p$, we reach the co-transiting criterion

$$\sin(\Delta i) \lesssim \frac{R_*}{a_1} + \frac{R_*}{a_2} \tag{3}$$

In reality, two planets that fail to satisfy equation (3) can still transit if the point at which their orbits intersect is close to the line of sight (Ragozzine & Holman 2010). This is a rare occurrence and will be excluded this work to maintain simplicity. Thus, I consider both planets to be detectable via the transit method only if the above expression holds true. (See Figure 1 for a visual aid.)

---

[1] https://www.nasa.gov/mission_pages/kepler/main/index.html
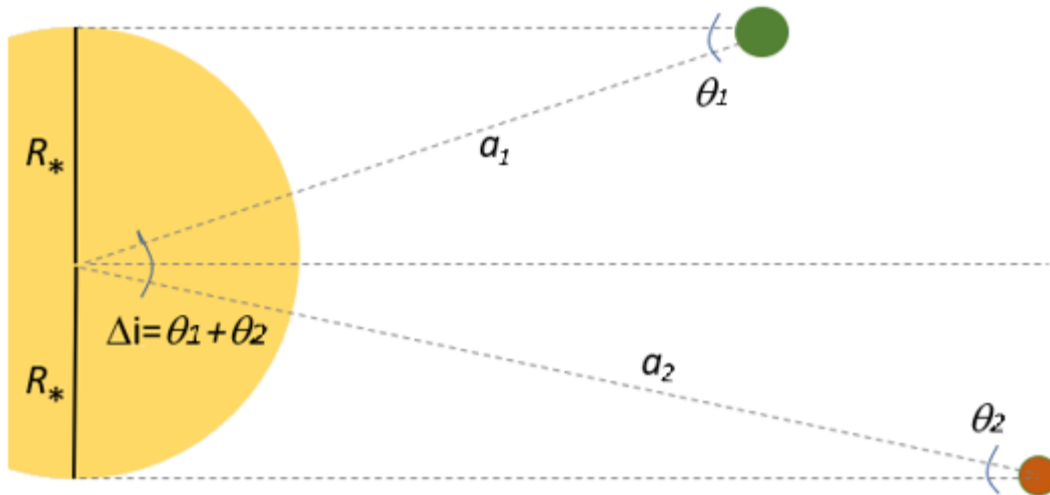
Figure 1. A two-planet system with nonzero mutual inclination. The two orbits straddle the boundary between singly transiting and doubly transiting.

If a system contains multiple planets, there is a chance that not all of those planets will be detected, particularly if their orbits relative to each other aren't fairly well aligned ("coplanar"). This sensitivity to orbital inclination increases as the semimajor axis of a planet is increased – greater distances from the host gives a planet less wiggle room before it is removed from transiting and becomes undetectable by the transit method. Therefore, it is possible, maybe even likely, that systems found by Kepler to host transiting planets possess additional, as yet unseen inclined planets.

Analyses of system architectural data came in soon after the project's onset (Borucki et al. 2011). An unexpected phenomenon revealed itself in the analyses of systems of planets with radii smaller than 6 Earth radii: while Kepler had found many systems containing different numbers of planets, the number of systems with only one planet detected by transit (a.k.a. a "single-tranet system" [Tremaine & Dong 2012]) comprised about 50% of the entire Kepler system set (Lissauer et al. 2011). Systems with multiplicities between two and six made up the other half of the set. This "overabundance of singles", now called the Kepler dichotomy, has

continued to exist even as we expand and refine our data set using complementary detection techniques and alternate telescopes (Ballard & Johnson 2016). See section 3.1 of this thesis for an up-to-date report on the Kepler dichotomy.

The cause of the Kepler dichotomy is still open to debate. Some believe that systems containing multiple planets are artificially pared down in transit multiplicity by the Kepler project's data processing method (e.g. Bovaird & Lineweaver 2017, Zink et al. 2019). Others prefer to view this as a genuine phenomenon with an astrophysical explanation. The aforementioned weakness in the transit method naturally leads one to wonder whether these single-tranet systems are truly single, or whether they contain planets that are simply too inclined to the observer's line of sight to be detected. One hypothesis proposes that the planetary birth environment around young stars tends to favor the formation of either one planet or many planets, perhaps due to the presence of a large planet (Johansen et al. 2012, Hansen & Murray 2013) – however, it has been shown that a single birth environment may produce the observed transit multiplicity rates, if one makes alternative assumptions about the protoplanetary disk's shape and density, as well as about the true distribution of modeled planet multiplicities at formation (Moriarty & Ballard 2016, Bovaird & Lineweaver 2017).

These formation-driven ideas assume that systems experience fairly dull lives once their formation disks disperse, undergoing little to no dynamical excitation. In contrast, another interpretation of the Kepler dichotomy is connected to dynamical excitation. It's theorized that systems leave the disk-hosting stage with fairly high multiplicities and low inclinations between planetary orbits (Kant 1755). Over time, these planets interact with each other, with objects exterior to them, and with their host star, potentially becoming misaligned in the process. In the context of the Kepler dichotomy, a system influenced by an inclination-exciting mechanism can

wind up with planets just spread out enough in their tilts relative to each other that only one planet will ever be seen to transit at a time – an orbit that is inclined and/or stretched out of circularity (made "eccentric") is called a "dynamically hot" orbit. Some interactions can be strong enough that the system goes "unstable", causing planets to collide with each other or with the host star, or get ejected from the system entirely, reducing the true multiplicity of the whole system. Planets that survive instability are often left on dynamically hot orbits (see for example Carrera et al. 2019). Thus, a system with a dynamical history may have a larger spread in inclinations between its constituent planets than it had initially, potentially enhanced further by instability and subsequent planet loss.

There are a number of mechanisms capable of dynamically heating planetary systems and pushing them to instability, including (but not limited to) secular chaos (Lithwick & Wu 2013), perturbations due to an external companion (and, as a special case of this, induced Kozai-Lidov oscillations) (Becker & Adams 2017, Hansen 2017, Naoz et al. 2011), planet-planet scattering (Ford & Rasio 2008, Johansen et al. 2012), and stellar oblateness (Spalding & Batygin 2016, Spalding et al. 2018). These mechanisms can each excite the mutual inclinations of planetary systems to greater or lesser extents, but require specific sets of initial conditions to do so. Consequently, as we strengthen our understanding of the true architectures of Kepler systems, and as we further explore these mechanisms and their unique effects on planetary systems, we will be in a better position to determine which mechanism/s is/are the dominant cause of the dynamical states of Kepler systems. I discuss each of these mechanisms in more detail in the next section.

One can begin to identify whether a particular mechanism is responsible for shaping the architecture of a Kepler system by comparing the system's observed properties – inclinations,

eccentricities, spacing, et cetera – to those typically resulting from the mechanism's operation. We have had some success in measuring the eccentricities of some Kepler systems using the transit timing variation (TTV) method of analysis (e.g. Xie et al. 2016), but inclinations between planets are much more difficult to measure in all but the most well-aligned systems. (Winn & Fabrycky 2015). Recently, though, Dai et al. (2018) analyzed transit data from approximately 100 stars to recover mutual inclinations between the two planets closest to their star in each system. They found that the closer a pair is to the star, the larger their mutual inclination is, especially among pairs within about 5 stellar radii from their hosts. This is consistent with the hypothesis that interactions with the host star are responsible. Of the mechanisms listed above, only the last in the list is associated with the central star of a planetary system. Within the past five years, it has been shown (Spalding & Batygin 2016) that inclinations between planets can become excited if their host star is spinning rapidly and has some nonzero tilt relative to the system in orbit around it. Like a ball of pizza dough, a rotating star becomes deformed about its equator ("oblate"), causing symmetric nonuniformities in its gravitational field. Planets will be driven into orbital precession about the host's spin axis if they are at all misaligned with the host star (see section 1.3); planets closest to the star will precess more quickly than those further away. As these orbits precess at different rates, they rotate away from each other, and the angle between them increases. One would expect this mutual inclination to grow more pronounced as the planets' distance from their host decreases, reflecting the trend observed by Dai et al. (2018). The oblate star mechanism is the focus of this thesis, and the first goal in chapter 2 is to demonstrate that such a mechanism does excite larger mutual inclinations between closer-in planet pairs.

While an analytic (mathematical) solution exists that predicts the evolution of mutual inclination between a planet pair orbiting this kind of star (Spalding & Batygin 2016), it only applies in the case where a star is rotating at a constant rate. In fact, stars begin to spin down very early in their lives, gradually losing the oblateness that powers the mutual inclination excitation process. As an analytic solution incorporating stellar spin-down doesn't yet exist, we must turn to N-body computer simulations to model the evolution of planetary systems in this scenario. Prior works have limited their application of this mechanism to specific, known Kepler systems (Spalding & Batygin 2016, Spalding et al. 2018) or to special cases designed to probe a particular part of the physics arising from the mechanism (Spalding & Batygin 2015). A broader N-body survey of the influence a young, tilted star has on its planets would improve our understanding of the mechanism's ability to alter the architecture and multiplicities of a wider variety of systems than have been previously examined. It's therefore my second goal in this thesis to determine the effect that different Kepler-like systems can achieve under the influence of such a star with varying levels of tilt and oblateness. I explore this effect in chapter two using two-planet (N=2) systems, and in chapter 3 with systems of more than two planets, creating a robust set of expected outcomes at a population level that can be used to more accurately evaluate the ubiquity of the oblate star mechanism than before.

Spalding et al. (2016, 2018) demonstrated that an oblate, tilted star can excite mutual inclinations between planets enough to reduce a multi-planet system to an apparently single-tranet system, potentially explaining the entire Kepler dichotomy – however, "can" is not the same as "does". For example, although emerging evidence suggests that giant planet are fairly common around compact inner systems (Bryan et al. 2019), and that their influence over inner planets *could* excite multis to the point of singledom (Pu & Lai 2018), a population-level set of

N-body simulations confirmed that an entire, as-yet-undetected group of Saturn-mass giant companions is required to reproduce the Kepler dichotomy through giant companion perturbation alone (Hansen 2017). By performing a suite of simulations on systems with physically-informed initial conditions, across different starting multiplicities, my third goal is to assess whether or not the oblate star mechanism naturally turns a large proportion of multis into singles, on par with the fraction present in our Kepler data. Doing so will either provide strong evidence that oblate, tilted stars are indeed responsible for the Kepler dichotomy, or emphasize observational and theoretical areas that need further study as we seek the truth about the Kepler singles.

We have seen, through telescopes and with mathematics, that planetary systems can play host to a wealth of interesting dynamics. Astrophysical interpretations of the Kepler dichotomy encourage us to push forward into this scientific frontier. A formation interpretation is difficult to confirm against modern Kepler observations: the planet formation process is still nebulous, and the dispersal of the formation disk early in systems' lifetimes means no information remains about the properties of a disk that created a given Kepler system. On the other hand, a dynamical interpretation can be directly checked against observational data – with a well-developed theoretical foundation, working knowledge of the occurrence rates of initial conditions for various mechanisms, and simulations to help us predict outcomes due to these mechanisms, we can begin to map out the possible histories that shaped modern Kepler system architectures. Many of these possible histories have been subject to scientific scrutiny in the decade since *Kepler* was launched; some, as seen in the next section, are still ripe for investigation.

1.2 A Brief Overview of Transit-Reducing Mechanisms

Among the different avenues by which planets can become mutually inclined, the first to be tested for single-tranet production was planet-planet scattering (Johansen et al. 2012). In this situation, planets in a system exert small perturbations on each other over long periods of time, culminating in large enough alterations to their original orbits to tip the system into instability. (Veras & Armitage 2004, Ford & Rasio 2008). It is an inevitability that a system will go unstable, if given enough time; the time scale for instability depends sensitively on the distance between planets (Davies et al. 2014). Leveraging this fact, Johansen et al. performed N-body simulations on a number of three-planet Kepler systems of different masses and separations, to determine whether their post-instability architectures and surviving multiplicities could reproduce the Kepler population of singles. The time scale on which instability occurred was longer than the expected lifetime of all but the most massive systems – thus, if planet-planet scattering creates singly transiting systems from initial multis, it can only do so with planets on the order of one Jupiter mass. This fails to explain the large number of low-mass planets observed in single-tranet systems. Planet-planet scattering was therefore ruled out early as a driver of the Kepler dichotomy.

Secular chaos is not so easy to eliminate. An explanation of the conditions under which it occurs will benefit the reader as they proceed through the remaining chapters of the text:

A closed orbit requires six coordinates to fully describe it: eccentricity, semimajor axis, orbital inclination, mean anomaly, longitude of ascending node, and argument of pericenter, the last three of which are circulating angular coordinates (see glossary for definitions). Because angles are measures of position on a circle, they can have any value from 0° to 360°. The mean anomaly represents a planet's position along its orbit, and therefore is constantly changing;

similarly, the ascending node and argument of pericenter are rarely static. Often they'll circulate periodically through the full 360° – this is called precession, and a single complete circuit can take many of the planet's orbits. Long-term behavior, usually involving the ascending node and/or argument of pericenter, is called "secular" behavior, and it's in this secular realm that much of the interesting dynamics in a planetary system occur.

When two planets' ascending nodes (or arguments of pericenter) precess at the same frequency, or when the ratio of their precession frequencies is a simple fraction, they're considered to be in a secular resonance. Resonances allow objects to influence each other much more strongly than in the non-resonant regime. An inner planet caught in two resonances simultaneously (a "resonance overlap") experiences impulsive changes in its eccentricity and inclination; this is the gist of secular chaos (Lithwick & Wu 2013).

For the most part, this mechanism has been invoked as an explanation for odd inner exoplanetary architectures in systems such as GJ 876 (Puranam & Batygin 2018) and 55 Cancri (Hansen & Zink 2015). Similar mean motion chaotic evolution was found to exist in Kepler-36 (Deck et al. 2012). Secular chaos has also been demonstrated to lurk at the edge of Mercury's current orbit (Lithwick & Wu 2011, Batygin & Laughlin 2008). Whether or not a planet enters the chaotic regime depends on the configuration of other planets in the system; Hansen & Zink (2015) present ten observed systems in which a planet may encounter two overlapping resonances if it occupies, or migrates through, the correct orbit. If future works confirm that chaos is present in these systems, it will strengthen the case that chaos is culpable for some portion of the Kepler excess of single-tranet systems. However, due to the nature of chaos, the outcome of such evolution at a population level is difficult to predict. As of the writing of this thesis, no attempt has been made to study the general dynamical signature of secular chaos,

10

implying that chaos' role is difficult to distinguish from a statistical perspective. Without a grasp of its unique signature, we cannot quickly discern whether it is responsible for the observed architectures of Kepler systems. It may be that we must continue to check for chaos-friendly conditions on a system by system basis, if we're to understand chaos' broader influence on exoplanetary systems.

Although the previous two mechanisms are associated with a wide range of final Δi, in truth it might not take more than a few degrees' separation to remove a planet from transit. A small amount of misalignment between planets is expected to be a natural outcome of planet formation (Lissauer et al. 2011). In a system of at least three planets, in the absence of other perturbers, the planets' orbits will "attempt" to realign with each other if even slightly mutually inclined. Secular coupling between the planets forces their orbital inclinations and ascending nodes to exhibit steady-state fluctuations (see Figure 2). If the amplitudes of these fluctuations are sufficiently large and the planets are far enough from their host, the total number of transit-observable planets can change periodically over time (equation 3).

Becker & Adams (2015) questioned whether this continuous "self-stirring" in a multi-planet system could achieve Δi amplitudes large enough to intermittently reduce that system's transit number. It is believed that the Kepler multis, being relatively coplanar, represent the state of a system just after birth (Kant 1755). Previous work has found that inclinations in the population of relatively coplanar Kepler multis can be modelled via a Rayleigh distribution with varying widths (Lissauer et al. 2011, Fabrycky et al. 2014). Thus, Becker & Adams drew their planets' initial inclinations from a Rayleigh distribution with 1.5° width and concluded that pristine four-planet systems would only rarely be able to oscillate with high enough amplitudes to affect their transit numbers. When combined with the results from Johansen et al. (2012), it
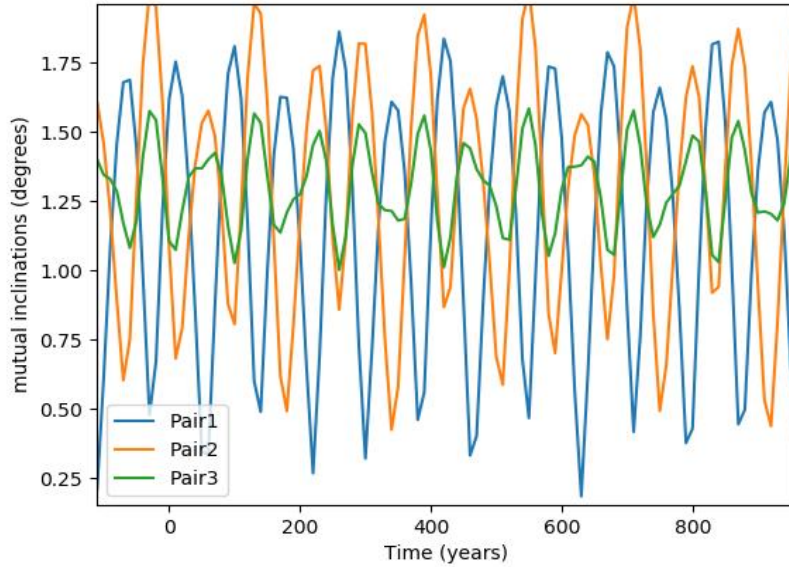
Figure 2. Self-stirring in a 3-planet system. Each planet pair's mutual inclination is represented by a different colored curve.

became clear that a system of multiple sub-Neptunes cannot excite itself into transit reduction. If we're to continue pursuing a dynamical explanation for the Kepler dichotomy, we must look for guilty parties outside of the compact multi-planet systems we're attempting to dynamically heat.

All other mechanisms oft invoked as exciters of inclination fall within the category of "one massive outer object acting upon the orbits of inner objects", the outer object ranging in mass from a giant planet to a companion star. An outer planetary or stellar companion must be inclined relative to the inner multiplanet system and sufficiently close/massive in order to stimulate the inner planets' mutual inclinations (Hansen 2017). In this general scenario, the companion's angular momentum vector is tilted relative to those of all of the other bodies in the system, and the planets' orbits precess about this vector (see Figure 3, next section). The (Eccentric) Kozai-Lidov mechanism is a special case of this scenario in which an outer, eccentric companion and inner system are mutually tilted by at least 39° (Naoz et al. 2011). In addition to forcing the usual Δi oscillations, the EKL companion can enter into a secular resonance with one

of the inner planets, stimulating chaotic eccentricity growth and instability (Denham et al. 2018).

Interestingly, Hansen & Zink (2015) noted that it may be necessary for a system to contain at

least one Jupiter-mass planet for chaotic (non-Kozai) evolution to take place. It is evident that

inner systems and giant companions can interact with each other in multiple, dynamically

exciting ways.

Interest in giant external perturbers as generators of single-tranet systems began to pick

up when observational data indicated the presence of such companions beyond known planetary

systems (Knutson et al. 2014, Bryan et al. 2016, Bryan et al. 2019). Lai & Pu (2016) and Pu &

Lai (2018) derived analytic solutions predicting RMS inclinations and eccentricities for N-planet

systems with a giant exterior companion[2]. Becker & Adams (2017) followed up on their self-

stirring work, introducing a giant planet exterior to a 5-planet Kepler-like system in order to

boost the system's mutual inclination oscillation amplitudes. They were able to constrain the

presence of a giant companion in a number of real Kepler systems this way. Perhaps the most

comprehensive and conclusive was Hansen (2017)'s work: after using a giant companion to

separately perturb eccentricity or inclination, he found that it was impossible to excite mutual

inclinations enough to reduce the transit number of the inner system without also exciting

eccentricities, causing the system to go unstable. Based on the observed occurrence rate of

Jupiter-size planets, he estimated that all low-mass single-tranet Kepler systems could be the

outcome of instability induced by a giant companion. However, his model couldn't account for

the slightly higher-mass portion of the Kepler single-tranet population unless a separate group of

---

[2] I attempted to apply the "recipe" laid out in Appendix B of Pu & Lai (2018) to reproduce the results therein, but
was not successful.

Saturn-sized planets exists, too small to be discovered by current distant planet detection methods.

Other work has followed that further discusses the influence that giant companions can have on planetary systems (Huang et al. 2017, Mustill et al. 2017, Pu & Lai 2019, Spalding & Millholland in prep), and data connecting long-period giant companions continues to come in (Foreman-Mackey 2016, Uehara et al. 2016, Zhu & Wu 2018, Bryan et al. 2019). It is clear, based on this sheer volume of data and scholarship, that a giant companion is the best contender among possible planetary perturbers when considering the dynamical creation of single-tranet systems. Indeed, the variety of ways in which a giant outer companion can excite inner systems makes it a powerful influencer.

However, if an outer giant is to stimulate inclination growth between inner planets, it must already be tilted away from the inner planets' orbits while they remain essentially coplanar, and it must be close enough that it doesn't simply lift the entire plane of planets at once (Hansen 2017). The prevailing theory proposes that an inclined binary companion gives the giant its tilt (Lai et al. 2018). Binary companions themselves have little effect on inner planetary systems, as shown by Mustill et al. (2017) – at the same time, they report that current observed occurrence rates of binaries+giants, and giants+inner systems, restrict the percentage of inner systems with giant, binary-tilted companions to about 13%. The proportion of inner systems excited by a giant companion to the point where their transit number is reduced is even lower (Hansen 2017). Even the best contender among planet-sized perturbers may not have a strong enough presence in the universe to be the main cause of the Kepler dichotomy. Fortunately, there remains an object present in *every* planetary system, active enough in its youth to potentially disrupt coplanarity, whose candidacy as top exciter has not been fully tested: the host star itself. In the following

section, I provide background and context for the mechanism by which a star alters the inclinations between its planets, as well as an overview of the work done thus far to investigate its effects.

1.3 The Stellar Agitator

Two conditions must be satisfied before a star can excite mutual inclinations (Δi) between its close-in planets: the star must be tilted relative to the system, and it must be rotating rapidly enough that its quadrupolar gravitational potential, driven by the resulting oblateness, has a stronger influence over the planets than they do on each other. Data from the Kepler mission as well as from multiple ground-based telescopes have enabled us to find limits for stellar tilts in multiple systems, and to learn that these tilts are often higher than the ~7° tilt of our own star (Lissauer et al. 2011). Until recently, most of our data has been associated with stars hosting a class of planets referred to as "hot Jupiters" – very close-in giant planets whose formation histories are a topic of active research. To address this mystery, a theory was developed that permits stars to become misaligned with entire coplanar systems of planets at once, removing the need for planets to undergo dynamical excitation individually. Meanwhile, it has been known for almost a century (Sterne 1939) that nonuniform gravitational fields arise from oblate stars, although this knowledge has rested largely (Ward et al. 1976) unapplied to star+planet systems until well into the 20th century.

Key to our search for information about a star's tilt is the Rossiter-McLaughlin effect. As a star rotates, one side of it always seems to be moving "toward" an observer as the other side moves "away". Light from the "toward" side is slightly shifted toward the blue end of the spectrum, while light from the "away" side is redshifted. If a planet transits across the face of the

star, it blocks light from some shifted region of the star, causing the star's entire spectrum to change slightly according to the shift of the unobscured region. This is the Rossiter-McLaughlin effect, and it happens periodically as the planet makes multiple transits. By observing this effect, as well as the trajectory of the transiting planet, one can measure the tilt of the spin axis against the plane of the sky and place constraints upon the true orientation of the star's spin axis relative to the orbital plane of the planet (Winn 2007). We refer to the latter angle as the star's "obliquity" or "spin-orbit misalignment". While measurements of the Rossiter-McLaughlin effect yield true stellar obliquities only when combined with radius and spin period measurements (which aren't always available), the angle between sky-projected spin axis and planet trajectory is still a useful observational parameter on which a number of important discoveries have been founded.

Winn et al. (2010) used a combination of radial velocity- and transit-detected planets, combined with measurements of the Rossiter-McLaughlin effect, to report on the projected obliquities of stars hosting hot Jupiters. They reported that hotter ($\gtrsim$ 6000 Kelvin) stars tended to be more strongly misaligned with their hot Jupiter than cooler stars. One possible explanation for this correlation is that the inner and outer layers of a cool star are relatively weakly coupled, allowing the outer layer – the part on which we rely for spin information – to realign with a close-in giant planet. Two years later, Steffen et al. (2012) found that hot Jupiters tend to be singly transiting, lacking neighbors. These two results tentatively link single-tranet systems with high misalignment relative to their stars (although observations of stellar obliquities in low-mass single-tranet systems had not yet been performed).

Similar findings followed from Albrecht et al. in 2012, with the concluding hypothesis that misalignments between hot Jupiter orbits and their host stars' spin axes occupy the entire

possible range, but that cooler hosts tended to realign with their giant planets, potentially via tides. Smaller planets were incorporated in a later analysis: Morton & Winn (2014) compared the projected stellar obliquity distributions of single-tranet Kepler stars and multi-tranet Kepler stars and found the former to be more misaligned with their planets. This study confirmed previous observations that planets in multi-tranet systems tend to have smaller radii than singly-transiting planets. However, the original report on the Kepler dichotomy had filtered for planets smaller than 6 Earth radii (Lissauer et al. 2011) – Morton et al.'s sample of single-tranet systems included planets with radii larger than 6 Earth radii, with no distinction between the two groups. It is therefore possible that their data set artificially boosted the expected stellar obliquity of single-tranet systems, as it had been previously shown by Winn et al. and Steffen et al. that hot Jupiters tend to be both lonely and out of alignment.

Mazeh et al. (2015) again demonstrated that hot stars tend to be more misaligned with their planets than cool stars, but again did not separate large and small planets, instead implementing the entire confirmed Kepler planet catalog in their analysis. However, it was clear at this point that a) stars and their largest, closest-in planets were often tilted relative to each other, and b) the chances that these giants formed at their current positions seemed slim, given that the inner regions of protoplanetary disks were thought to contain too little material to form the massive cores required to accrete gas on Jupiter scales (Rafikov 2006) . Therefore, it was presumed that hot Jupiters must have migrated inward from farther out, implying that the migration and lifting onto higher inclinations may have happened via the same post-disk mechanism. Many attempts have been made to explain the existence of hot Jupiters using dynamical excitation processes, such as Kozai forcing (Nagasawa et al. 2008, Naoz et al. 2011,Teyssandier et al. 2013), secular chaos (Wu & Lithwick 2011), and planet-planet scattering

(Weidenschilling & Marzari 1996, Petrovich et al. 2014, Nagasawa et al. 2008), none of which depend directly on the properties of the star, despite evidence that spin-orbit misalignments in systems of hot Jupiters are related to the host's effective temperature (and therefore also to stellar mass).

Inspired by this conundrum, Batygin (2012) proposed an alternate route to increased stellar obliquities in planetary systems. In this theory, the protoplanetary disk is torqued by a distant stellar companion, causing the disk to precess about the angular momentum vector of the binary pair. As the disk precesses, it oscillates between perfect initial alignment with its host and total misalignment. The maximum angle between disk and star is determined by the geometry of the host-disk-companion system, as well as the strength with which the host star is coupled to the disk itself, the latter itself a rich area of study (Batygin & Adams 2013, Spalding & Batygin 2014, Spalding & Batygin 2015). The final inclination between the embedded, fully-formed planets and their host star becomes fixed once the gaseous disk dissipates.

There have been multiple follow-up papers to this work: Batygin & Adams (2013) modelled in more detail the interactions that affect star-disk coupling and found that as the disk begins to dissipate, a resonance can be excited between the precession frequencies of the disk and of the star (which is still coupled to the disk, and therefore lagging behind it). The resonance causes a sudden jump in spin-orbit misalignment, but is only encountered if the star's spin rate is held constant or is decreasing. Further exploration of the theory with more refined star-disk interaction modeling and a wider range of initial conditions led Spalding & Batygin (2014) to conclude that disk torqueing could result in any degree of misalignment. The temperature-misalignment trend, rebranded as a mass-misalignment trend, was revisited in Spalding & Batygin (2015), where it was found to arise due to the stronger magnetic coupling of cool, low-

mass (<1.2 M$_\odot$) stars – and therefore the weaker magnetic coupling of hot, high-mass stars –

with their disks. Weaker star-disk coupling leads to longer required timescales for realignment

with the disk, once it becomes misaligned. By comparison, hot, massive stars effectively "run out

of time" to realign before their disk dissipates.

It should be noted that the disk-torqueing pathway proposed by Batygin (2012) is only

accessible to star-disk systems that have a wide, inclined stellar companion during the early parts

of their lifetimes. From their multi-year direct imaging survey of hot Jupiter hosts, Ngo et al.

(2015) observed that only 50% of misaligned hot Jupiter systems had binary companions,

suggesting that at best, companion disk-torqueing can only explain half of the observed instances

of close-in, highly inclined giant planets[3]. A survey for wide binary companions around Kepler

single-tranet systems has not been conducted, although Winn et al. (2017) studied high-

resolution spectral data of stars hosting mostly sub-Neptune-sized planets (R $\lesssim 4$R$_\oplus$) and

determined that Kepler systems that don't contain hot Jupiters tend to have a mean stellar

obliquity of about 20°. They state that this is an upper limit, but also that their data is biased

toward lower obliquities. As it's unclear which of the two caveats is dominant, we'll assume a

fixed mean stellar obliquity of 20° in this work.

Likewise vital to the operation of the star-driven excitation mechanism is the oblateness

of a star early in its lifetime. The gravitational potential due to an oblate central object is

modelled in Murray & Dermott (1999) as the azimuthally-symmetric solution to the Laplace

equation in terms of spherical harmonics:

---

[3] It is important to point out that binary pairs can become decoupled early in life (Duchene & Kraus 2013), allowing
modern systems to possess misalignments without currently being part of a binary.

$$V = -\frac{GM}{r}\left[1 - \sum_{n}^{\infty} J_n \left(\frac{R}{r}\right)^n P_n(\cos\theta)\right] \tag{4}$$

where G is the universal gravitational constant, M is the mass of the object, R is its radius at the

most oblate part, r is viewer's distance away from the center of mass of the object, and θ is the

angle of the viewer with respect to the object's equatorial plane. The generic Legendre

polynomial Pn($\cos\theta$) represents the set of spherical harmonics that define the object's shape in

space, symmetric about its spin axis. J_n is a set of parameters expressing oblateness as a function

of the object's evolution; the first, J_2, is dominant and usually sufficient when modelling

perturbations due to this type of central body. It is directly related to the unique structure of the

object itself, and must therefore either be directly measured or approximated analytically. J_2 is

known as the "second-order quadrupole moment", or simply the "quadrupole moment" in this

work. It fixes n at 2, conveniently leaving us with only one surviving term in the entire sum. The

relevant Legendre polynomial is $P_2 = \frac{3}{2}\cos^2\theta - \frac{1}{2}$.

The relationship between rotation and deformation has been more thoroughly studied in

planets and satellites than in stars (Clairaut 1743, Cook 1980, Murray & Dermott 1999 and

sources therein). Modern investigations involving the quadrupole moment of stars (e.g. Li et al.

2020, Spalding & Batygin 2016) take their model from T.E. Sterne (1939), who derived an

expression for J_2 when calculating variations in the potentials of stars in elliptical binaries:

$$J_2 = \frac{1}{3}k_2 \left(\frac{\Omega}{\Omega_{br}}\right)^2 \tag{5}$$

Ω is the rotational frequency of the star ($2\pi/T$ for spin period T). Ω_{br} is the "breakup frequency",

defined as $\sqrt{GM/R^3}$. k_2 is the Love number, related to the mass distribution of the star, and can

have different values depending on our stellar model (Sterne 1939). Based on observations of spin periods and physical properties of young stars in the Orion Molecular Cloud Complex (Briceño 2005, Karim 2016), the typical range of J_2 early in a star's lifetime falls between 10^{-6} and 10^{-2} if the star is modelled as fully convective. With equations (4) and (5) in hand, one is equipped to simulate the evolution of a planetary system in orbit around a misaligned, rapidly rotating star.

To summarize the salient points: Observations of Kepler stars have revealed that the stars' spin vectors aren't always perfectly parallel to the angular momentum vectors of the planets in orbit around them – indeed, they can be quite misaligned. Although this signal is strongest among massive, hot stars hosting close-in giant planets, systems with low-mass singly transiting planets also demonstrate nonzero spin-orbit misalignments. In an attempt to allow systems of giant planets to retain coplanarity and other architectural features that would be erased by dynamical excitation, but still become tilted relative to their host stars, Batygin (2012) and others explore the possibility that the star itself became tilted within its own protoplanetary disk. This opens up the possibility that any system, not just systems of giant planets, could have started out with some measure of misalignment, as long as it was part of a wide binary pair in its youth.

In addition, it is well established that celestial objects with short rotational periods can become oblate, creating a nonuniform gravitational field that will cause objects in tilted orbits around them to precess about the central host's spin axis (Figure 3). A young star is capable of achieving rotational periods of about 1-10 days (Bouvier et al. 2013), much faster than those of modern stars (the Sun, by comparison, rotates with a period of about 25 days at the equator, slower at the poles). Thus, the quadrupolar gravitational potential of a young star may be
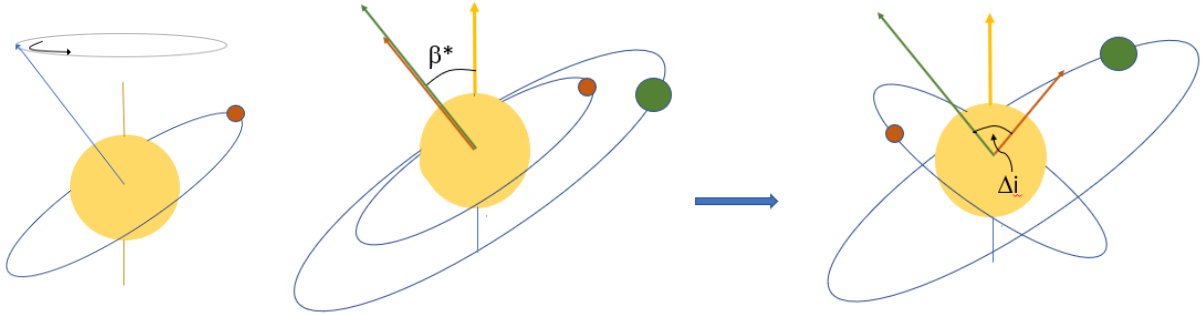
Figure 3. Left**:** A single planet precessing about its host's spin axis. Right: Same as left, with a two-planet system to illustrate the potential for misalignment.

sufficient to induce precession in the orbits of its closest planets, altering their mutual inclinations. It was in this context that Spalding & Batygin (2016) proposed a new mechanism by which planets' mutual inclinations could be excited, potentially hindering our ability to observe all of the planets in a multi-planet system. The details of excitation are as follows.

An object on a tilted, circular orbit around a perfectly spherical host experiences acceleration due only to the first term in equation (4). As long as its orbit remains circular, it will stay the same distance from its host, pass through the same gravitational potential, and feel the same acceleration, at every point in its orbit. By contrast, the same object orbiting an oblate host feels an acceleration caused by both terms in equation (4) – the second of which depends not only on distance from the host, but also on the object's angular position relative to the host's equatorial plane. Orbiting bodies in this scenario feel nonuniform accelerations as they move. It is this nonuniform acceleration that leads to orbital precession. In terms of Keplerian coordinates, the component of an orbit that changes under this type of precession is the "ascending node", and the motion is called "nodal precession". Figure 3 depicts a simple example of a single tilted planet precessing about its host's spin axis; one full revolution appears on the accompanying plot as one completed cycle of the ascending node through 360°.

22

When two or more planets are in close orbits around this type of star, the closer-in planet experiences a larger acceleration and will precess at a higher frequency (shorter period) than its outer neighbor. If they start on coplanar orbits, this mismatched precession will cause the inner planet's orbit to outpace the outer, increasing the angle between the two orbital planes (Figure 3). The maximum possible angle between the two planets is restricted by their initial tilt (β_*) relative to the star – as long as the inner planet has less orbital angular momentum than the outer, their maximum Δi can't exceed $2\beta_*$ (see Spalding & Batygin 2016).

In a simpler system with a perfectly spherical star, the orbits of planets in the system will still undergo small oscillations in some of their elements due to the presence of all of the other planets, as discussed in the previous section. So, too, do planets orbiting a tilted, oblate star cause oscillations in each other's orbital inclinations as the star attempts to increase their misalignment. This results in a sort of complex wobbling motion of each planet's angular momentum vector, a phenomenon difficult to capture in a static figure.

These planets don't experience constant-amplitude oscillations eternally, however. After its disk dissipates, a young star begins to gravitationally contract, shrinking onto the main sequence (Batygin & Adams 2013, Bouvier et al. 2013) and spinning up until internal pressure balances gravitation and it enters the fusion phase (Asimov 1977). The influence of a spinning-up star on its planets has not been explored yet. After spin up, however, stars of up to $1.2M_\odot$ will begin to slowly spin down as their angular momentum is carried away by stellar winds (Schatzman 1962). Slower rotation leads to a weaker quadrupole moment, decreasing the acceleration that drives planet precession and causing the precession frequencies to decrease as well. Eventually the quadrupolar contribution to the star's gravity becomes negligible, and the

23

orbits in the system continue to oscillate in one form or another about the final mutual

inclinations they acquired while experiencing quadrupolar torqueing.

Spalding & Batygin's (2016) first steps were to calculate a proof-of-concept analytic

solution for the evolution over time of the mutual inclination Δi between two planets orbiting an

oblate, tilted star. Their solution derives from Laplace-Lagrange secular theory, and is based on

the assumptions that a) both planets are on initially circular, nearly coplanar orbits, b) the ratio of

their periods is not a simple fraction (a.k.a. the planets are not near mean motion resonance), c)

the stellar spin axis points along the same direction at all times, and d) the star's spin rate is

constant. The solution, shown below, is a simple sine function with an amplitude less than or

equal to twice the obliquity, β_*, of the host star.

$$\Delta i(t) = 2\beta_* \mathcal{G} \sin\left(\frac{\omega_0 t}{2}\right) \tag{6}$$

where

$$\mathcal{G} = \mathcal{L}\left[1 + \mathcal{L}^2 + 2\left[\frac{\Lambda_2 - \Lambda_1}{\Lambda_2 + \Lambda_1}\right]\mathcal{L}\right]^{-\frac{1}{2}} \tag{7}$$

$$\mathcal{L} = \frac{v_2 - v_1}{B_2 + B_1} \tag{8}$$

$$\omega_0 = [(B_1 + B_2)^2 + (v_1 - v_2)(v_1 - v_2 + 2[B_1 + B_2])]^{\frac{1}{2}} \tag{9}$$

$$B_1 = \frac{1}{4} n_1 \left(\frac{a_1}{a_2}\right)^2 \left(\frac{m_2}{M_*}\right) b_{3/2}^{(1)}\left(\frac{a_1}{a_2}\right)$$

$$B_2 = \frac{1}{4} n_2 \left(\frac{a_1}{a_2}\right) \left(\frac{m_1}{M_*}\right) b_{3/2}^{(1)}\left(\frac{a_1}{a_2}\right) \tag{10}$$

$$v_p = \frac{3}{2} n_p J_2 \left(\frac{R_*}{a_p}\right)^2$$

Λ_p is approximately the angular momentum of planet p, and is given by $m_p\sqrt{GM_*a_p}$. The mass and semimajor axis of planet p are m_p and a_p, respectively. For the period T of one orbit, the orbital frequency, or mean motion, n_p is equal to $2\pi/T$. M_* and R_* are the mass and radius of the host star, and b is the Laplace coefficient, a special integral function of a_1/a_2, given by

$$b_{3/2}^{(1)}\left(\frac{a_1}{a_2}\right) = \frac{1}{\pi}\int_0^{2\pi}\left[\frac{\cos\psi}{\left[\left(1 + \left(\frac{a_1}{a_2}\right)^2 - 2\left(\frac{a_1}{a_2}\right)\cos\psi\right)^{\frac{3}{2}}\right]}\right]d\psi \tag{11}$$

The amplitude $\mathcal{G}$ of equation (6) was inspected to gain insight into the limits of the planets' Δi under different sets of physical parameters. Perhaps most interestingly, they found that when the inner planet has more angular momentum than the outer, the two enter a secular resonance, meaning that they precess at similar frequencies and achieve maximum inclinations larger than $2\beta_*$. Such a result was the backbone of their subsequent paper, in which they explored the possibility that hot Jupiters with low-mass exterior neighbors cannot be seen transiting with those neighbors, again due to resonant precession driven by a tilted, oblate star (Spalding & Batygin 2017). According to equation (6), it should be possible for that kind of star to decrease the number of transiting planets in a system by increasing their mutual inclinations.

In order to lend robustness to their solution, incorporate stellar spin-down, and look into the specific evolution of a system all throughout its life, they performed 110 N-body simulations using Kepler-11 (6 planets) as a basis system, using different combinations of initial J_2 (denoted as $J_{2,0}$ in this work) and β_* when initiating each run. In the end, these test systems not only saw a reduction in their transit number – in some cases they went unstable, losing a minimum of three, or a maximum of five planets in the process, and always appearing as a single-tranet system

afterward. A majority of possible combinations of β_* and $J_{2,0}$, from 0° to 90° and 10^{-4} to 10^{-2} respectively, resulted in a reduction in transit number. Systems with β_* above approximately 30° and/or $J_{2,0}$ above ~10^{-3} nearly always went unstable, losing their smallest planets first.

Kepler systems are generally expected to have 3 or so planets per host star (Lissauer et al. 2011, Zhu et al. 2018), so the results of Spalding & Batygin (2016) were lacking in information about excitation and stability at the N>2-planet level. The physics underlying instability was likewise uninvestigated. Consequently, Spalding et al. (2018) performed a larger collection of N-body simulations on different known Kepler systems of 2, 3, or 4 planets, again mapping their final maximum transit numbers and instability rates. They concluded the following:

i.   the stellar oblateness mechanism can reduce the transit number of any Kepler system, through Δi excitation (all) or by triggering instability (most);

ii.   the average eccentricity of a planet surviving instability in an initially two-planet system may be 0.3-0.4, although more sophisticated collision models in simulations would produce more accurate estimates on eccentricity outcomes. Tidal interactions will circularize the closest-in planets, and distant planets are unlikely to;

iii. in the two-planet case, instability seems to occur as the result of a secular resonance, this time between the two planets' arguments of pericenter. They predict that, for a planet pair where the outer planet has more angular momentum, the two planets must reach Δi of approximately 40° before instability occurs.

Using the initial properties of each 2-planet system in the set, they solved equation (6) for β_* as a function of $J_{2,0}$ and predicted the β_* and $J_{2,0}$ values above which the given planet pair will

be excited out of transit. The resulting curve very roughly followed the boundary between fully transiting and partially transiting systems, with varying levels of accuracy.

This paper opened multiple avenues for future work. It was noted that a young system's spin-orbit misalignment is sensitive to the time scale on which the disk dissipates; a slowly-dispersing disk has the potential to damp inclination growth between system and star, a factor that was not accounted for in the 2018 paper. Disk dispersal is an elusive phenomenon, and not much is known about it. Spalding & Millholland (in prep) are currently investigating this era of stellar evolution, seeking to clarify the conditions under which a star will retain appreciable misalignment as it loses its disk. Their results will help distinguish the stellar oblateness mechanism's ubiquity in planetary systems.

The authors also note that their small sample size of 11 systems prevented them from placing tighter constraints on the occurrence rate and conditions for instability. They again cite $J_{2,0} \sim 10^{-3}$ and $\beta_* \approx 30°$ as approximate limits above which systems go unstable, but point out that the range varies widely from system to system. The ensemble of simulations conducted within this thesis can provide instability criteria for Kepler-like systems as a function of the measurable properties of the system, with which we can more precisely predict the frequency of planetary instability due to this mechanism.

The Kepler dichotomy is fundamentally a question of true multiplicity: are we seeing all of the planets that are really there, or are we missing planets? Put another way, what is the transit distribution of a population of Kepler systems orbiting an oblate star, and what is the true multiplicity distribution? Spalding et al. (2018) have shown that Kepler systems respond diversely to young, inclined, rapidly rotating stars, and so their results cannot be used to predict the multiplicity of a randomly selected transiting system. Thus, with our knowledge as it

27

currently stands, we can't answer those questions most pertinent to the Kepler dichotomy. It is the goal of this thesis to begin answering those questions.

CHAPTER 2

PERTURBED COUPLES: N=2

2.1 Introduction and Assumptions

The oblate, tilted star (referred to as OTS from this point forward) mechanism has only been applied to a handful of Kepler systems (Spalding 2016, 2018, Li et al. 2020), too small a collection to be considered representative of the entire Kepler/K2 set of over 1800 systems. In this chapter, I perform N-body simulations on 45 different artificial planetary systems with different average planet masses m and innermost semimajor axis a_1, each evolved under 105 unique combinations of initial quadrupole moment ($J_{2,0}$) and stellar tilt β_*. These systems have been constructed based on recent analyses of the Kepler population (Weiss et al. 2017, Millholland et al. 2018); their responses to an OTS generate a framework of parameters that will help us contextualize our past and future observations of close-in planetary systems. I compare my results to those of Dai et al. (2018) to show that the observable inclinations of the closest-in transiting systems could easily have originated from interactions with an OTS. I further discuss the relationship between a system's fate and its initial conditions, confirm and improve upon predictions from other work about instability triggers, and address the implications of my findings.

Assumptions:

1. The protoplanetary disk dispersed quickly.

As mentioned in chapter 1, spin-orbit misalignment in young systems is theorized to be the product of multiple interactions between star, disk, and companion. Not only does the disk influence its host star's evolution through magnetic, gravitational, and accretionary interactions, it also hosts its own potential that can competitively torque planets embedded within it. A

suitably massive disk will keep its planets in fairly good alignment within it as the companion-driven precession described in Batygin (2012) occurs, even as the host star attempts to excite the orbits out of coplanarity. However, Spalding & Millholland (in prep) show that a slow transfer of dominance from disk to host star (slow disk dissipation) will allow the entire collection of coplanar orbits to drift from disk-aligned to star-aligned, erasing any stellar obliquity previously attained and disempowering the OTS mechanism. On the other hand, if the disk dissipates quickly, the planets are unable to 'drift' into stellar realignment before OTS-induced nodal precession begins to dynamically excite them. "Slow" and "quick" are defined relative to the precession frequency due to the OTS, but because very little is understood about this phase of a system's life (Spalding et al. 2018), a precise boundary between the two dispersal rates is difficult to define. Thus, for the sake of simplicity, we assume that the disk dispersed rapidly enough that planets and star remained misaligned. Future work will help place this assumption into better perspective.

2. The young star has already fully contracted, and the planets lie on modern orbits.

A young star in the post-disk, pre-main-sequence (PMS) stage will both shrink in radius and increase in spin rate over several tens of millions of years; its initial radius can be as large as twice its final radius (Shu et al. 1987), and it will rotate with a period between 1 and 10 days at the onset of contraction, potentially on the order of tenths of days just after contraction (Bouvier et al. 2013). After this point, its size remains relatively constant and, if lower than around 1.2 $M_\odot$, it gradually slows its rotation over the next several Gyr (see previous chapter). Previous applications of the OTS mechanism were confined to the spin-down phase, choosing an inflated stellar radius and spin periods representative of the PMS stage and essentially ignoring the complications introduced by the spin-up phase. It is beyond the scope of this thesis to explore the

dynamics between an OTS and a close-in system in the spin-up phase, but the issue is still important to address. Among the systems simulated in this work, the closest-in contain an inner planet in orbit at only a few *final* stellar radii away from the center of mass of its host. If the host's *initial* radius is twice its final, the host will engulf the closest-in planets in simulations, depriving us of data on those planets with very short periods. It is for this reason that I have chosen a stellar radius of 1 Solar radius ($R_\odot$) as an initial condition, and hold it fixed while J_2 decays over the course of the simulation. The outcome of the spin-up phase of evolution, perhaps in tandem with disk dissipation, is a question left for future work.

I further assume that modern Kepler architecture is a good representation of the organization of a planetary system just after emergence from its disk. This is supported by evidence from Weiss et al. (2018), which suggests that planets form close to their final positions. Ultra-short-period planets (USPs), which comprise those planets in our sample set with the smallest semimajor axes, are unlikely to have formed where they currently lie for the reason mentioned above, in addition to the lack of solid materials at such small separations from the star (see Petrovich et al. 2018 for a possible migration scenario for this class of planets, invoking secular chaos). I therefore assume that all necessary planet migration has taken place before OTS precession begins, and that it occurs with no dynamical excitation so that all planets start on coplanar, circular orbits. Massive companion + OTS excitation is explored in greater detail in Pu & Lai (2019) as another pathway to USP creation.

2.2 Methods

All simulations in this work were performed using the "well-tested" (Spalding & Batygin 2016) N-body integration software package mercury6 (Chambers 1999). In its essence, the integrator starts with the planetary system in an initial configuration; it calculates all

accelerations on all objects due to all other objects, and applies a user-defined time step to evolve the objects' new velocities due to those accelerations; using different approximation methods, it solves for the position of each object at this new point in time; finally, it re-calculates accelerations based on the updated positions of the objects and repeats the process with the next time step. The algorithm one implements to perform these calculations dictates the relative speed and accuracy of the simulation. Accuracy is measured by the degree to which a simulation conserves the total initial energy of a system – smaller time steps lead to smaller deviations away from the system's would-be state if it were evolving in reality, and thus results in better conservation of energy. At the same time, a smaller time step means that more iterations are required to evolve a system for the desired duration. One must choose between efficiency and accuracy when selecting a time step and algorithm.

I employed mercury6's hybrid Bulirsch-Stoer/symplectic algorithm with a time step of $1/20^{th}$ of the shortest planet period in the system. This time step conserved energy to within 0.0001%. The symplectic part of this algorithm incorporates Hamiltonian mechanics to additionally preserve the system's volume in phase space, improving energy conservation, and operates for a majority of the duration of the simulation. The Bulirsch-Stoer method takes over when planets enter close encounters with each other, performing more "brute force" calculations like the ones outlined above to provide more accurate close-encounter outcomes than the symplectic algorithm.

Because part of the goal of this chapter is to compare OTS-driven outcomes to the data from Dai et al. (2018, henceforth called the "Dai set"), the innermost semimajor axis a_1 in each artificial system is drawn from a set of values expressed as a multiple of stellar radius R_*, ranging from 2 to 20:

$$\frac{a_1}{R_*} \in \{2, 3, 4, 5, 6, 7, 8, 9, 10, 11, 12, 14, 16, 18, 20\} \tag{12}$$

The exact value of each a_1 in the Dai set depends on the radius of the host star attached to a given data point. I choose to evolve my artificial systems around a Sun-like ($R_*=R_\odot=0.005$ AU, $M_*=M_\odot$) star, resulting in values of a_1 between 0.01 and 0.1 AU.

Recent analyses of Kepler data presented interesting trends amongst planets in a system of multis: it was found that they tend to be evenly spaced, with a mean separation of 20 mutual Hill radii (Weiss et al. 2017). The mutual Hill radius between a planet j and its next outer neighbor $j+1$ is defined as

$$R_H = \left(\frac{m_j + m_{j+1}}{3M_*}\right)^{\frac{1}{3}} \frac{(a_j + a_{j+1})}{2} \tag{13}$$

so the mean separation between Kepler planets is simply

$$a_{j+1} - a_j = 20R_H \tag{14}$$

Each pair of neighbors in a system is separated by 20 mutual Hill radii based on the above expressions. Every successive semimajor axis depends on the one before it:

$$a_{j+1} = a_j \frac{1 + 10\left(\frac{m_j + m_{j+1}}{3M_*}\right)^{\frac{1}{3}}}{1 - 10\left(\frac{m_j + m_{j+1}}{3M_*}\right)^{\frac{1}{3}}} \tag{15}$$

Likewise, Millholland et al. (2018) discovered that all planets within a randomly selected Kepler system had masses more similar to each other than if they had all been thrown together by chance. This uniformity of mass allows us to select a single value that represents the average planet mass of planets in a system, and assign that same value to each planet in the system

without diverging far from the organization of a true Kepler system. According to Weiss & Marcy (2014), planets with radii $<4R_\oplus$ have an average mass of about 4.3 $M_\oplus$; therefore, each planet in a pair of planets in my simulations has the same mass, equal to 1, 5, or 10 Earth masses. Their radii are calculated using the piecewise mass-radius power law from Weiss & Marcy (2014), where mass m_p and radius R_p are in Solar units:

$$m_p = 2.69 R_p{}^{0.93} \tag{16}$$

From there, assuming perfectly spherical planets, their densities are simple to calculate ($\rho=m/V$).

Most of the 2-planet systems studied by Spalding et al. (2018) remained stable at tilts below $\sim30°$. In order to more thoroughly investigate stable cases, multiple cases of β_* ranging between $0°$ and $30°$ were simulated, with two additional, large-obliquity runs included for comparison:

$$\beta_* \in \{1°, 6°, 10°, 20°, 30°, 50°, 70°\} \tag{17}$$

Ten spin periods, evenly distributed in log space (10^X, where x is between 0 and 1 in multiples of 0.1), were plugged into equation (5) along with the relevant physical properties of the star to generate input values for $J_{2,0}$. The Love number k_2 can take on values spanning an order of magnitude (0.014 to 0.28) depending on whether one chooses to model a young star as fully radiative or fully convective, respectively – a PMS star can evolve from the former to the latter as it contracts, so either may suffice (Batygin & Adams 2013). $J_{2,0}$ values will turn out to span several orders of magnitude regardless, so the choice is more or less moot. In keeping with past literature (Spalding & Batygin 2016, Spalding et al. 2018), k_2 is set to 0.28 for a fully convective young star, leading to a possible over-estimate of the quadrupolar potential. However, as mentioned above, we chose a smaller stellar radius than may exist in reality. Thus, our results are representative to real, PMS stars within an order of magnitude.

Over 30 young, Solar-mass PMS stars, called T-Tauri stars, in the Orion Molecular cloud have had their masses and radii (Briceño et al. 2005) as well as their spin periods (Karim et al. 2016) characterized. When modelled as fully convective, their calculated J_2 values range from $\sim 10^{-5}$ to $\sim 10^{-3}$, with a small number pushing as high as $\sim 10^{-2}$. The above set of $J_{2,0}$, based on previously observed T-Tauri spin rates, doesn't exceed $\sim 10^{-3}$. To bridge the gap, five more $J_{2,0}$ between $\sim 10^{-3}$ and $\sim 10^{-2}$ were selected. The complete set of $J_{2,0}$, with values rounded, is:

$$J_{2,0} \in \left\{ \begin{array}{l} 1.98 \times 10^{-5}, 3.14 \times 10^{-5}, 4.98 \times 10^{-5}, 7.89 \times 10^{-5}, \\ 1.25 \times 10^{-4}, 1.98 \times 10^{-4}, 3.14 \times 10^{-4}, 4.98 \times 10^{-4}, 7.89 \times 10^{-4}, \\ 1.25 \times 10^{-3}, 1.98 \times 10^{-3}, 3.14 \times 10^{-3}, 4.98 \times 10^{-3}, 7.89 \times 10^{-3}, 1.25 \times 10^{-2} \end{array} \right\} \quad (18)$$

The quadrupole moment is allowed to exponentially decay over time, to simulate stellar spin-down:

$$J_2 = J_{2,0} \, e^{\frac{-t}{\tau}} \quad (19)$$

Actual spin-down lasts a star's whole lifetime (Bouvier et al. 2013). It would be computationally inefficient to perform over 3000 ~Gyr-long simulations. In a system where nothing else dynamically interesting is expected to happen on time scales longer than the planets' precession periods, we have the freedom to assign any value to the decay parameter τ, as long as it is large relative to those precession periods. Behavior that occurs on much longer time scales than other periodic effects in a physical system is called "adiabatic" (discussed more thoroughly in Lichtenberg & Lieberman 1992). Following Spalding & Batygin (2016), I set the decay parameter to 1Myr.

Although mercury6 does have the option to include the influence of an oblate star when integrating, there's no way to incorporate stellar spin-down without implementing a custom subroutine. Fortunately, mercury6 allows users to define their own additional forces (mfo_user).

An object in orbit around an OTS experiences a gravitational potential per unit mass defined by equation (4). The acceleration due to this potential is simply the gradient, ∇V, of its oblateness-induced component where n=2:

$$V = \frac{GM}{r} J_2 \left(\frac{R}{r}\right)^2 \left(\frac{3}{2}\cos^2\theta - \frac{1}{2}\right) \tag{20}$$

With $r=\sqrt{x^2 + y^2 + z^2}$ and $\cos\theta = z/r$, and incorporating equation (19), the three-dimensional Cartesian gradient of the above potential is

$$a_{Jx} = -J_{2,0}\, e^{\frac{-t}{\tau}} \left(\frac{GM_*}{r^3}\right)\left(\frac{R_*}{r}\right)^2 x\left[7.5\left(\frac{z}{r}\right)^2 - 1.5\right]$$

$$a_{Jx} = -J_{2,0}\, e^{\frac{-t}{\tau}} \left(\frac{GM_*}{r^3}\right)\left(\frac{R_*}{r}\right)^2 y\left[7.5\left(\frac{z}{r}\right)^2 - 1.5\right] \tag{21}$$

$$a_{Jx} = -J_{2,0}\, e^{\frac{-t}{\tau}} \left(\frac{GM_*}{r^3}\right)\left(\frac{R_*}{r}\right)^2 z\left[7.5\left(\frac{z}{r}\right)^2 - 4.5\right]$$

General relativistic effects were modelled using an approximation from Nobili & Roxburgh (1986):

$$a_{GR,x} = 1.625 \times 10^{-11} \left(\frac{x}{r^2}\right)\left(\frac{M_*}{K_2}\right)^2$$

$$a_{GR,y} = 1.625 \times 10^{-11} \left(\frac{y}{r^2}\right)\left(\frac{M_*}{K_2}\right)^2 \tag{22}$$

$$a_{GR,z} = 1.625 \times 10^{-11} \left(\frac{z}{r^2}\right)\left(\frac{M_*}{K_2}\right)^2$$

K_2 in this context is the Gaussian gravitational constant squared, equal to around 2.59×10^{-4}. These accelerations as they appear in the mercury6 subroutine mfo_user are in Appendix A.

The duration of the simulations was 5Myr, long enough for the closest-in systems to settle into steady state oscillation about a fixed Δi. Upon completion, I calculated the mutual

inclination between each surviving planet pair using the following relations and the definition of

r, above. (The second expression is a vector cross product, the third a dot product.)

$$\dot{r} = \sqrt{\dot{x}^2 + \dot{y}^2 + \dot{z}^2} \tag{23}$$

$$\vec{h} = \vec{r} \times \dot{\vec{r}} \tag{24}$$

$$|\Delta i| = \mathrm{acos}\left(\frac{\vec{h_1} \cdot \vec{h_2}}{\|\vec{h_1}\| \|\vec{h_2}\|}\right) \tag{25}$$

This calculation was performed at each time step for the last 10,000 years of an integration and

averaged together, to smooth over the planets' ambient oscillations.

To give the resulting data an organic appearance while retaining the trends inherent in it,

I fed it to the Mathematica machine learning function Predict[]. Like any function-fitting

method, Predict[] takes real, N-dimensional input+result data and processes it with a

combination of fitting algorithms to best model the relationships between inputs and result. As

the name implies, it can then generate predictive sets of data based on alternative input sets. I

drew values of a_1, m, $J_{2,0}$, and β_* from different distributions to create physically-informed

inputs; a_1 came from a uniform distribution on [0.01, 0.1] AU, m from a uniform distribution on

[1, 10] Earth masses, $J_{2,0}$ from a distribution fitted to the aforementioned T-Tauri J_2 set, and β_*

from a Rayleigh distribution, as suggested by Winn et al. (2017). In fact, multiple distributions

have been proposed to fit the current stellar obliquity data (Li et al. 2020). I investigated whether

the choice of β_* distribution and mean significantly affected the inclination outcome produced by

Predict[]. As such, I created four separate fabricated input sets following the process outlined
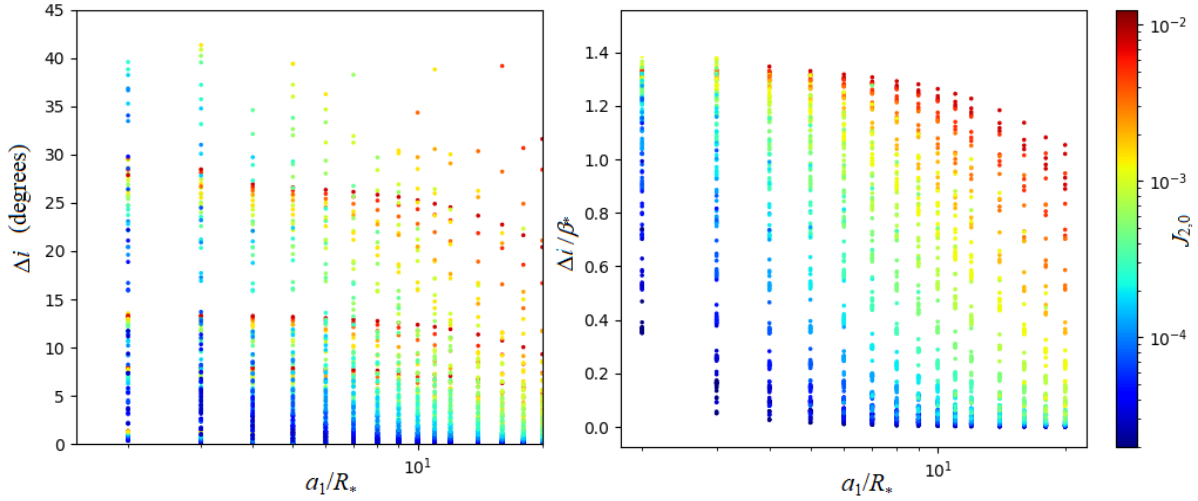
Figure 4. The complete set of N-body simulation results, colored according to $J_{2,0}$. Left (a) is a plot of mutual inclination against the innermost planet's distance from the host. Right (b) is the same plot, with mutual inclination scaled according to initial stellar tilt.

above, each set containing β_* drawn from a different distribution: Rayleigh with means 20°, 30°,

and 45°, and a uniform distribution on [0, 90]°.

Finally, to clearly illustrate the dependence of Δi on stellar parameters $J_{2,0}$ and β_*, I

performed a second-order polynomial interpolation on the original N-body data set using

Mathematica's Interpolate[]. The resulting curves can be found in Appendix B.

2.3 Results and Discussion

2.3.1 a_1

Figures 4 and 5 contain the direct results of my simulations. Mutual inclinations between

same-mass planets in the constant-spin regime are capped off at $2\beta_*$ (Spalding & Batygin 2016).

However, a notable feature of the simulations is that, as the stellar J_2 decays, planetary mutual

inclinations adiabatically decrease, reducing the maximum final misalignment between them to

$1.4\beta_*$. This can be seen in the right-hand panel of Figure 4, where Δi of a system is scaled by that
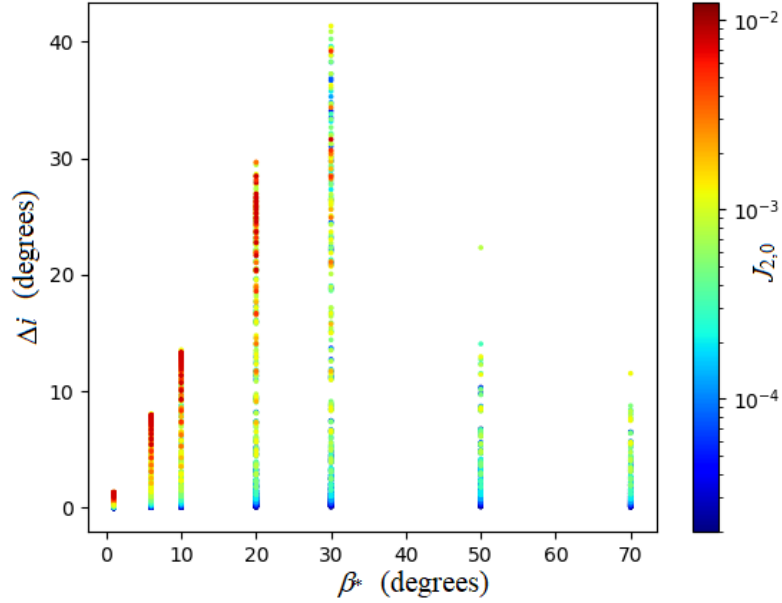
Figure 5. Δi vs β_* for the entire surviving set of simulated systems, colored according to $J_{2,0}$.

system's initial stellar obliquity. The left-hand panel in the same figure can be thought of as seven separate layers of data, one for each initial β_*, superimposed over each other. The warmer the color, the higher $J_{2,0}$ was at initialization. Red banding, corresponding to the highest $J_{2,0}$, appears at approximately $1.4\beta_*$ for each initial β_*, most prominently at about 14° ($\beta_*=10°$) and 28° ($\beta_*=20°$), with hints of a band around 8° ($\beta_*=6°$). As expected, the more strongly misaligned a star is, and the more oblate, the larger an impact it has on its planets' mutual inclinations.

Despite the new upper limit imposed on Δi by stellar spin-down, there appears to be a lack of mutual inclinations higher than 30-40°, and no high $J_{2,0}$ band for $\beta_*=30°$, 50°, or 70°, in Figure 4a. Figure 5 more clearly shows this pattern. A majority of systems with high β_*/high $J_{2,0}$ went unstable (and therefore have no mutual inclination to plot), while the high β_*/low $J_{2,0}$ systems wound up with only a few degrees' excitation as a consolation prize for surviving. Mutual inclinations at $\beta_*=50°$ and 70° in Figure 5 rarely exceed 15° or so, in contrast with the Δi of $\beta_*=30°$ systems, which bump right up against the instability limit. Spalding et al. (2018)

found that the barrier between stability and instability is marked by $\beta_* \approx 30°$ and $J_{2,0} \sim 10^{-3}$, regardless of system multiplicity; they predicted that a planet pair would go unstable upon reaching a mutual inclination of about 40°, and that systems with β_* at or above 50° would experience inclination growth unlike that at lower obliquities. The deficit of mutual inclinations above the 40° line in Figure 4a, combined with the absence of mutual inclinations above 15° at high obliquities in Figure 5, support their conclusions.

A second data deficit appears at $\Delta i \approx 15°$ in Figure 4a; this is an artefact of a combination of real behavior and input-selection effects. The amplitude [equation (7)] in Spalding & Batygin's (2016) constant-spin solution for Δi was shown in that paper to increase nearly asymptotically to its maximum value as $J_{2,0}$ was increased. Here we see similar behavior, where for a given value of β_*, values of $J_{2,0}$ between $\sim 10^{-3}$ and $\sim 10^{-2}$ do relatively little to increase Δi further toward $1.4\beta_*$. Similarly, choosing $J_{2,0}$ that grow on orders of magnitude mean that low-end $J_{2,0}$ are fairly well clustered together on a linear scale, progressively spreading out at higher $J_{2,0}$. This causes the lowest and highest parts of a Δi versus a_1/R_* plot to appear denser than the middle (see Figure 7) – clustering at the higher end is a natural result, while clustering at the lower end is a selection effect. The deficit of points at 15° occurs in the "slice" of Δi data associated with $\beta_* = 20°$, and would be filled if the β_* set had included values between 10° and 20°.

While there does appear to be an anticorrelation between innermost semimajor axis and mutual inclination in Figure 4a, the trend can be made clearer. Figure 6b is a 2D histogram of 5,000 Predict[] points, created by following the procedure laid out in the previous section,
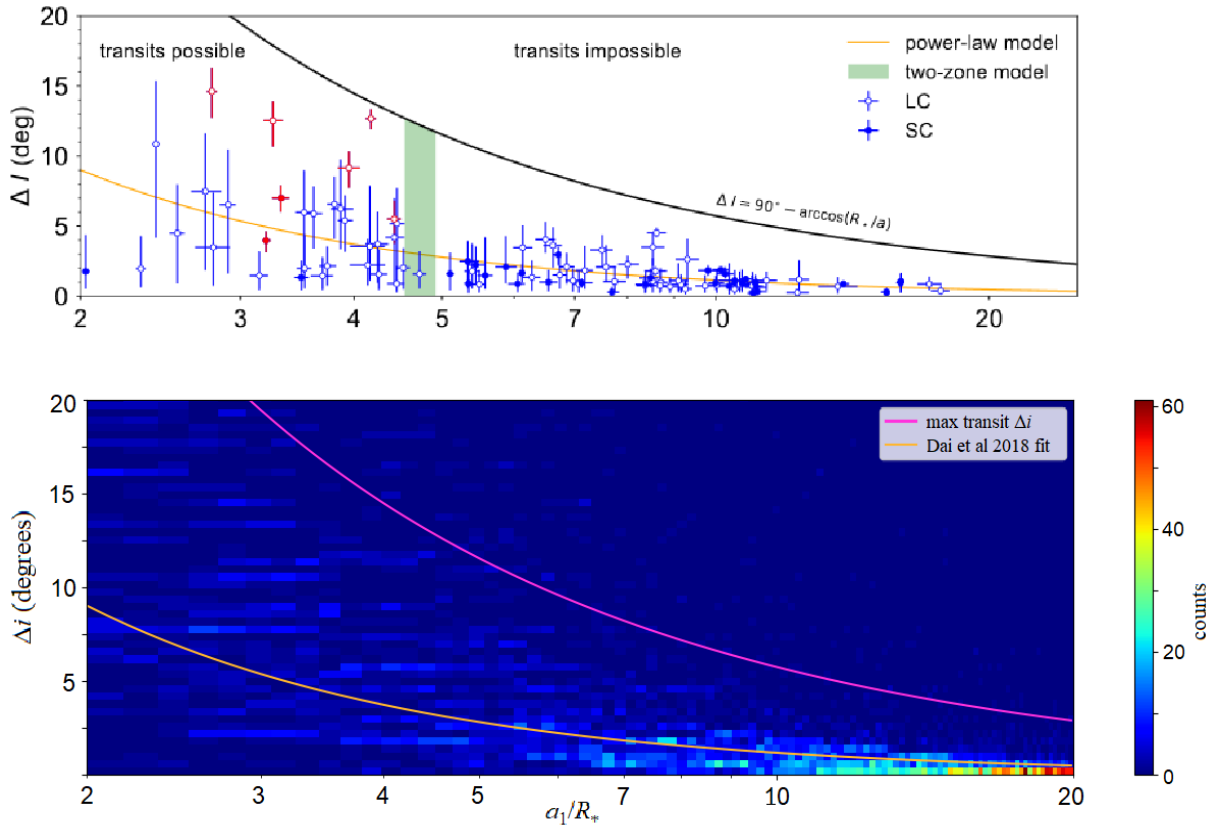
Figure 6. Δi versus a_1/R_* for observational and artificial data sets. **(a)** Figure 3 from Dai et al. (2018), showing mutual inclinations extracted from the light curves of multi-transiting systems. The black line demarcates the boundary between mutually transiting and singly transiting; the orange is a best fit line chosen by the authors. The green region separates pairs that are strongly coupled from pairs that are weakly coupled. The color of each point is related to the method employed to extract Δi. **(b)** A 2D histogram comprised of artificial data from Mathematica's Predict[] function, trained on N-body data. The artificial input data selection process is described in the text. Color corresponds to the density of data points within each bin. The magenta and orange lines are equivalent to the black and orange lines, respectively, from the Dai et al. plot.

drawing β_* from a Rayleigh distribuuion with mean 20°. Only those data points with $J_{2,0} \lesssim 10^{-3}$ are included on this histogram in order to reduce the high-$J_{2,0}$ density banding described above. In the top panel of Figure 6, I have included the original Δi versus a_1/R_* plot published in Dai et al. (2018, Figure 3 in that work). The important curves from the Dai et al. figure have been superimposed over the 2D histogram for ease of comparison: the orange line is a best fit line derived by Dai et al., where at a given a_1/R_*, inclinations are Rayleigh-distributed with a scale parameter

$$\sigma = \sigma_0 \left(\frac{a_1}{R_*}\right)^m \tag{26}$$

specified by σ_0 and m (not related to this thesis' input variable m), which are equal to 0.382 and -1.28, respectively (see Dai et al. 2018, table 2). This scale parameter σ represents the statistical mode, in radians, of all mutual inclinations at a specific a_1/R_*. The orange curve on both plots is this mode converted to degrees.

The two parts of Figure 6 complement each other in a number of ways. First, and most importantly, they both demonstrate that mutual inclinations between planet pairs are larger and more spread out as proximity to the host star decreases. Second, the orange Dai curve is qualitatively a good fit to this simulated data set. In light of the fact that the Dai data set is supposed to represent only a lower bound on possible mutual inclinations between planets, this is a particularly interesting result, suggesting that the Dai method for extracting mutual inclinations from light curves is fairly accurate. A statistical comparison between the two data sets, observational and theoretical, is beyond the scope of this thesis. Third, most of the simulated systems lie below the no-transit line. If systems with $J_{2,0} > 10^{-3}$ had been included on the 2D histogram, they would appear above the no-transit line; however, these high $J_{2,0}$ stars are relatively rare (Briceño et al. 2005, Karim et al. 2016) and are not expected to constitute more

than a small fraction of real systems, so their removal doesn't significantly alter the big picture. This abundance of simulated systems below the transit line implies that most of the time, two-planet systems can be fully observed if the viewing geometry is just right. It may be that the Dai set, though limited, is fairly well representative of the true relationship between Δi and innermost semimajor axis of planet pairs across the universe.

2.3.2 β_*

Varying β_* in the simulations did not reveal any interesting behavior beyond what has already been reported in the literature and above. Likewise, a comparison of 2D histograms of predictive data sets based on the different β_* distributions yields very little discernible difference between them (Appendix B). The underlying distribution of stellar obliquities in the universe cannot be constrained using this data set. As an OTS's obliquity is linked to the survivability of its planets, one may be able to estimate the true mean stellar obliquity by studying instability rates and residue in Kepler systems; chapter 3 delves into this possibility in greater detail.

2.3.3 m

Figure 7a is a single constant-β_* slice of Figure 4a, colored according to the average planet mass m assigned to each planet pair. The points overlap for the most part at low Δi – indeed, systems with the largest mass seem to pull ahead very slightly between 1° and 3°. Above 3°, the smallest-mass systems begin to experience sharper inclination growth than either of the two other mass classes, becoming most widely separated from them at small distances from the star and creating 'smeariness' in the upper regions of the plot. The relative differences in Δi are
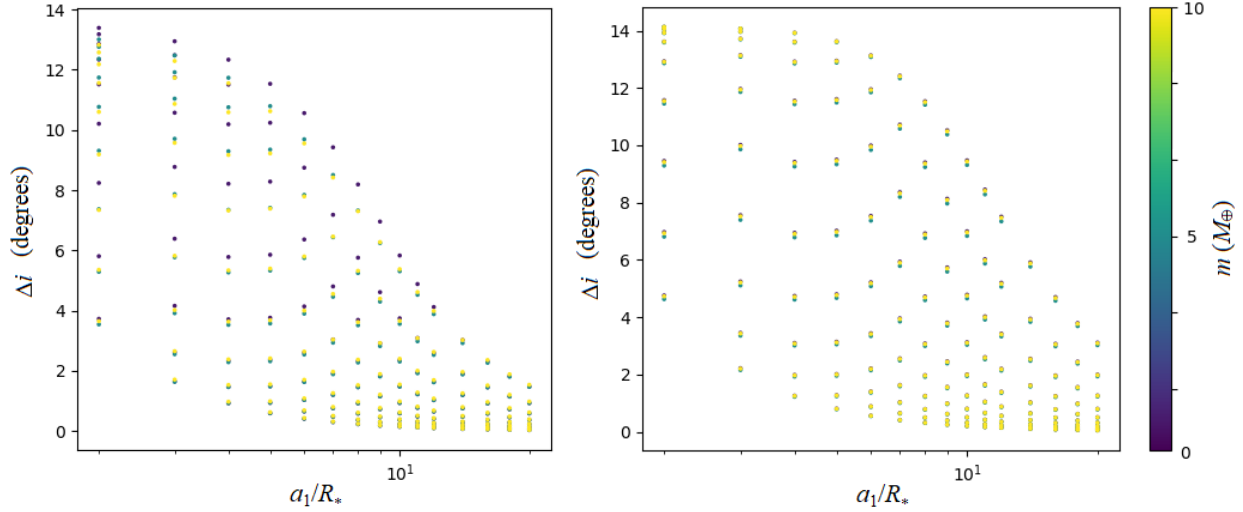
Figure 7. Plots of Δi vs a_1/R_* with colors indicating average planet mass. Navy is the lowest mass, green is middle, and yellow is highest. **(a)** Left, a "slice" of Figure 4a at $\beta_*=10°$. **(b)** Right, the same set of inputs as in figure (a), plugged into the RMS amplitude of Spalding & Batygin's (2016) solution for Δi in an OTS-planet-planet system [equation (6) in this work].

not necessarily remarkable – mass group 2 is five times as large as mass group 1, but mass group 3 is only twice as large as mass group 2, so it's reasonable that mass groups 2 and 3 are close together in Δi. The general trend is notable, however, and becomes somewhat more pronounced at higher β_*. Evidently, average planet mass corresponds to slightly higher Δi, particularly for moderate-to-large $J_{2,0}$ and small a_1/R_*. However, the differences are so small that system mass is not likely to be a determining factor in whether a surviving OTS-evolved planet pair appears singly or doubly transiting. Low-mass systems tended to go unstable around 15% of the time, compared to a 12% instability rate for both of the other mass groups – it is therefore slightly more probable that a truly single-planet system is lower in mass, according to this data.

This mass dependence becomes more interesting when compared to the set of Δi produced by equation (6). Using the same inputs as went into Figure 7a, but calculating the root-mean-squared mutual inclination of equation (6) (amplitude/$\sqrt{2}$), we arrive at Figure 7b. A small measure of mass group/inclination divergence is present in this constant-spin solution, though

44
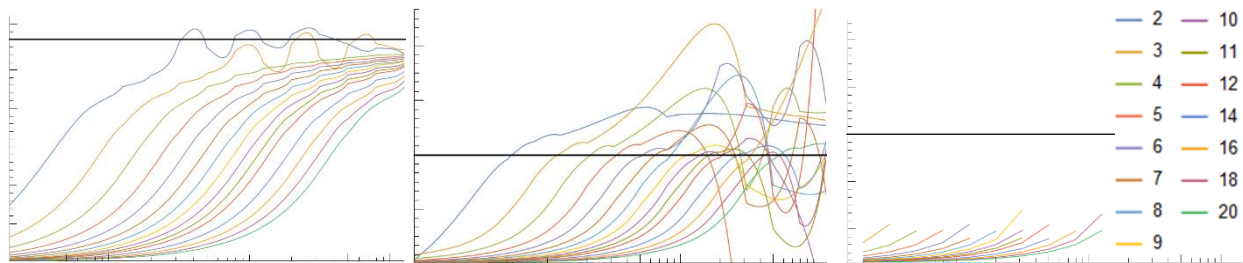
Figure 8. The evolution of a group of systems as stellar obliquity is increased. Each panel represents a "slice" of N-body data at $\beta_*=20°$, 30°, and 50° (left to right). The curves are high order fits of Δi vs $J_{2,0}$, color coded according to a_1/R_*. The systems that would have gone unstable if allowed to evolve past 5Myr create disruptions in otherwise smooth mutual inclination curves. The black line marks where $\Delta i\approx30°$. All systems here are from the $m=5M_\oplus$ subset.

not to the same extent as in the simulated data – the spin down process separates out masses while exciting all systems somewhat anemically. Hence, the RMS of equation (6) may be an approximate predictor of a pair's Δi for the closest-in systems, but will overpredict with more severity as the pair is moved farther out and its mass is increased.

2.3.4 $J_{2,0}$

Although the range of β_* in this experiment was selected to keep systems stable, based on estimated stability boundaries established by Spalding et al. (2018), it still provides us with valuable information about instability prerequisites from system to system. The β_* slices seen in Figure 8, represent systems on the lower edge of stability (20°), in the thick of it (30°), or all fully unstable (50°). In the leftmost panel, systems at $a_1/R_*=2$ and 3 exhibit discordant behavior in their upper $J_{2,0}$ regions; these data points represent systems that did not go unstable on the 5Myr time scale, but did when evolved for a further 2Myr beyond that. Thus, disorderly changes in Δi after smooth growth through low $J_{2,0}$ are indicators that a system is close to or in the middle of chaotic mutual inclination evolution and, given enough integration time, will go unstable. The
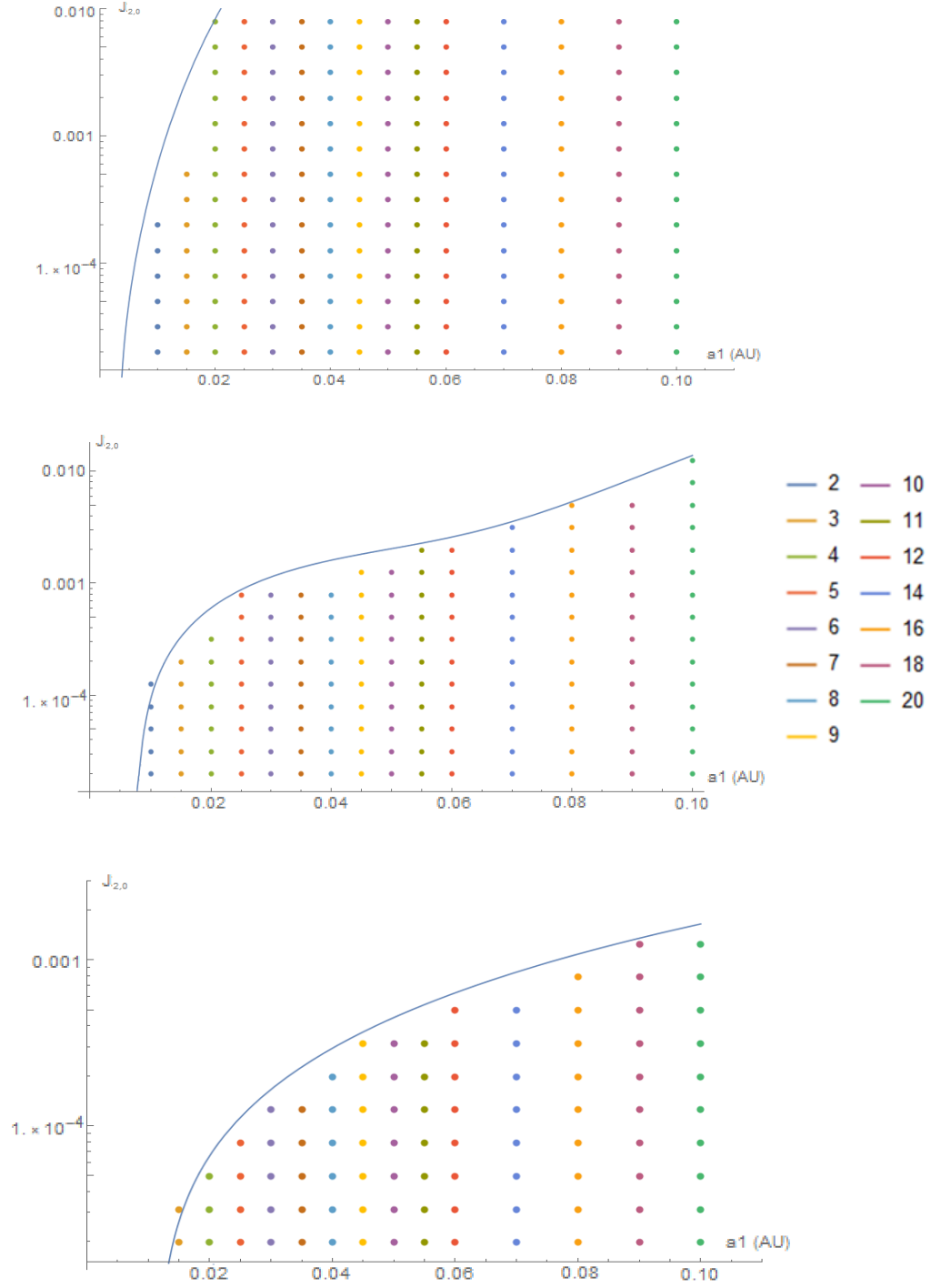
Figure 9. Instability boundaries for surviving systems with $m=5M_\oplus$, from the N-body set. The y-axis is $J_{2,0}$, the x-axis is a_1/R_*. As in the previous figure, each panel contains a "slice" of data at constant β_* (20°, 30°, and 50° top to bottom). All of the systems from Figure 8 appear here, with the exception of those showing signs of long-term instability. The blue curves are approximate fit lines relating a_1/R_* to the critical value $J_{2,0,\text{crit}}$ above which a system with that position and obliquity will go unstable [equations (27)-(29)].

middle panel in Figure 8 even more clearly shows this disorder. At 50° of obliquity, rightmost panel, every system destined for instability has achieved it by 5Myr.

That only the close-in systems start to go unstable at $\beta_* = 20°$ suggests there may be a more subtle relationship between the critical stellar obliquity/$J_{2,0}$ values leading to instability than has been previously reported. Each dot in Figure 9 is a planet pair that showed no signs of instability over the entire integration. The blue curves, expressions for $J_{2,0crit}$ as a function of a_1, are estimated fits of the boundary above which systems do not survive integration. For $\beta_* = 20°$, 30°, and 50°, respectively, these take on the form

$$J_{2,0crit} = -0.0003 + 0.006x + 0.68x^2 + 50{,}000x^4 \qquad (27)$$

$$J_{2,0crit} = -0.0015 + 3.1x^2 - 72x^3 + 550x^4 \qquad (28)$$

$$J_{2,0crit} = -0.00005 + 0.003x + 0.14x^2 \qquad (29)$$

The $\beta_* = 70°$ equivalent to Figure 9 is identical to the $\beta_* = 50°$ panel in that figure, and so the boundary in equation (29) fits both obliquities. It appears that at some point between 30° and 50°, an OTS has reached its maximum destructive potential, and the boundary between stable and unstable is fixed.

It's important to keep in mind that these boundaries cannot be extrapolated beyond the range of a_1 explored in this work. They are intended to illustrate that $J_{2,0crit}$ can vary by several orders of magnitude for very close-in systems, such that the previous estimate of $\sim 10^{-3}$ is valid when $\beta_* = 30°$, but only for the most distant systems at higher obliquities, and only for the closest at lower obliquities. Using these three curves, one may find an approximate $J_{2,0crit}$ for any obliquity between 20° and 50°, for any star-inner planet separation in the designated range,
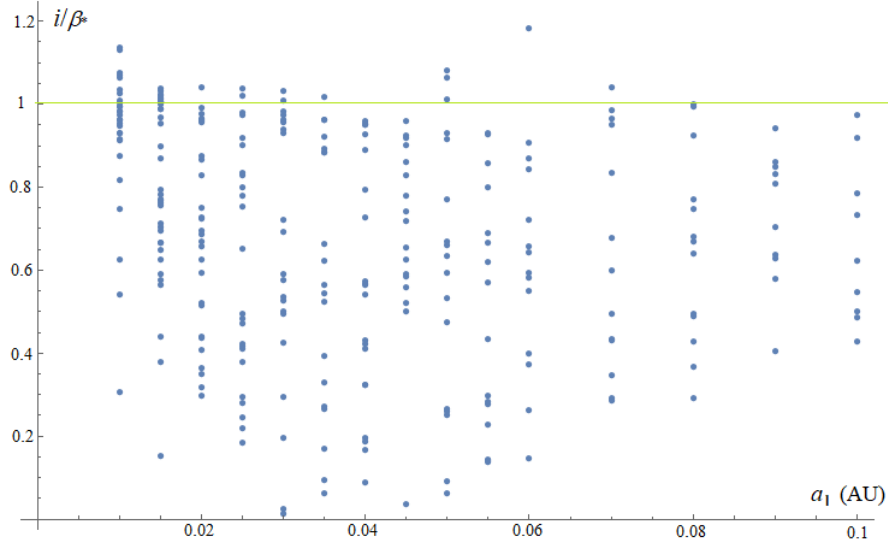
Figure 10. The final orbital inclinations of lone post-instability planets, as a function of a_1. The vertical axis expresses inclination as a fraction of the system's initial stellar obliquity (which also served as the planets' initial orbital inclination). The green line marks planets whose final inclinations remain unchanged. Note that the horizontal axis isn't a measure of the survivor's final semimajor axis, only the initial position of the inner edge of the system.

provided that the two planets are of roughly equal mass close to $m=5M_\oplus$. (This may seem a tall order, but recall that the mean mass of a Kepler system with $R<6R_\oplus$ is at least $4.3M_\oplus$, that masses are fairly similar within a system, and that the inner edges of Kepler systems often fall within the range examined here.)

2.3.5 The Survivors

No mention has yet been made of the planets that are left behind after instability. In general, instability in a multi-planet system leaves behind planets with increased orbital inclinations (e.g. Hansen 2017). Upon inspection of the surviving planets' inclinations, however, I have found that in a majority of cases, instability due to an OTS reduces the final misalignment between star and planet. Figure 10 demonstrates this trend. Most of the points above the green line come from $\beta_*=70°$ systems, the rest from $\beta_*=50°$ systems. This pattern has interesting implications: if a single-tranet system is truly single, made lonely by an OTS, then the obliquity

48

of the modern system will read as lower, potentially much lower, than its initial obliquity. Winn et al. (2017) observed that single-tranet and multi-tranet systems both appeared to have low obliquities; on the face of it, this seems to put a damper on the viability of the OTS mechanism in creating single-tranet systems, as it does so most effectively at higher obliquities than Winn et al. reported. However, these results reduce the damping somewhat by opening up the possibility that large spin-orbit misalignments early in a star's life can lead to low misalignments and single-tranet systems later on. More investigation, using systems of higher multiplicity, is needed to determine whether single-tranets are always accompanied by a drop in spin-orbit misalignment, or if this effect is different when multiple planets are lost from a system.

2.4 Conclusions

The OTS mechanism is an area of celestial mechanics heretofore explored only for unique, individual Kepler systems. While previous works (Spalding & Batygin 2016, Spalding et al. 2018) mapped out the effects that physically-informed ranges of β_* and decaying J_2 have on transit numbers in these individual systems, it was not well known to what level the properties of the systems themselves affected their fates. This chapter set out to improve our understanding of this mechanism's dynamical signatures, as well as the initial conditions that ultimately drive a planetary system to instability. I put forth the following conclusions:

1. An OTS excites larger mutual inclinations for the shortest-period planet pairs. Indeed, it seems to reproduce quite well the data at the core of Dai et al.'s (2018) paper. The authors incorporate an additional factor into their study which has not been included in mine: they draw a distinction between small-a_1 planet pairs with large mutual separations and more distant, closely packed systems – the boundary between these two groups appears as the green box situated

around $a_1/R_* = 5$ in Figure 6a. The innermost planets in former group can be loosely categorized

as USPs (see section 2.1) the formation histories of which are an area of active research (e.g.

Petrovich et al. 2018, Pu & Lai 2019, Li et al. 2020). Because planets in these USP pairs are

physically farther from each other than typical Kepler pairs (more than the 20 mutual Hill radii

used in this work), they aren't as strongly coupled, and thus respond more to dynamical stimuli

than strongly-coupled pairs. Had I chosen a larger spacing for the planet pairs closer than 0.025

AU from their star, they likely would have ended up with larger mutual inclinations and possibly

a higher rate of instability, increasing the already substantial inclination spread in Figure 6b and

thinning out the data below the transit line.

It has been suggested in the aforementioned works (and in the assumption statement at

the beginning of this chapter) that USPs migrated inward from farther out in their systems. Their

final inclinations and survival probably depend on the timing of this migration relative to the age

of the star; the longer it takes them to move in, the weaker the OTS's quadrupole moment will be

once they get there, and the smaller their inclinations (Pu & Lai 2019). We might therefore

expect that inner planets with relatively low Δi in the USP region of Figure 6a had finished

migrating inward some time after their star had begun to spin down, whereas more excited USPs

fell into place more quickly.

2. An OTS with decaying spin rate excites lower-mass systems somewhat more than

higher-mass systems, which could lead to a slight preference for lower masses in single-tranet

systems. This is in contrast with findings in Johansen et al. (2012), which showed that singles

tend to have larger radii than multis. However, no distinction was made between the population

of lonely hot Jupiters and the collection of smaller planets first reported on in Lissauer et al.

(2011). Weiss et al. (2018) remedied this and concluded that, for sub-Neptunes in the Kepler data

set, there is no difference in average radius between singles and multis. The remainder of the single-tranet population consists of hot Jupiters and distant ice planets, both with histories likely very different from the Kepler sub-Neptunes.

Further, Spalding & Batygin (2016) demonstrated that the smallest planets are destroyed first when a given system goes unstable. Had I retained the average mass parameter m in the lowest-mass systems in my simulations, but allowed the planets in a pair to be different sizes, the larger planet would likely survive instability, perhaps weakening the already weak preference shown here for low-mass single tranet systems. Regardless, the OTS-planet mass relationship, while stronger than in the constant spin scenario, is still relatively minor.

3. The planet that survives OTS-induced instability in a system of two planets almost always realigns somewhat with its star after instability. This can partially, if not entirely, erase the star's initial obliquity if no other planets exist in the system, leading to low modern obliquities in single-tranet systems. This may partially explain the similarities in obliquities among singles and multis as reported by Winn et al. (2017). That hot Jupiters continue to exhibit strong obliquities, while smaller singles do not, suggests that hot Jupiters form/migrate without giant, nearby neighbors to potentially scatter off them and change their misalignment.

One interesting point that cannot be explained by the work done in this thesis is the lack of high-obliquity Kepler multis. All OTS investigations have allowed for combinations of high β_* and low $J_{2,0}$, which has been shown to have very little influence over an initially coplanar multi-planet system; if such combinations exist, we might expect to see multis with extremely tilted stars that never reached high enough spin rates to excite their systems. This does not seem to be the case. Perhaps there's an association between stellar obliquity and spin rate – perhaps all misaligned stars are oblate enough to excite the planets closest to them? This also doesn't seem

to be the case: Batygin & Adams (2013) concluded that stars with low to moderate spin rates, not high ones, are more likely to retain their misalignment after their disks have dispersed. It may take further study of the intricate physics of misalignment to show that high β_*, low $J_{2,0}$ systems don't exist, or that well-aligned Kepler multis occupy only the low β_*, low $J_{2,0}$ quadrant of the obliquity/oblateness box. Perhaps an OTS with low O and high T occurs under conditions that also favor the formation of hot Jupiters. Though beyond the scope of this thesis, it is certainly a question worth addressing in the future.

4. In addition to the above observations, I have more fully explored the parameter space of the OTS mechanism. My results allow us to make predictions about the survivabilty of a two-planet system based on a set of initial conditions, as well as the architecture of surviving systems.

Concurrent with the data analysis phase of this chapter, a separate group arrived at the main part of conclusion (1) independently (Li et al. 2020). My work diverges from theirs in that it considers full spin-down dynamics, while the methods in that work are almost purely analytical. Though quantitatively different, our combined work makes a stronger case for the OTS mechanism than either work does alone.

The work presented in this chapter lends itself to a number of additional questions, not least of which is: what happens when you throw more planets into the mix? Do they stabilize each other against excitation? Inspection of the Dai data set hints that planet pairs that are part of larger systems do lie fairly close to the horizontal axis in Figure 6a. If N>2 systems are flatter than N=2 systems, they would appear to fully transit more often than N=2 systems. What kinds of transit frequencies can we expect from higher-multiplicity systems? How does that relate to transit multiplicities in our current data? With these questions, let's proceed to the next chapter.

CHAPTER 3

BRITTLE GROUPS: N>2

3.1 Reintroduction

Nearly ten years have passed since it was first reported that the Kepler data contains an

unexpectedly high number of single-tranet systems (Lissauer et al. 2011). Our database of

confirmed exoplanets has only grown since then, supplemented by other telescopes (e.g. Keck;

Marcy et al. 2014) and other detection methods (e.g. radial velocity; Ford et al. 2011, Bryan et al.

2016). One is led to wonder if any of the original Kepler singles have been found to possess non-

transiting neighbors that impose transit timing variations on the single, or are large enough to

influence the host star itself. According to the database[4], as of April 2020, only a fraction (about

30 in several thousand) of *all* transit-detected singles, across multiple observatories, have

additional planets that were found using non-transit methods. Giant planets comprise more than

half of this set; the other part largely consists of small singles with radial velocity companions.

Two systems (KOI-124 and Kepler-19) had singles with enough variation in their transit timing

that an additional planet could be confirmed in the system. For the most part, Kepler singles have

remained in the singles club, gathering more members as observations go on.

The RV method is best at detecting large planets, preferably with short orbital periods.

The TTV method is favored when searching for planets that are still fairly well aligned, closely

packed, and bordering mean-motion resonances, but just out of transit sight. Neither of these is

ideal if one is looking for small, inclined planets in a single-tranet system. "Inclined" is, of

course, a relative term – if a multi-planet system does resist OTS excitation more than a lone

---

[4] https://exoplanetarchive.ipac.caltech.edu/
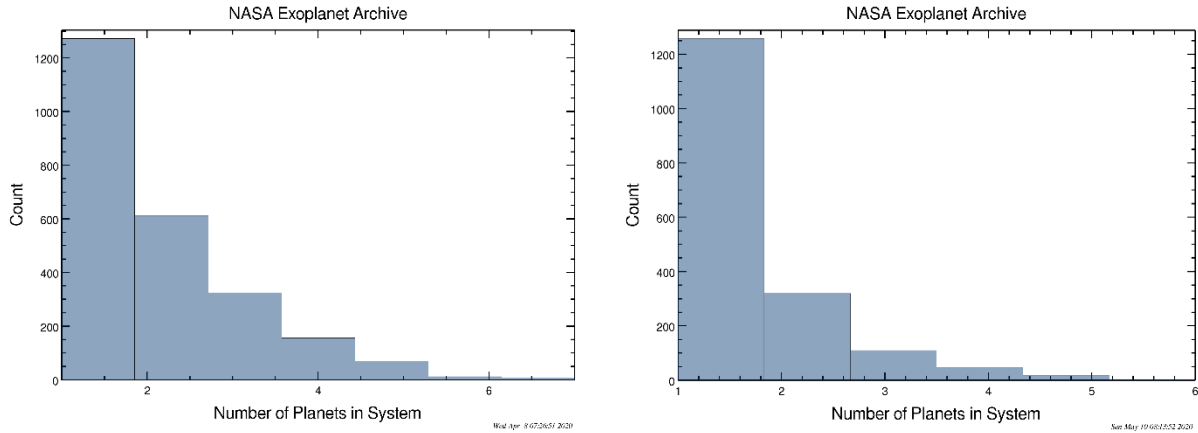
Figure 11. Histograms of current exoplanet data. **a)** The number of planets that are part of N-planet systems, and **b)** the number of systems containing N planets, from N=1 to N=6. Singles dominate the population at both levels.

planet pair does, then it might be more easily detectable by TTV or transit. The low number of transiting singles with TTV neighbors implies otherwise. This is where our knowledge about OTS systems fails us: we know that a system of multiple planets will go unstable before it starts looking like a single-tranet system (Spalding & Batygin 2016, Hansen 2017, Spalding et al. 2018), but the number of survivors and their final inclinations after OTS instability have not been thoroughly examined.

Weiss et al. (2018) confirmed that the majority of Kepler sub-Neptunes are still singles. While they looked at a smaller set of data than is currently available, an inspection of the larger set tells the same story: the proportion of singles among all planets is roughly 0.5 (Figure 11a), and the proportion of single-tranet systems among all systems is accordingly higher (about 75%, Figure 11b). All of our questions about underlying versus apparent multiplicity, the creation of singles, and the possible architectures of multi-planet systems are all still valid.

At this point, it is valuable to point out that the "dichotomy" part of the Kepler dichotomy is somewhat subtle. Lissauer et al. (2011) reported that the Kepler multis alone are much easier to fit a suitable orbital inclination distribution to than both multis and singles together – it

seemed that Kepler multis and singles had completely separate, "dichotomous" inclination distributions. However, recent works (Zhu et al. 2018, Sandford et al. 2019, He et al. 2019) have proposed inclination distributions that reproduce both multis and singles. They maintain that dynamical 'heat' increases inversely with true system multiplicity, and that two separate inclination distributions are consequently not required to describe the Kepler data set. Unfortunately, this resolves the Kepler dichotomy only in a semantic sense; there still firmly exists a surplus of singles, now suggested to be part of undetected multis, and it begs explanation. Moreover, as has been demonstrated time and again (e.g. Ford & Rasio 2008, Johansen et al. 2012, Spalding & Batygin 2016, Hansen 2017, Spalding et al. 2018), instability is a key player in dynamical heating and transit reduction – how often is a single truly single, and how often can it have the hidden neighbors that recent studies claim it to have? Does the OTS mechanism naturally lead to successively weaker excitation in higher-N systems?

In the previous chapter, I confirmed the hypothesis that close-in planet pairs become more mutually inclined by an OTS than distant pairs do. Most pairs exhibited stability on large time scales with final mutual inclinations as large as ~35°. In this chapter, I combine N=2 data with simulation data from N=3, 4, 5, and 6 systems and inspect the relationship between initial multiplicity N_i, final multiplicity N_f, and number of transiting planets N_T in OTS systems. I determine the resilience of N>2-systems to OTS excitation, establish the requirements that must be met in order for the OTS mechanism to explain the excess of single-tranet systems in the Kepler set, and comment on the viability of these requirements in light of current observations and the results from chapter 2.

All of my assumptions from the previous chapter carry over to this one.

3.2 Methods

The basic setup for this experiment is identical to the previous chapter's, with a few alterations made to save computation time and maintain physical accuracy. A half-set of innermost semimajor axes is used, based on equation (12):

$$\frac{a_1}{R_*} \in \{2, 4, 6, 8, 10, 12, 16, 20\} \tag{30}$$

The stellar parameters are the same, so a_1 again ranges from 0.01 to 0.1 AU. Successive semimajor axes calculated using equation (13). However, Weiss et al. (2017) reported that high multiplicity Kepler systems ($N \geq 4$) are more closely packed than N=2 and N=3 systems. It's possible that extra non-transiting planets are present between known planets in these Kepler systems, such that observed planet-planet separations misrepresent the true organization (and multiplicity) of Kepler systems, particularly in the low-multiplicity cases. As shown by Fang & Margot (2013), though, at least 30% of 2-, 3-, and 4-planet Kepler-like systems with observed spacings and multiplicities are not long-term stable if extra unseen planets exist between extant orbits. This proportion increases with increasing system multiplicity, and is only a lower limit on the proportion of Kepler systems that are "dynamically packed" – a.k.a. do not and cannot hold additional undetected intra-orbit planets, and so are likely genuinely separated by the observed distances. In keeping with the observations of Weiss et al. (2017), then, separations of 20, 15, 14, and 13 mutual Hill radii are used for the N=3, 4, 5, and 6 sets of simulations, respectively. As there was only a small difference in excitation and instability rates across the masses assigned in chapter 2, I use only the middle mass ($5M_\oplus$) from that set in these simulations. Five $J_{2,0}$ are drawn evenly from the lowest 10 values from equation (18):

$$J_{2,0} \in \{3.14 \times 10^{-5}, 7.89 \times 10^{-5}, 1.98 \times 10^{-4}, 4.98 \times 10^{-4}, 1.25 \times 10^{-3}\} \tag{31}$$

Stellar obliquity is again taken from the full range in equation (17). All simulations – a total of 960 -- are run for 5Myr or until only one planet remains.

At every point for the final 10,000 years in a simulation, the mutual inclination between each surviving planet pair is calculated using equations (23)-(25). The mean of these mutual inclinations is also recorded. Based on these individual instantaneous mutual inclinations, the maximum possible transit number at that point in time can be calculated using equation (3) and the method implemented in Spalding & Batygin (2016) and Spalding et al. (2018). Starting with the entire group of surviving planets (p total planets), every mutual inclination between pairs in the group is checked against the transit criterion in equation (3). If all pairs satisfy the criterion, then the maximum transit number at epoch is p. If any planet pair fails to satisfy the criterion, it's impossible to observe p transits in this system. The required transit number is then lowered to p-1 and new groups are made out of all possible combinations of p-1 planets; each of these groups is checked via the above method, and if all of the pairs in at least one group satisfy the transit criterion, then the maximum transit number at epoch is p-1. If not, the next lowest transit number is sought out, and the process repeats until some sub-group of the surviving planets passes the test. The three calculations – mutual inclinations, mean mutual inclination, and maximum transit number – are performed at each time step and averaged over at the end. In this chapter, "the mutual inclination of an N=n system" refers to the mean-mean-mutual-inclination ($\Delta\sigma$) associated with a system, as opposed to the collection of average individual Δis. If only one planet survived at the end, the mean-mean-mutual-inclination $\Delta\sigma$ is set equal to its final orbital inclination. Note that in the surviving N=2 case, only one planet pair exists to be averaged over, so $\Delta\sigma$ and Δi are the same. Only the N=2 systems with initial conditions from the above sets are used in this chapter.
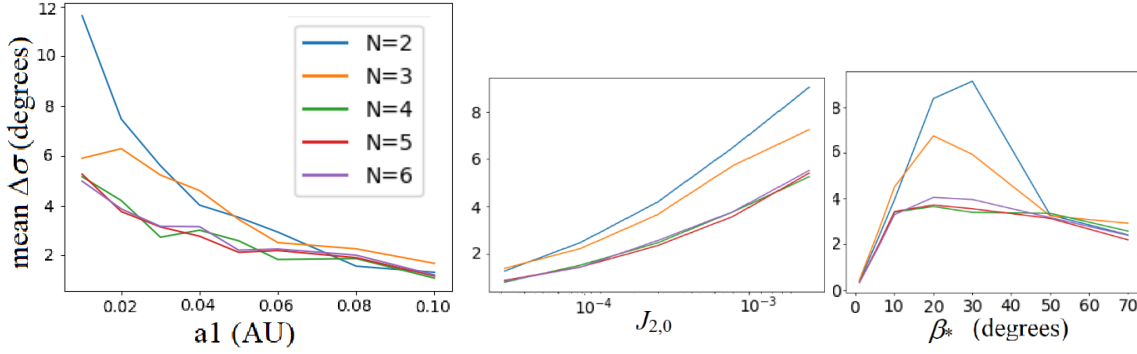
Figure 12. Mean final mutual inclinations for completely intact N-planet systems, as functions of a_1 (left), $J_{2,0}$ (middle), and β_* (right). Each point is the average of about 20 simulated systems.

3.3 Results and Discussion

3.3.1: N>3 Systems Are Stiff

I will first address the population of systems that remained completely intact throughout the simulation (same final and initial multiplicities). To create Figure 12, for each N_i, all of the $\Delta\sigma$ for systems with a given value of the relevant parameter were averaged together. All three panels generally demonstrate a tendency for excitation to decrease with increasing multiplicity. The $N_i=2$ and $N_i=3$ cases were constructed almost identically – $N_i=3$ is simply an $N_i=2$ system with another planet tacked on to the outside edge. When comparing these two sets of curves, it appears generally true that extra planets in a system makes it more resistant to excitation. The story is a bit more complicated at the $N_i>3$ level: although separation between planets was decreased while extra planets were added, neither of these actions seemed to make much of a difference in the final mean inclination in $N_i=4$, 5, or 6 planets. It seems logical to guess that either would result in stronger resistance to excitation, and so together make a system very resistant. However, the sudden jump in mean inclinations between the low (2 and 3) multiplicities and the high (4, 5, and 6) multiplicities, accompanied by a sudden jump in planet separations ($20R_H$ to about $14R_H$), points to planet separation being a much stronger determining

factor than multiplicity in a system's final architecture. This makes sense: an extra planet placed

far away is likely going to exert less force than a nearby planet moved in closer. The exact cause

for the tight clustering among $N_i > 3$ systems is unclear – six-planet systems still have the most

distant outer edges, which would respond sluggishly to OTS excitation, keeping $\Delta\sigma$ low. Perhaps

there's a 'resistance limit' against outside influence that high-N_i Kepler systems have attained.

More research into this is required to elucidate close-packed systems' response to external

perturbers. Nevertheless, when taken as a whole, it appears that the more planets occurring in a

young Kepler-like system, the less an OTS will be able to excite it, largely thanks to the

association between multiplicity and small planet-planet separations. The signal is strongest as a

function of $J_{2,0}$, at moderate values of β_*, and in systems with an inner edge within about

0.07AU.

3.3.2: The Bigger They Are, The Harder They Fall

Evidently, high-N_i systems take more effort to excite to higher inclinations. Does this

resilience also apply to instability? Broadly speaking, the values of β_* and $J_{2,0}$ associated with

instability in the N>2 cases are about the same as those that resulted in instability in the N=2

cases, if a little lower. The instability rate in this data set is only slightly higher – 15% in the N=2

cases, around 20% in the N>2 cases, with no further multiplicity dependence in the latter set of

cases. In these ways, high-N_i systems are somewhat *less* resilient to instability than lone planet

pairs are. The most striking distinction between low-N_i and high-N_i systems, stable versus

unstable, can be seen in Figure 13. The set of systems featured represent a typical instability

outcome: upon crossing the threshold from stable to unstable, a high-multiplicity system will
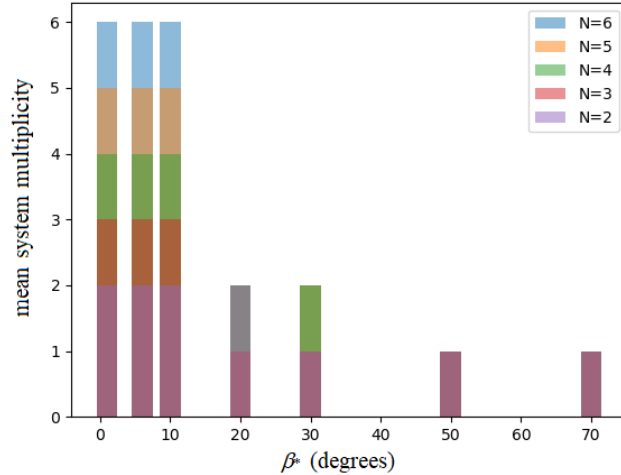
Figure 13. A histogram of the final multiplicities of N-planet systems when evolved around an OTS with different stellar tilts. This is a slice of data taken at $a_1/R_*=2$ and $J_{2,0}=1.98\times10^{-4}$, a mild value for $J_{2,0}$.

lose at least half of its planets, if not all of them. Post-instability systems are further estranged from stable systems by their dynamically heated orbits (Figure 14a), almost always appearing as single-tranet systems instead of smaller multis (Figure 14b). Lower surviving multiplicities combined with larger inclinations seems to force young Kepler-like multis into a nearly binary final state: either the system stays whole, and appears whole, or it loses parts of itself and appears single (Figure 15). For every N_i in Figure 15, the most frequent outcome was intact coplanarity (between 60% and 80%, lowest for $N_i=6$ and increasing with decreasing N_i). The second-most frequent outcome was true singleness (10-15%) or a pair appearing single (10% for $N_i\geq5$).

These pieces come together to form an interesting whole. A Kepler-like multi ($N_i>2$) orbiting an OTS at small distances will most likely evolve into a dynamically hot, highly reduced system or a dynamically cool, intact multi. The outcome depends more sensitively on stellar obliquity than in the $N_i=2$ case, especially for the closest-in systems; a few degrees' tilt one way or the other could mean the difference between a lifetime of companionship and a Red Wedding. All-or-nothing planet loss was also encountered in Spalding & Batygin (2016), but only briefly acknowledged; here I add robustness to that observation.
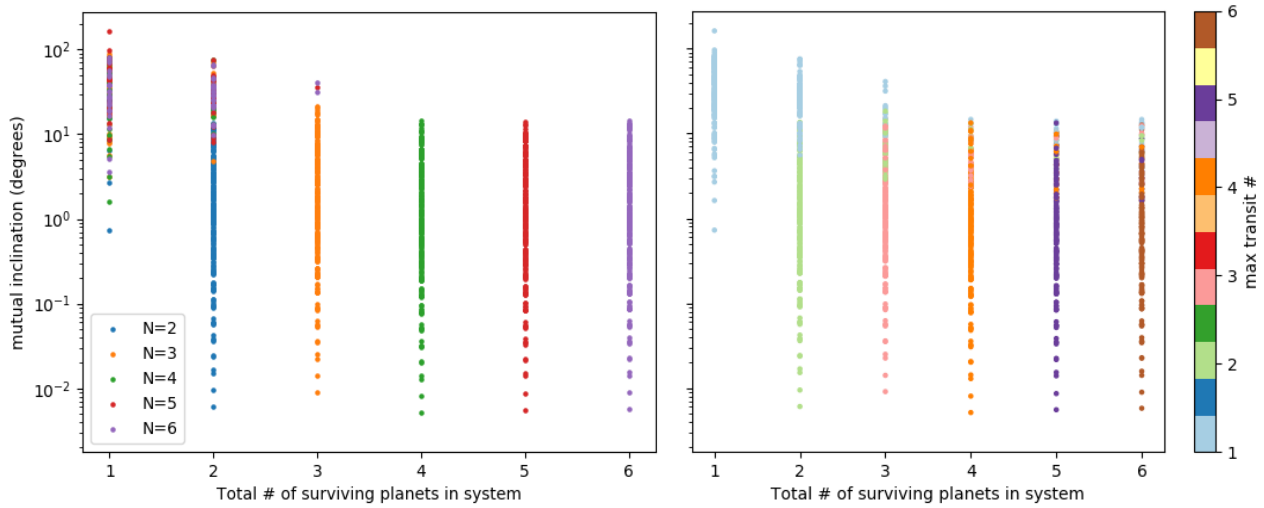
Figure 14. $\Delta\sigma$ vs true final multiplicity N_f, **(a)** colored according to initial multiplicity N_i, and **(b)** colored according to final transit number N_T.
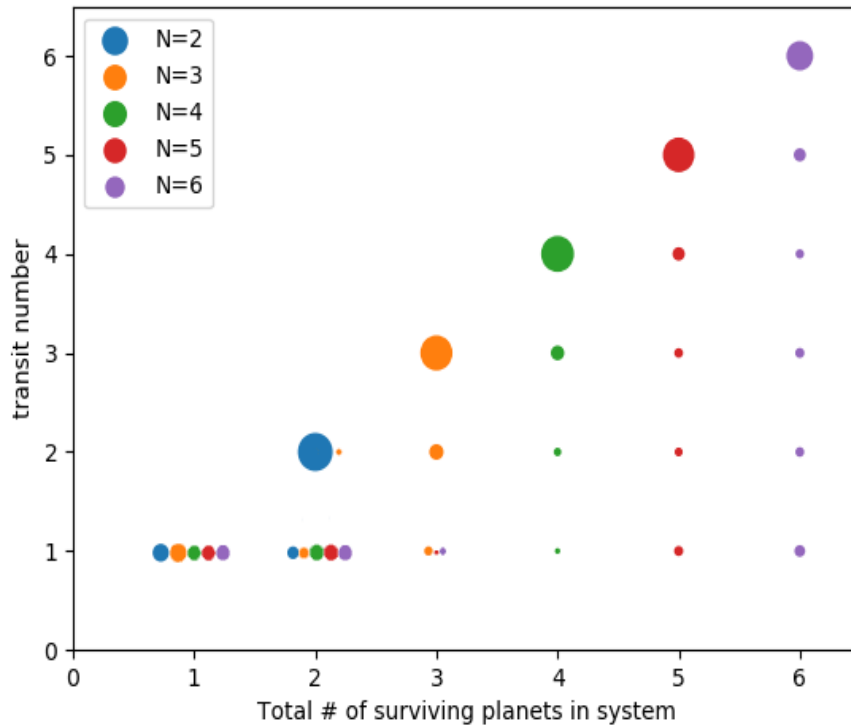
Figure 15. A frequency plot of N_T versus N_f. Each dot is colored by initial multiplicity N_i and sized according to the percentage of systems that ended up with the given combination of N_f and N_T.
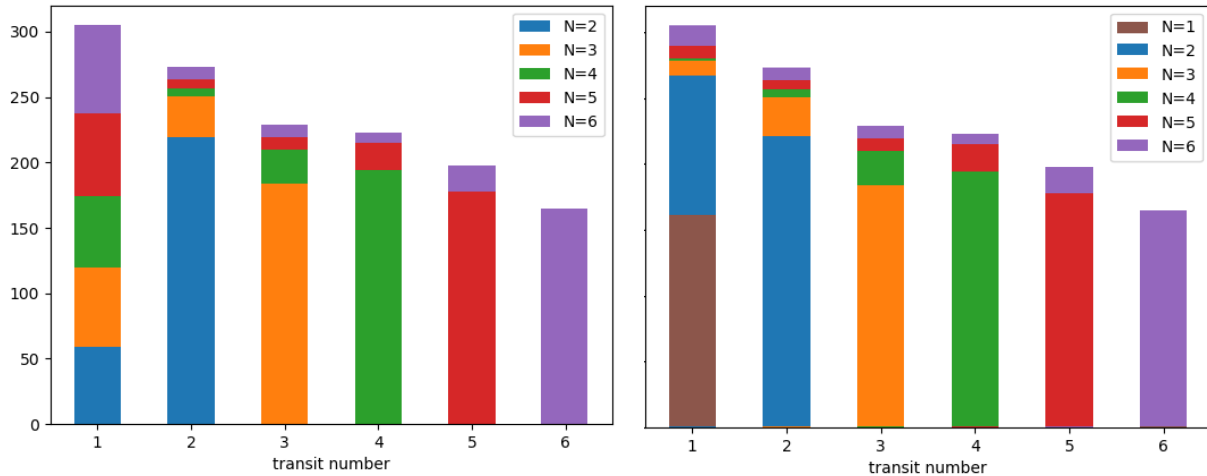
Figure 16. A histogram of final maximum transit number, colored according to the original (left) and final (right) number of planets in the system.

3.3.3: We're Gonna Need a Bigger Tilt

With a basic grasp of the relationship between N_i, N_f, and N_T under the influence of the OTS mechanism, we can puzzle together a rudimentary answer to the question, "could OTSs be the cause of the Kepler dichotomy?" It's important to keep in mind that the initial conditions on which this data set is based were not selected to encapsulate all of Kepler parameter space – most Kepler systems' inner edges are further from their host than mine. The mean period of the innermost edge of a Kepler system is about 7 or 8 days, equivalent to 0.07AU around a Sun-like star, or $a_1/R_* = 14$. In addition, the initial β_* set was chosen mainly to ensure that the full possible range of Δi could be accessed while minimizing instability. The true rates at which young Kepler-like multis lose planets and/or have their transit number reduced will be different than those appearing in this work, although real systems should still exhibit the bimodality of fates that simulated systems do.

Figure 16 tabulates final transit numbers according to initial multiplicities -- it's is the equivalent of rotating Figure 15 90° clockwise, combining all of the dots in each column by

color, and condensing them into a bar. This histogram doesn't resemble Figure 11b very closely because during the input selection process, I've assumed that young Kepler-like systems have planet multiplicities drawn from a discrete uniform distribution between 2 and 6; in reality, we've detected very few high-multiplicity systems. The bars in Figure 16 require scaling in order to more closely match Figure 11b. In turn, this scaling will tell us how many systems of each N_i are needed to reproduce the transit counts associated with the Kepler dichotomy, and whether the inputs I've selected can cause instability frequently enough to create a large population of singles.

If we assume that the relative rates at which different N_i systems turn into each N_T system are fixed (i.e. would be about the same for larger data sets – again, this may not be exactly true, but bear with me for argument's sake), Figure 16 can be translated into a set of linear equations and scaled to match the current set of transiting Kepler data (Figure 11b). For example: if the total number of systems that started with $N_i=5$ (red bars) is X_{5i}, then some proportion of X_{5i} is systems that have five maximum transiting planets (the biggest red bar, comprising most of $N_T=5$) – call that proportion $P_{5i,5}$, and call the total number of systems in the biggest red bar $N_{5i,5}$. So

$$X_{5i}P_{5i,5} = N_{5i,5}.$$

(32)

The rest of the $N_T=5$ bar is a sliver of purple $N_i=6$ systems. The number of initially 6-planet systems with maximum transit number 5 is $N_{6i,5}$. As above, we can relate the total number X_{6i} of initially 6-planet systems to the number that appear to quintuply transit:

$$X_{6i}P_{6i,5} = N_{6i,5}$$

(33)

63

The total number of systems Y_5 in the $N_T=5$ bar is the sum of $N_{6i,5}$ and $N_{5i,5}$. Substituting in equations (32) and (33):

$$X_{5i}P_{5i,5} + X_{6i}P_{6i,5} = Y_5 \tag{34}$$

Reducing the height Y_5 of the $N_T=5$ bar to match the equivalent bar in Figure 11b requires decreasing X_{5f} and X_{6f} by undetermined amounts. These amounts can be constrained when the full set of equations is constructed via the same method. If there are 1257 single-tranet, 320 double-tranet, 110 triple-tranet, 46 quadruple-tranet, 17 quintuple-tranet, and 3 sextuple-tranet systems in Figure 11b, then the system of equations relating initial multiplicities to final maximum transiting multiplicities is

$$X_{1i} + 0.212X_{2i} + 0.220X_{3i} + 0.193X_{4i} + 0.229X_{5i} + 0.240X_{6i} = 1250$$

$$0.788X_{2i} + 0.116X_{3i} + 0.021X_{4i} + 0.025X_{5i} + 0.032X_{6i} = 320$$

$$0.664X_{3i} + 0.093X_{4i} + 0.032X_{5i} + 0.036X_{6i} = 110 \tag{35}$$

$$0.638X_{4i} + 0.075X_{5i} + 0.029X_{6i} = 46$$

$$0.638X_{5i} + 0.072X_{6i} = 17$$

$$0.591X_{6i} = 3$$

where the coefficients in both sets have been rounded for display. The resulting scaled histogram is shown in Figure 17.

Too few systems went unstable in my data to fill the entire single-tranet quota – only about 10% of the single-tranet systems in Figure 17 were created by exciting a system of multis. In addition to a collection of young multis, over 1000 of the Kepler-observed systems would need to be born naturally single, making an OTS ultimately responsible for only a small portion
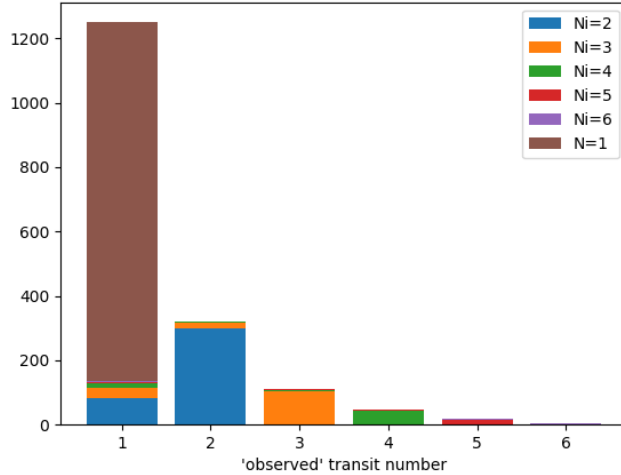
Figure 17. The spread of initial multiplicities required to reproduce the Kepler dichotomy by the OTS mechanism, based on transit rates from N-body simulations. 1116 singles, 380 doubles, 155 triples, 64 quadruples, 26 quintuples, and 5 sextuples are needed in this scenario, where transit reduction is infrequent.

of all single-tranet systems. This is to be expected from a data set that was chiefly designed to avoid instability while probing parameter space as widely as possible.

There are a number of ways to considerably boost the instability rate among planetary systems: one could push systems' inner edges close to their host, or increase the host's quadrupole moment, or perhaps decrease the planets' masses and increase their separations (though the last two may not boost instability "considerably"). Any of these would be in violation of observation, however – Kepler systems are often more distant from the star than mine, hosts' $J_{2,0}$ rarely exceed the upper limit enforced in this chapter, and Kepler masses and separations are well-documented and have already been incorporated in my simulations. The obvious answer is that I have underrepresented stellar obliquity. β_* is still the most mysterious parameter of all, and as seen in the previous section, just few degrees' tilt can mean the difference between long-term companionship and a community tragedy.

The most distant systems to go unstable in this data set did so at obliquities above 30° -- this limit decreases to somewhere in the teens for the closest-in systems. To boost instability

rates at all levels, then, would require stellar tilts distributed with a moderately high mean. I observed in chapter 2 that, in almost all cases, the sole surviving planet of an instability erases part of its spin-orbit misalignment by dropping to a lower inclination; the same trend is found across all OTS systems in this data set (Figure 18), where 82% of survivors settled into lower-inclination orbits after their last remaining neighbor was destroyed. Single-tranet systems are truly single most of the time (Figure 16b); the remainder are very likely to be doubles on highly mutually inclined orbits (Figure 14b). The oscillations in inclination caused by these misaligned pairs may also help conceal the host's true original obliquity. Due to these effects, it is clear that the spin-orbit misalignments we have measured and will measure likely do not reflect the true distribution of initial misalignments that contribute to the OTS mechanism.
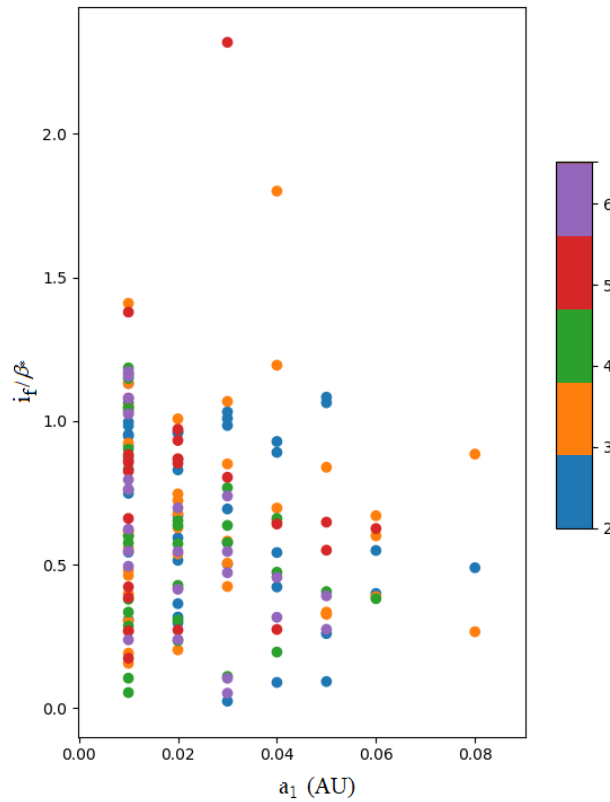
Figure 18. The final orbital inclinations of the lone survivors of instability, scaled by initial stellar tilt and colored according to initial system multiplicity. As in Figure 10, the horizontal axis represents the initial inner edge of the system.

3.4 Conclusions

In a universe where all planetary systems are born compact, with similar masses and close to their star, the only way they can become a Kepler single with hidden neighbors is to experience inclination excitation between planet pairs. A Kepler single with many hidden neighbors is a science fictionist's dream – a central star surrounded by a web of orbits. The reality seems to be much less fantastical. The purpose of this chapter was to investigate the way that systems born with more than two planets respond to inclination excitation while in orbit around an oblate, tilted star, and to use this knowledge to move us one step closer toward identifying the source of the excess of Kepler singles. I conclude the following:

1. Multi-planet, Kepler-like systems with N>3 are less excitable in mutual inclination than low-multiplicity systems, assuming that the multiplicity/spacing data we've gathered from *Kepler* accurately represent true system spacings. This is likely because they are more closely packed than low-N systems; close neighbors bolster each other against outside perturbations (Becker & Adams 2017). Moreover, the N>3 systems exhibit very similar levels of mutual inclination excitation across multiplicities, though intuition expects their resistance to increase as planets are added and separations are decreased. Most of the planet pairs in the Dai set that are part of reportedly higher-multiplicity systems all demonstrate low excitations, in agreement with this result. Previous work (Zhu et al. 2018, Sandford et al. 2019) conclude that mean inclinations in the Kepler systems increase inversely with multiplicity; while is true in the broadest sense that an OTS excites mutual inclinations at the lowest multiplicities more than at the highest, the transition is not smooth.

2. A Kepler-like system with more than two planets will lose at least half, if not all but one, of those planets if it encounters instability. While it's not news that close-packed multis go

thoroughly unstable (Spalding & Batygin 2016, Pu & Wu 2015), this result is important when combined with the previous point. Multi-planet systems that go unstable are bound to nearly binary destinies: most will remain flat enough that, from the perfect vantage point, all of their planets can be seen to transit, while most of the rest will almost completely fall apart and acquire large mutual inclinations with any surviving neighbors. The states in between occur less frequently.

If a single-tranet system is almost always the product of instability, and if instability always reduces the number of planets in a system to a maximum of three, but usually only one or two, then the Kepler singles' prospects for companionship are looking grim. In light of this, it seems probable that most of the planet pairs in the Dai set without additional reported neighbors are genuinely just pairs, assuming that they originate from an OTS-evolved system. This is again in contrast with Zhu et al. (2018) and others that single-tranet systems are mostly part of excited multi-planet systems.

3. The OTS mechanism could lead to the creation of a large number of single-tranet systems if conditions favor instability more than they do under the conditions set up in this chapter and the previous one. Stellar obliquity is the wild card in this situation – it has been suggested (Spalding & Batygin 2015) that any possible degree of misalignment is achievable through disk torqueing, so it's conceivable that hosts are tilted enough (>30° for distant, ≳15° for very close systems) often enough to boost instability rates beyond those recovered in this work. At first glance, this seems unlikely in light of recent observations of stellar obliquities in Kepler singles and multis, which show little difference between the two populations, with a mean at or below 20°. However, conclusion (4) in the previous chapter has only been strengthened by simulations of higher-multiplicity systems – regardless of initial system multiplicity, the spin-

orbit misalignment between a star and the sole surviving member of its unstable system will appear reduced relative to its original value. Thus, if the initial obliquities of host stars are widely spread, they'll be somewhat compressed and pushed down toward lower – perhaps considerably lower – values post-instability. Where before the OTS mechanism's prospective power was restrained by reports of low obliquity in singles, it is now somewhat freer. It depends now on the relationship between initial and final misalignment in the OTS regime, a topic worth further investigation.

CHAPTER 4

SUMMARY

4.1 Recapitulation and Predictions

In chapter 2, we opened the door onto a crowd of planetary pairs whose stars were all misaligned and fast-rotating in their youth – a larger crowd than we'd ever met before. From this crowd we picked out patterns across couples: the ones that lived close to their stars had larger mutual inclinations, seemed a little more distant from each other. The smaller ones also seemed more misaligned, and there were fewer low-mass pairs in the crowd, though only by a bit in both cases. By asking around, we learned about the couples who couldn't make it to the party of survivors because they had broken up; we saw trends, we mapped out the properties of young host stars that put strain on planet pairs to the point of instability. It was confirmed that the unstable couples had all reached the same breaking point by different means, a breaking point previously predicted based on a smaller group of data and some theory. We asked about the planets left behind after instability – most of the time, they had realigned somewhat with their star after everything was said and done. Without having prior knowledge of the situation, one might look at a single and its star and not know whether the potential for instability had ever existed.

In chapter 3, the multis came in. They all seemed less susceptible to perturbation by their host star compared to the pairs – particularly the fours, fives, and sixes. The intact groups were all fairly well-aligned. However, they showed us that they were also more sensitive to upset than the pairs – an instability among them causes many members to leave, leaving at best a triple, possibly a pair, all made more inclined away from each other by the event. We learned that most of the time, a multi almost completely self-destroys and became a single which, like the other

70

singles, usually falls onto a lower-inclination orbit. Current observations of singles and multis find low obliquities in both sets, which suggests that these lonely singles may be good at concealing their turbulent histories.

If future observations of stellar obliquities in systems of Kepler singles continue to yield low (<~30°) misalignments, this obliquity-erasing behavior could be the essential factor that lends credence to the mechanism discussed in this thesis. Assume for now that initial spin-orbit misalignments are evenly distributed between 0° and 90° -- perhaps weighted toward the low end, taking into account that certain physics in the disk-hosting stage do operate to realign star and planets, so call the mean misalignment 40° or so. As demonstrated in this work, 40° is sufficient to cause instability in most close-in Kepler-like systems, and should increase the rate of instability among multis above the conservative rates simulated in chapter 3. Based on the apparently randomly scattered final singleton inclinations in Figure 18, I tentatively predict that stellar obliquities in Kepler singles will be observed with a mean of around ½ the mean of the true distribution of initial stellar obliquities. This puts the observed mean misalignment in Kepler singles at around 20°, which is the estimated average observed obliquity among Kepler singles and multis as put forth by Winn et al. (2017).

The two most common outcomes for a multi in orbit around an oblate, tilted star are intact and coplanar, or single/surviving as a pair and appearing single. I predict that most Kepler singles are truly single, with only one other neighbor similar in size to it, two neighbors in rare cases. While it isn't impossible for a single to be part of a very excited multi of similar sizes, the chances of that are slim. Thus, I further predict that any neighbors we do discover in Kepler single-tranet systems will be very distant from the original transiting planet, or have migrated

inward from farther out post-instability and be of a different size and composition than the original single.

4.2 Future Work

At the time that Spalding & Batygin (2016) proposed the oblate, tilted star mechanism, evidence suggested that single-tranet systems were more common around misaligned stars (Winn et al. 2010, Albretch 2012), and that misaligned stars tended to be hot. However, followup work (Winn et al. 2017, Weiss et al. 2018) has shown that this signal was biased by hot Jupiters, and that Kepler stars hosting small singles versus small multis are essentially the same. This is at odds with our assumption that the final transit multiplicity of a Kepler-like system depends on stellar properties. Moreover, as addressed in chapter 2, current observations reveal a deficit of high-obliquity, coplanar Kepler multis – if we assume that a star's misalignment is not correlated, or even anticorrelated, with the strength of its quadrupole moment, then that leaves us with either an entirely unobserved group of misaligned, coplanar multis that a star was unable to excite, or with the prediction that stellar obliquity and oblateness are linked. It is therefore vital that we continue to study the process (or processes) by which stars acquire their misalignments, to determine whether such a link does exist.

Obliquity erasure is also an interesting new result. It is likely generic to all destabilizing mechanisms that force precession about some perturber's angular momentum axis. Right now, those all involve large objects on wide orbits, with smaller objects inside (see chapter 1). Should a giant perturber be responsible for creating some fraction of the Kepler singles, we might expect to see mild, but not severe, misalignment between them as we discover more giants around close-in systems. The physics behind this relaxation is another topic for future inquiry.

REFERENCES

Albrecht, S. *et al.* 2012, Obliquities of Hot Jupiter Host Stars: Evidence for Tidal Interactions and Primordial Misalignments, *The Astrophysical Journal* **757**, 18

Asimov, I. 1977, *The Collapsing Universe*, Walker & Co

Ballard, S. & Johnson, J. A. 2016, The Kepler Dichotomy Among the M Dwarfs: Half of Systems Contain Five or More Coplanar Planets, *The Astrophysical Journal* **816**, 66

Batygin, K. 2012, A Primordial Origin for Misalignments Between Stellar Spin Axes and Planetary Orbits, *Nature* **491**, 418–420

Batygin, K. & Adams, F. C. 2013, Magnetic and Gravitational Disk-Star Interactions: An Interdependence of PMS Stellar Rotation Rates and Spin-Orbit Misalignments, *The Astrophysical Journal* **778**, 169

Batygin, K. & Laughlin, G. 2008, On the Dynamical Stability of the Solar System, *The Astrophysical Journal* **683**, 1207–1216

Becker, J. C. & Adams, F. C. 2017, Effects of Unseen Additional Planetary Perturbers on Compact Extrasolar Planetary Systems, *Monthly Notices of the Royal Astronomical Society* **468**, 549–563

Becker, J. C. & Adams, F. C. 2016, Oscillations of Relative Inclination Angles in Compact Extrasolar Planetary Systems, *Monthly Notices of the Royal Astronomical Society* **455**, 2980–2993

Borucki, W. 2011, Characteristics of Planetary Candidates Observed by Kepler. II. Analysis of the First Four Months of Data, *The Astrophysical Journal* **736**

Borucki, W. *et al.* 2009, KEPLER: Search for Earth-Size Planets in the Habitable Zone, in *Proceedings of the International Astronomical Union* No. IAUS253, 2008

Bouvier, J. *et al.* 2013, Angular Momentum Evolution of Young Low-Mass Stars and Brown Dwarfs: Observations and Theory, in *Protostars and Planets VI* 433–450

Bovaird, T. & Lineweaver, C. H. 2017, A Flat Inner Disc Model as an Alternative to the Kepler Dichotomy in the Q1–Q16 Planet Population, *Monthly Notices of the Royal Astronomical Society* **468**, 1493–1504

Briceño, C. *et al.* 2005, The CIDA Variability Survey of Orion OB1. I. The Low-Mass Population of Ori OB1a and 1b, *The Astronomical Journal* **129**, 907–926

Bryan, M. L. *et al.* 2016, Statistics of Long Period Gas Giant Planets in Known Planetary Systems, *The Astrophysical Journal* **821**, 89

Bryan, M. L. *et al.* 2019, An Excess of Jupiter Analogs in Super-Earth Systems, *The Astronomical Journal* **157**, 52

Carrera, D., Raymond, S. R. & Davies, M. B. 2019, Planet-Planet Scattering as the Source of the Highest Eccentricity Exoplanets, *Astronomy & Astrophysics* **629**,

Chambers, J. E. 1999, A Hybrid Symplectic Integrator that Permits Close Encounters Between Massive Bodies, *Monthly Notices of the Royal Astronomical Society* **304**, 793–799

Clairaut, A. C. 1743, *Théorie de la Figure de la Terre*

Cook, A. H. 1980, *Interiors of the Planets*, Cambridge University Press

Dai, F., Masuda, K. & Winn, J. N. 2018, Larger Mutual Inclinations for the Shortest-period Planets, *The Astrophysical Journal* **864**, L38

Davies, M. B. *et al.* 2014, The Long-Term Dynamical Evolution of Planetary Systems, in *Protostars and Planets VI*, University of Arizona Press

Deck, K. M. *et al.* 2012, Rapid Dynamical Chaos in an Exoplanetary Eystem, *The Astrophysical Journal Letters* **755**

Denham, P., Naoz, S., Hoang, B.-M., Stephan, A. P. & Farr, W. M. 2019, Hidden Planetary Friends: On the Stability of Two-Planet Systems in the Presence of a Distant, Inclined Companion, *Monthly Notices of the Royal Astronomical Society* **482**, 4146–4154

Duchêne, G. & Kraus, A. 2013, Stellar Multiplicity, *Annual Review of Astronomy and Astrophysics* **51**, 269–310

Fabrycky, D. C. *et al.* 2012, Architecture of Kepler's Multi-transiting Systems: II. New Investigations with Twice as Many Candidates, *The Astrophysical Journal* **790**

Fang, J. & Margot, J.-L. 2012, Architecture of Planetary Systems Based on Kepler Data: Number of Planets and Coplanarity, *The Astrophysical Journal* **761**, 92

Ford, E. B. & Rasio, F. A. 2008, Origins of Eccentric Extrasolar Planets: Testing the Planet-Planet Scattering Model, *The Astrophysical Journal* **686**, 621–636

Ford, E. B., Rowe, J. F., Fabrycky, D. C., Carter, J. A. & Al, E. 2011, VizieR Online Data Catalog: Transit Timing Observations from Kepler. I. (Ford+, 2011), *VizieR Online Data Catalog* **219**,

Foreman-Mackey, D., Hogg, D. W. & Morton, T. D. 2014, Exoplanet Population Inference and the Abundance of Earth Analogs from Noisy, Incomplete Catalogs, *The Astrophysical Journal* **795**, 64

Hansen, B. M. S. & Murray, N. 2013, Testing In Situ Assembly with the Kepler Planet
Candidate Sample, *The Astrophysical Journal* **775**, 53

Hansen, B. M. S. & Zink, J. 2015, On the Potentially Dramatic History of the Super-Earth P 55
Cancri e, *Monthly Notices of the Royal Astronomical Society* **450**, 4505–4520

Hansen, B. M. S. 2017, Perturbation of Compact Planetary Systems by Distant Giant Planets,
Monthly Notices of the Royal Astronomical Society **467**, 1531–1560

He, M. Y., Ford, E. B. & Ragozzine, D. 2019, Architectures of Exoplanetary Systems. I: A
Clustered Forward Model for Exoplanetary Systems around Kepler's FGK Stars, *Monthly
Notices of the Royal Astronomical Society* **490**, 4575–4605

Huang, C. X., Petrovich, C. & Deibert, E. 2017, Dynamically Hot Super-Earths from Outer
Giant Planet Scattering, *The Astronomical Journal* **153**, 210

Johansen, A., Davies, M. B., Church, R. P. & Holmelin, V. 2012, Can Planetary Instability
Explain the Kepler Dichotomy?, *The Astrophysical Journal* **758**, 39

Kant, I. 1755, *Universal Natural History and Theory of the Heavens*

Karim, M. T. *et al.* 2016, The Rotation Period Distributions of 4–10 Myr T Tauri Stars in Orion
Ob1: New Constraints on Pre-Main-Sequence Angular Momentum Evolution, *The
Astronomical Journal* **152**, 198

Knutson, H. A. *et al.* 2014, Friends of Hot Jupiters. I. A Radial Velocity Search for Massive,
Long-Period Companions to Close-In Gas Giant Planets, *The Astrophysical Journal* **785**,
126

Lai, D. & Pu, B. 2016, Hiding Planets Behind a Big Friend: Mutual Inclinations of Multi-Planet
Systems with External Companions, *The Astronomical Journal* **153**, 42

Lai, D., Anderson, K. & Pu, B. 2018, How Do External Companions Affect Spin–Orbit
Misalignment of Hot Jupiters? *Monthly Notices of the Royal Astronomical Society* **475**,
5231–5236

Li, G., Dai, F. & Becker, J. 2020, Mutual Inclination Excitation by Stellar Oblateness, *The
Astrophysical Journal* **890**, L31

Lichtenberg, A. & Lieberman, M. 1992, *Regular & Chaotic Dynamics*, Springer Science

Lissauer, J. J. *et al.* 2011, Architecture and Dynamics of Kepler's Candidate Multiple Transiting
Planet Systems, *The Astrophysical Journal Supplement Series* **197**, 8

Lithwick, Y. & Wu, Y. 2013, Secular Chaos and Its Application to Mercury, Hot Jupiters, and the Organization of Planetary Systems, *Proceedings of the National Academy of Sciences* **111**, 12610–12615

Marcy, G. W. *et al.* 2014, Masses, Radii, and Orbits of Small Kepler Planets: The Transition from Gaseous to Rocky Planets, *The Astrophysical Journal Supplement Series* **210**,

Mazeh, T., Perets, H. B., McQuillan, A. & Goldstein, E. S. 2015, Photometric Amplitude Distribution of Stellar Rotation of KOIs—Indication for Spin-Orbit Alignment of Cool Stars and High Obliquity for Hot Stars, *The Astrophysical Journal* **801**, 3

Millholland, S., Wang, S. & Laughlin, G. 2017, Kepler Multi-Planet Systems Exhibit Unexpected Intra-System Uniformity in Mass and Radius, *The Astrophysical Journal Letters* **849**, 1–7

Moriarty, J. & Ballard, S. 2016, The Kepler Dichotomy in Planetary Disks: Linking Kepler Observables to Simulations of Late-Stage Planet Formation, *The Astrophysical Journal* **832**, 34

Morton, T. D. & Winn, J. N. 2014, Obliquities of Kepler Stars: Comparison of Single- and Multiple-Transit Systems, *The Astrophysical Journal* **796**, 47

Murray, C. & Dermott, S. 1999, *Solar System Dynamics*, Cambridge University Press

Mustill, A. J., Davies, M. B. & Johansen, A. 2017, The Effects of External Planets On Inner Systems: Multiplicities, Inclinations and Pathways to Eccentric Warm Jupiters, *Monthly Notices of the Royal Astronomical Society* **468**, 3000–3023

Nagasawa, M., Ida, S. & Bessho, T. 2008, Formation of Hot Planets by a Combination of Planet Scattering, Tidal Circularization, and the Kozai Mechanism, *The Astrophysical Journal* **678**, 498–508

Naoz, S., Farr, W. M., Lithwick, Y., Rasio, F. A. & Teyssandier, J. 2011, Hot Jupiters from Secular Planet–Planet Interactions, *Nature* **473**, 187–189

Ngo, H. *et al.* 2015, Friends of Hot Jupiters. II. No Correspondence Between Hot-Jupiter Spin-Orbit Misalignment and the Incidence of Directly Imaged Stellar Companions, *The Astrophysical Journal* **800**, 138

Nobili, A. M. & Roxburgh, I. W. 1986, Simulation of General Relativistic Corrections in Long Term Numerical Integrations of Planetary Orbits, *Symposium - International Astronomical Union* **114**, 105–111

Petrovich, C., Tremaine, S. & Rafikov, R. 2014, Scattering Outcomes of Close-In Planets: Constraints on Planet Migration, *The Astrophysical Journal* **786**, 101

Pu, B. & Lai, D. 2019, Low-Eccentricity Migration of Ultra-Short-Period Planets in Multiplanet Systems, *Monthly Notices of the Royal Astronomical Society* **488**, 3568–3587

Pu, B. & Lai, D. 2018, Eccentricities and Inclinations of Multiplanet Systems with External Perturbers, *Monthly Notices of the Royal Astronomical Society* **478**, 197–217

Puranam, A. & Batygin, K. 2018, Chaotic Excitation and Tidal Damping in the GJ 876 System, *The Astronomical Journal* **155**, 157

Rafikov, R. R. 2006, Atmospheres of Protoplanetary Cores: Critical Mass for Nucleated Instability, *The Astrophysical Journal* **648**, 666–682

Ragozzine, D. & Holman, M. J. 2010, The Value of Systems with Multiple Transiting Planets, arXiv preprint arXiv:1006.3727

Sandford, E., Kipping, D. & Collins, M. 2019, The Multiplicity Distribution of Kepler's Exoplanets, *Monthly Notices of the Royal Astronomical Society* **489**, 3162–3173

Schatzman, E. 1960, A Theory of the Role of Magnetic Activity During Star Formation, <https://resolver.caltech.edu/CaltechAUTHORS:20120209-091528636>

Shu, F. H., Adams, F. C. & Lizano, S. 1987, Star Formation in Molecular Clouds: Observation and Theory, *Annual Review of Astronomy and Astrophysics* **25**, 23–81

Spalding, C. & Batygin, K. 2017, A Secular Resonant Origin for the Loneliness of Hot Jupiters, *The Astronomical Journal* **154**, 93

Spalding, C. & Batygin, K. 2016, Spin-orbit Misalignment as a Driver of the Kepler Dichotomy, *The Astrophysical Journal* **830**, 5

Spalding, C. & Batygin, K. 2014, Early Excitation of Spin-Orbit Misalignments in Close-In Planetary Systems, *The Astrophysical Journal* **790**, 42

Spalding, C. & Batygin, K. 2015, Magnetic Origins of the Stellar Mass-Obliquity Correlation in Planetary Systems, *The Astrophysical Journal* **811**, 82

Spalding, C., Marx, N. W. & Batygin, K. 2018, The Resilience of Kepler Systems to Stellar Obliquity, *The Astronomical Journal* **155**, 167

Steffen, J. H. *et al.* 2012, Kepler Constraints on Planets Near Hot Jupiters, *Proceedings of the National Academy of Sciences* **109**, 7982–7987

Sterne, T. E. 1939, Apsidal Motion in Binary Stars, *Monthly Notices of the Royal Astronomical Society* **99**, 451–462

Teyssandier, J., Naoz, S., Lizarraga, I. & Rasio, F. A. 2013, Extreme Orbital Evolution from Hierarchical Secular Coupling of Two Giant Planets, *The Astrophysical Journal* **779**, 166

Tremaine, S. & Dong, S. 2012, The Statistics of Multi-Planet Systems, *The Astronomical Journal* **143**, 94

Uehara, S., Kawahara, H., Masuda, K., Yamada, S. & Aizawa, M. 2016, Transiting Planet Candidates Beyond the Snow Line Detected by Visual Inspection of 7557 Kepler Objects of Interest, *The Astrophysical Journal* **822**, 2

Ward, W. R., Colombo, G. & Franklin, F. A. 1976, Secular Resonance, Solar Spin Down, and the Orbit of Mercury, *Icarus* **28**, 441–452

Weidenschilling, S. J. & Marzari, F. 1996, Gravitational Scattering as a Possible Origin for Giant Planets at Small Stellar Distances, *Nature* **384**, 619–621

Weiss, L. M. *et al.* 2018, The California-Kepler Survey. VI. Kepler Multis and Singles Have Similar Planet and Stellar Properties Indicating a Common Origin, *The Astronomical Journal* **156**, 254

Weiss, L. M. *et al.* 2017, The California-Kepler Survey V. Peas in a Pod: Planets in a Kepler Multi-planet System are Similar in Size and Regularly Spaced, *The Astronomical Journal* **155**, 1–15

Winn, J. N. & Fabrycky, D. C. 2015, The Occurrence and Architecture of Exoplanetary Systems, Annual Review of Astronomy and Astrophysics 53, 409–447

Winn, J. N. *et al.* 2017, Constraints on the Obliquities of Kepler Planet-hosting Stars, *The Astronomical Journal* **154**, 270

Wu, Y. & Lithwick, Y. 2011, Secular Chaos and the Production of Hot Jupiters, *The Astrophysical Journal* **735**, 109

Xie, J.-W. *et al.* 2016, Exoplanet Orbital Eccentricities Derived from LAMOST–Kepler Analysis, *Proceedings of the National Academy of Sciences* **113**, 11431–11435

Zhu, W., Petrovich, C., Wu, Y., Dong, S. & Xie, J. 2018, About 30% of Sun-like Stars Have Kepler-Like Planetary Systems: A Study of Their Intrinsic Architecture, *The Astrophysical Journal* **860**, 101

Zhu, W. & Wu, Y. 2018, The Super Earth–Cold Jupiter Relations, *The Astronomical Journal* **156**, 92

Zink, J. K., Christiansen, J. L. & Hansen, B. M. S. 2019, Accounting for Incompleteness Due to Transit Multiplicity in Kepler Planet Occurrence Rates, *Monthly Notices of the Royal Astronomical Society* **483**, 4479–4494

MERCURY6 CUSTOM SUBROUTINE

This is the custom code implemented in all mercury6 N-body simulations performed during the data gathering phase of this inquiry. It assumes that the user has modified mercury6 to read two additional lines from the input file param.in, defining $J_{2,0}$ (called cusJ2 in the code) and the quadrupole moment decay constant τ (called tDecy). To remove this requirement and insert the code directly into mercury6_2.for, a few simple changes can be made:

- delete cusJ2 and tDecy on lines 4 and 12

- add cusJ2 and tDecy to the end of line 16

- define cusJ2 and tDecy at some point between lines 19 and 25, including desired values

Note that editing mercury6_2.for requires that the executable mercury6 be recompiled to incorporate the changes. Ensure that no lines contain extra tabs or spaces preceding content – otherwise the code won't compile.

mercury6 can be downloaded from GitHub at https://github.com/4xxi/mercury.

```
1    c---------------------------------------------------------------------
2    c
3         subroutine mfo_user (time,jcen,nbod,nbig,m,x,v,a,
4        % cusJ2,tDecy,rcen)
5    c
6         implicit none
7         include 'mercury.inc'
8    c
9    c Input/Output
10        integer nbod, nbig
```

```fortran
11        real*8 time,jcen(3),m(nbod),x(3,nbod),v(3,nbod),a(3,nbod)

12        real*8 cusJ2,tDecy,rcen

13  c

14  c Local

15        integer j, k

16        real*8 acen(3),j2,G

17        real*8 jr2,r2,r_1,r_2,r_3,u2,tmp1,tmp2,tmp3,tmp4

18  c

19  c-----------------------------------------------------------------------------

20  c

21        acen(1)=0.0d0

22        acen(2)=0.0d0

23        acen(3)=0.0d0

24

25        j2 = cusJ2 * (rcen ** 2) * exp(-time/tDecy)

26

27        G= 2.9599027E-4

28

29        do j=2,nbod

30

31         r2 = x(1,j)*x(1,j) + x(2,j)*x(2,j) + x(3,j)*x(3,j)

32         r_1 = 1.d0 / sqrt(r2)

33         r_2 = r_1 * r_1

34         r_3 = r_2 * r_1

35         jr2 = j2 * r_2

36         u2 = x(3,j) * x(3,j) * r_2

37

38         tmp1 = m(1) * r_3 * G
```

```fortran
39        tmp2 =jr2*(7.5d0*u2 - 1.5d0)

40        tmp3 = jr2*3.d0

41

42        a(1,j) = x(1,j) * tmp1 * tmp2

43        a(2,j) = x(2,j) * tmp1 * tmp2

44        a(3,j) = x(3,j) * tmp1 * (tmp2 - tmp3)

45

46          a(1,j) = a(1,j) - 1.62506E-11 * x(1,j)

47     %    /((x(1,j)*x(1,j)+x(2,j)*

48     %     x(2,j) + x(3,j)*x(3,j) )**2)

49     %     *((m(1)/K2)**2)

50        a(2,j) = a(2,j) - 1.62506E-11 * x(2,j)

51     %    /((x(1,j)*x(1,j)+x(2,j)*

52     %     x(2,j) + x(3,j)*x(3,j) )**2)

53     %     *((m(1)/K2)**2)

54        a(3,j) = a(3,j) - 1.62506E-11 * x(3,j)

55     %    /((x(1,j)*x(1,j)+x(2,j)*

56     %     x(2,j) + x(3,j)*x(3,j) )**2)

57     %     *((m(1)/K2)**2)

58

59        acen(1) = acen(1)  -  (m(j) / m(1)) * a(1,j)

60        acen(2) = acen(2)  -  (m(j) / m(1)) * a(2,j)

61        acen(3) = acen(3)  -  (m(j) / m(1)) * a(3,j)

62

63      end do

64

65      do k = 2, nbod

66
```

```
67        a(1,k) = a(1,k) - acen(1)

68        a(2,k) = a(2,k) - acen(2)

69        a(3,k) = a(3,k) - acen(3)

70

71     end do

72   c

73   c---------------------------------------------------------------------------
```

APPENDIX B

ADDITIONAL PLOTS AND INTERPOLATED CURVES

This contains three additional density histograms excluded from chapter 2, as well as a set of interpolated curves connecting initial oblateness $J_{2,0}$, stellar obliquity β^*, and innermost semimajor axis a_1 to the mutual inclination of a surviving simulated planet pair. The dotted line appearing on Figures 26 and 27 is the curve expressed by equation (29), and marks the point above which systems would go unstable rather than continuing to gain mutual inclination.

Curves that terminate at $\beta_*=80°$ in Figures 28-42 are systems that remained stable at all stellar tilts; curves that terminate elsewhere or are concave up went unstable, usually between 30° and 50° of obliquity.
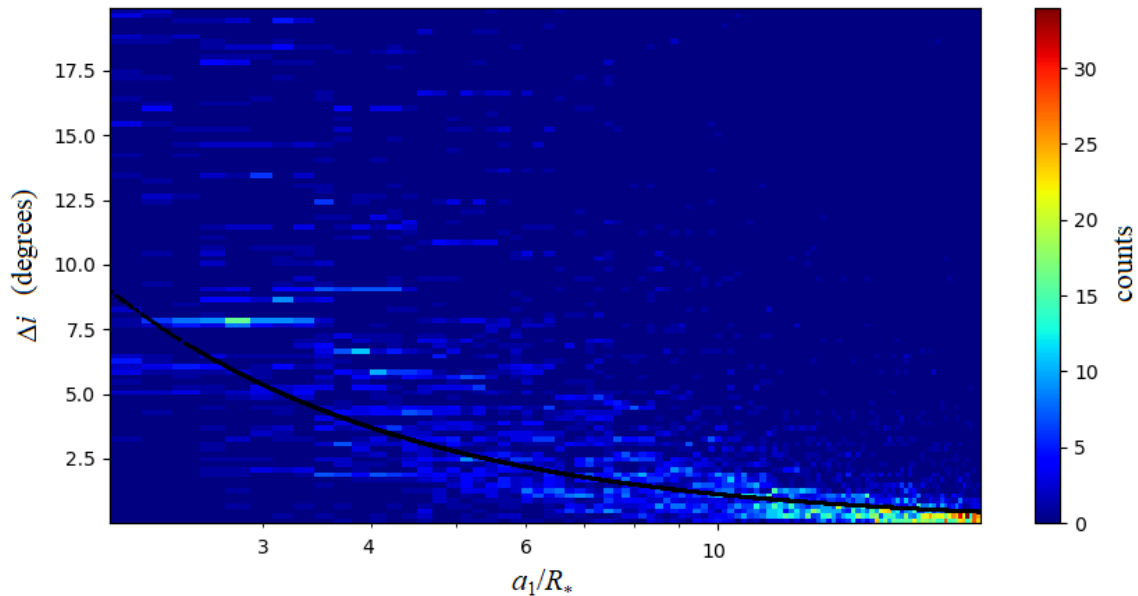
Figure 19. A 2D histogram of Predict[] data, where β_* is drawn from a Rayleigh distribution with mean 30°.
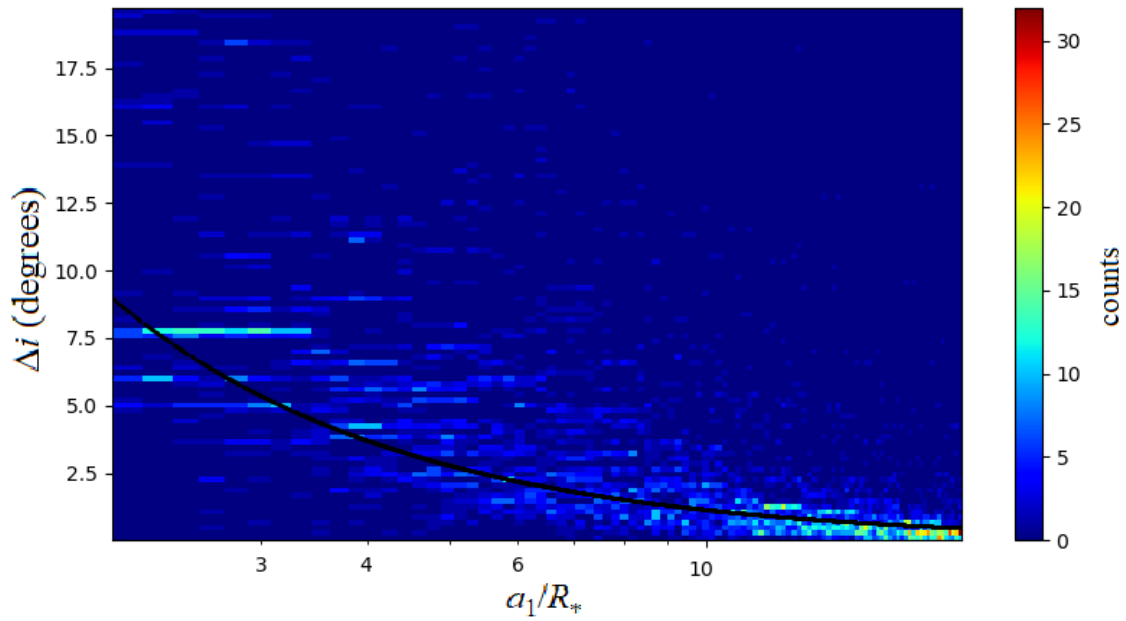
Figure 20. A 2D histogram of Predict[] data, where β_* is drawn from a Rayleigh distribution with mean 45°.
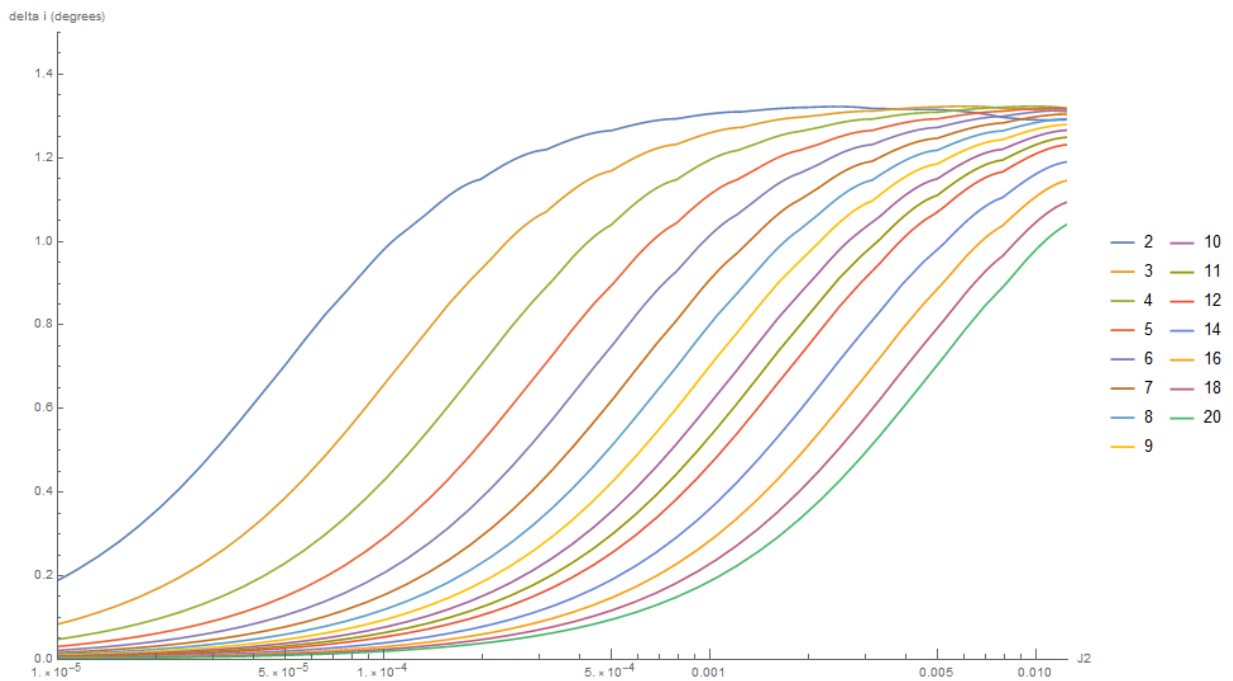
Figure 21. Interpolated Δi vs $J_{2,0}$ curves for different a_1 at β_*=1°.

84
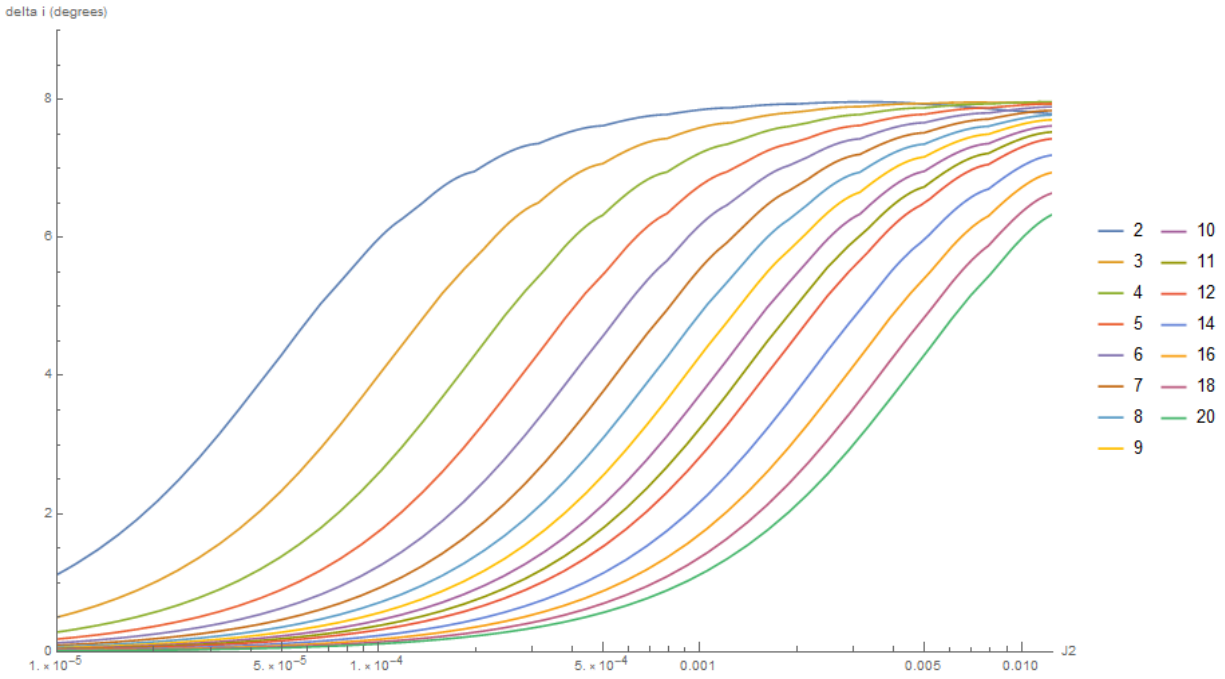
Figure 22. Interpolated Δi vs $J_{2,0}$ curves for different a_1 at $\beta_*=6°$.
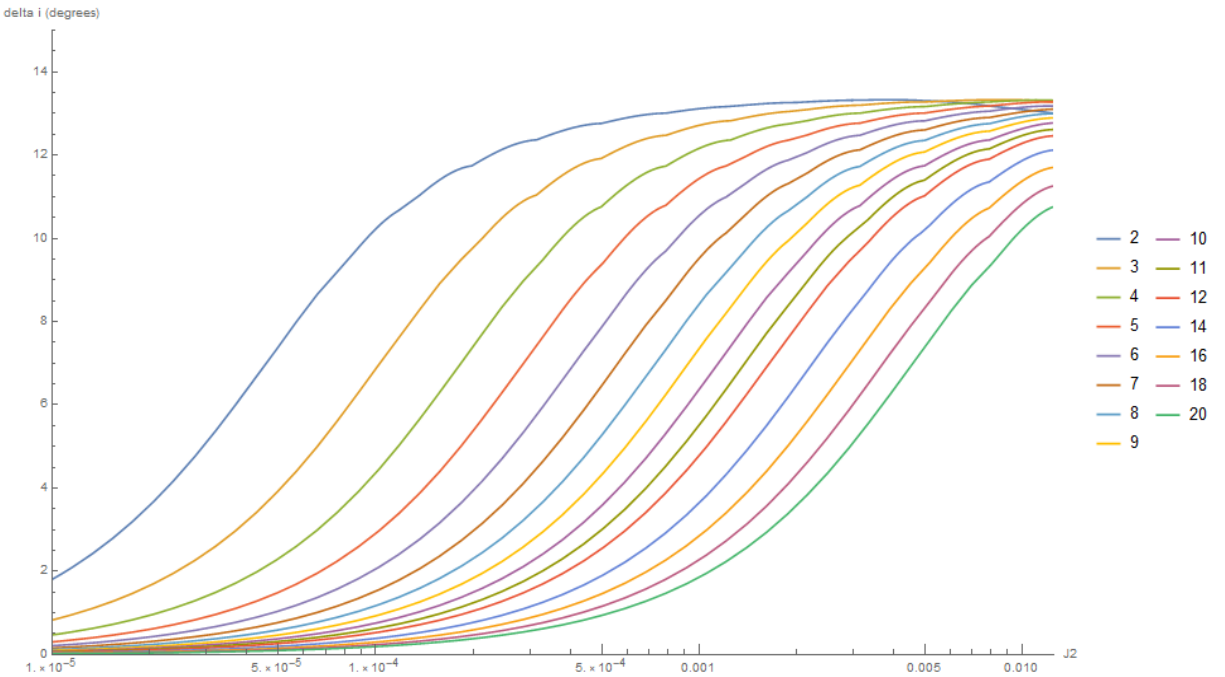
Figure 23. Interpolated Δi vs $J_{2,0}$ curves for different a_1 at $\beta_*=10°$.
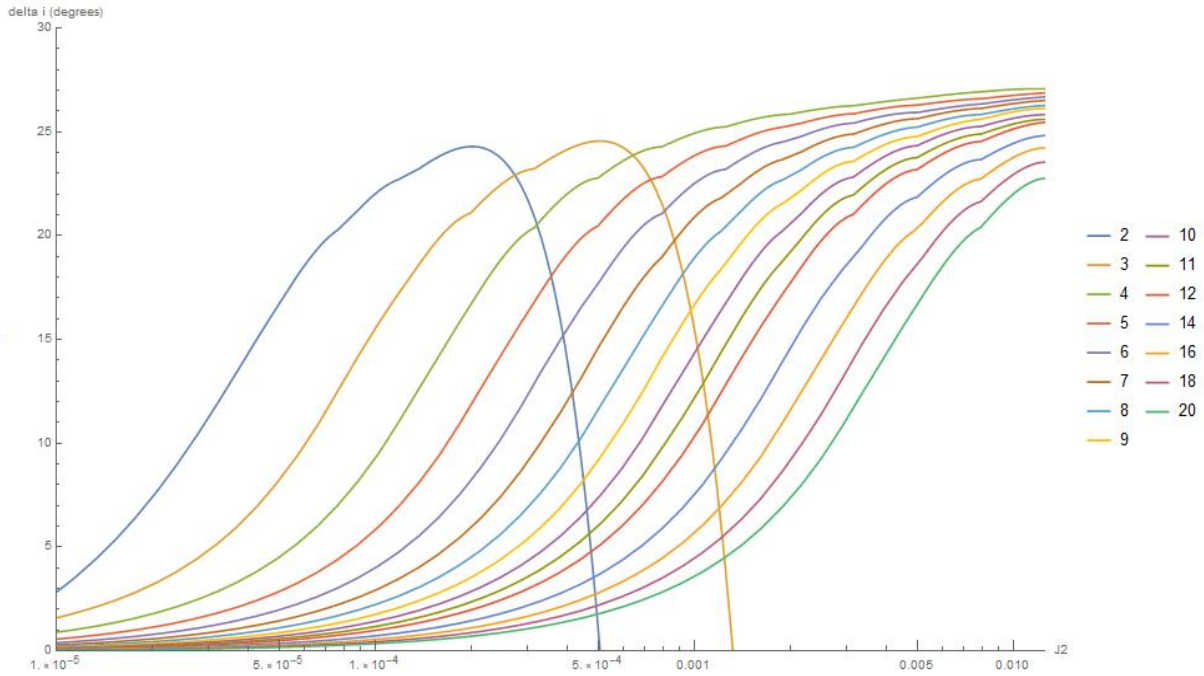
Figure 24. Interpolated Δi vs $J_{2,0}$ curves for different a_1 at $\beta_* = 20°$.
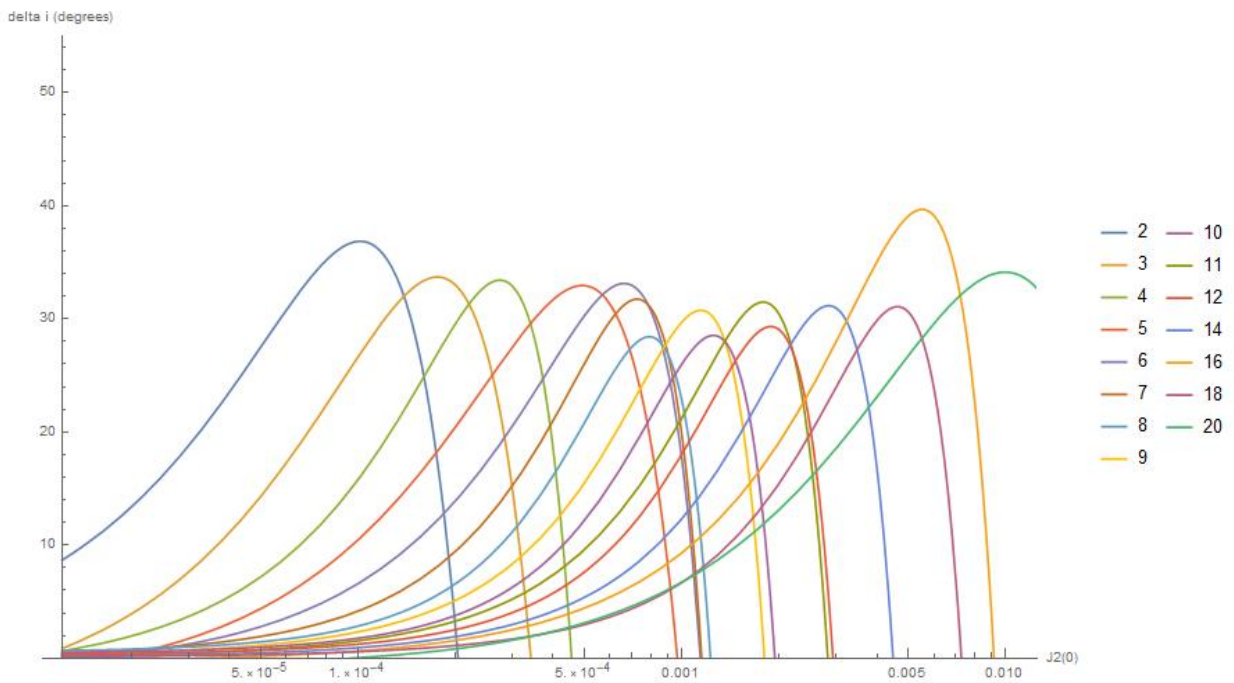
Figure 25. Interpolated Δi vs $J_{2,0}$ curves for different a_1 at $\beta_* = 30°$.
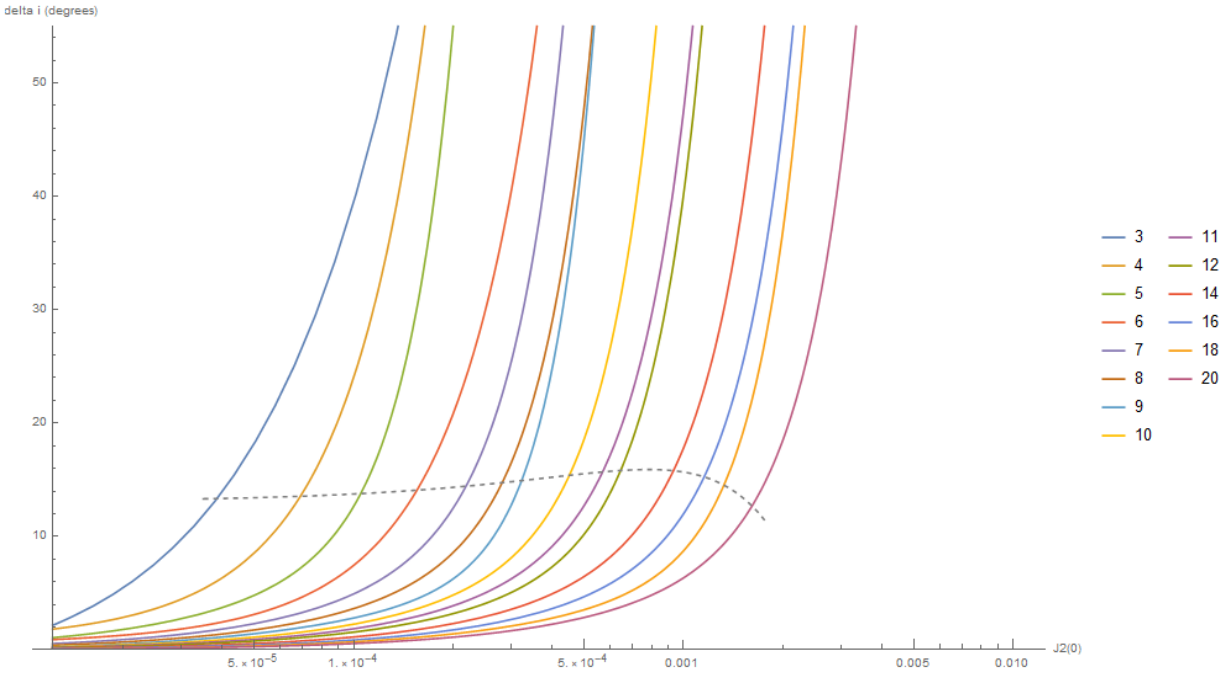
Figure 26. Interpolated Δi vs $J_{2,0}$ curves for different a_1 at $\beta_*=50°$.
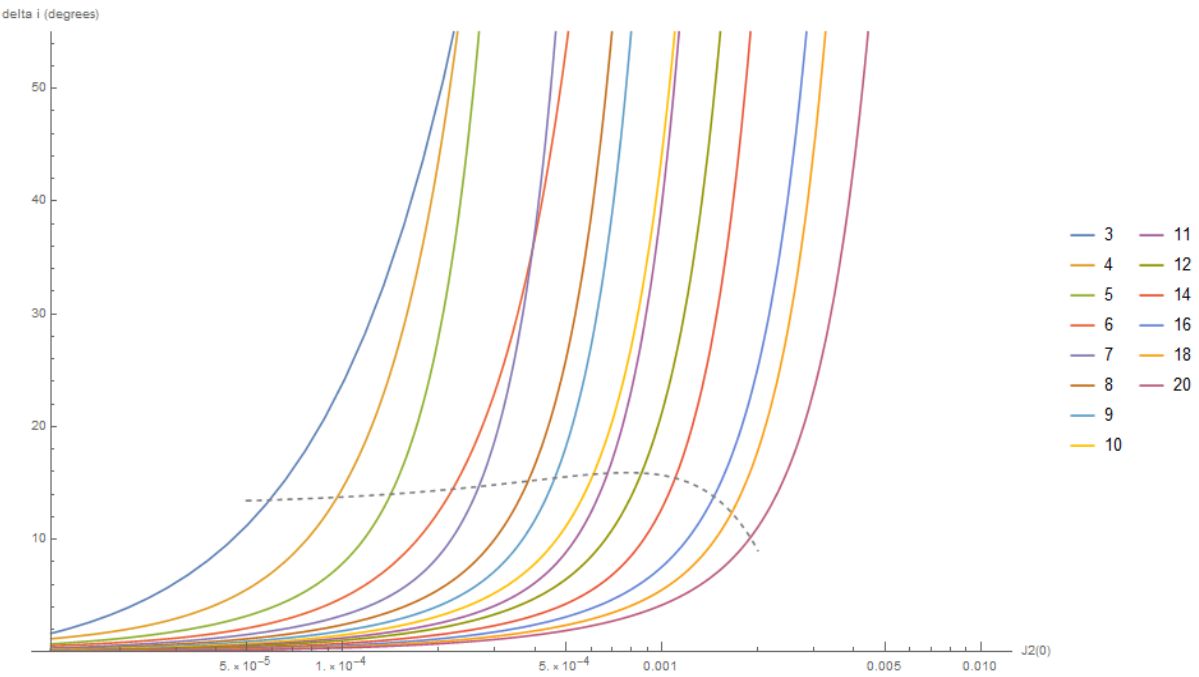
Figure 27. Interpolated Δi vs $J_{2,0}$ curves for different a_1 at $\beta_*=70°$.
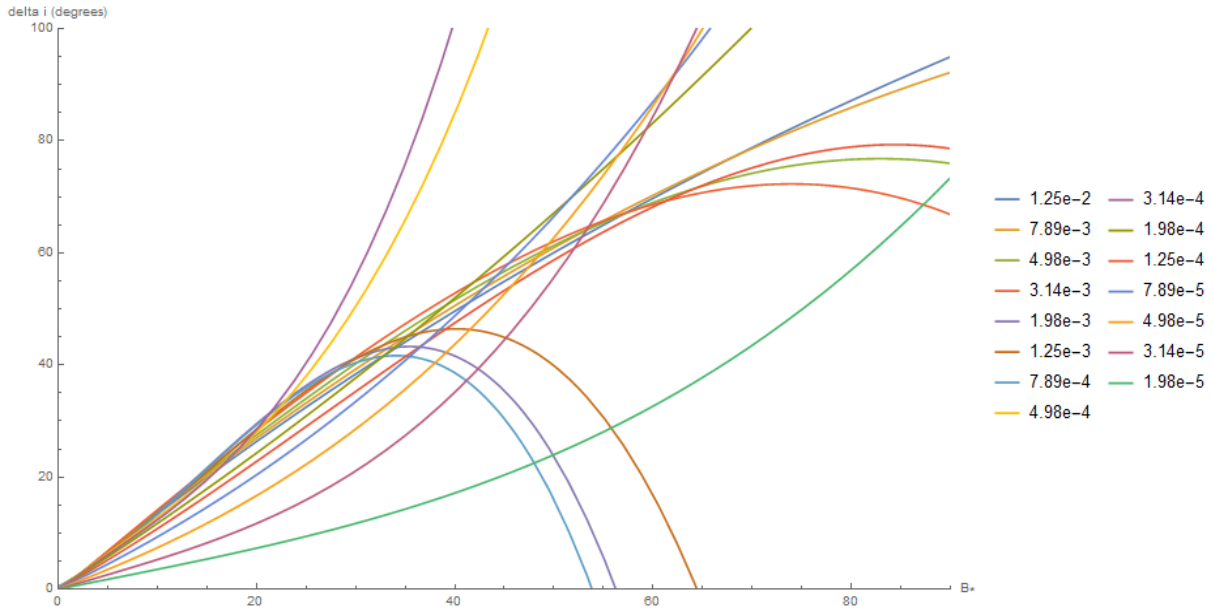
Figure 28. Interpolated Δi vs β_* curves for different $J_{2,0}$ at a_1=0.01 AU.
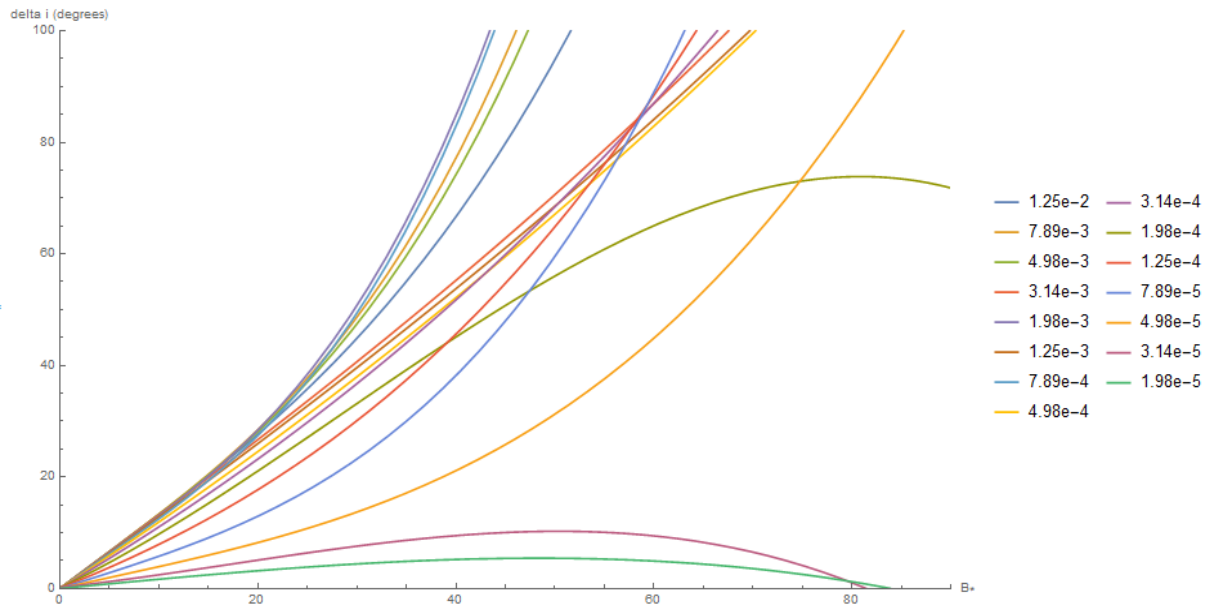
Figure 29. Interpolated Δi vs β_* curves for different $J_{2,0}$ at a_1=0.015 AU.
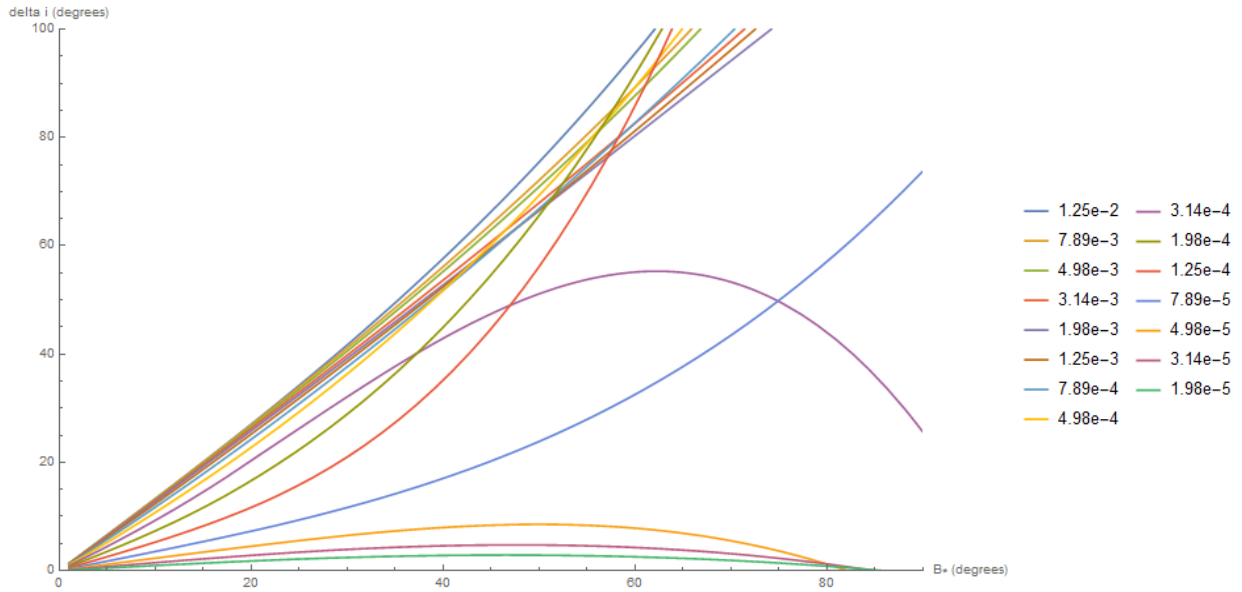
Figure 30. Interpolated Δi vs β_* curves for different $J_{2,0}$ at a_1=0.02 AU.
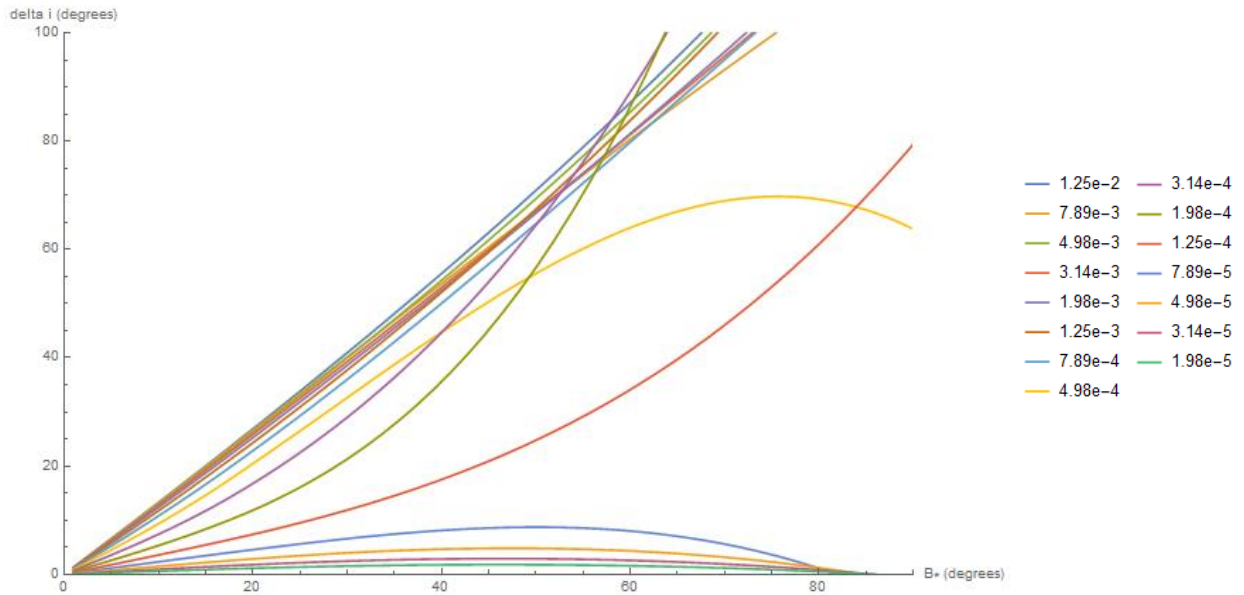
Figure 31. Interpolated Δi vs β_* curves for different $J_{2,0}$ at a_1=0.025 AU.
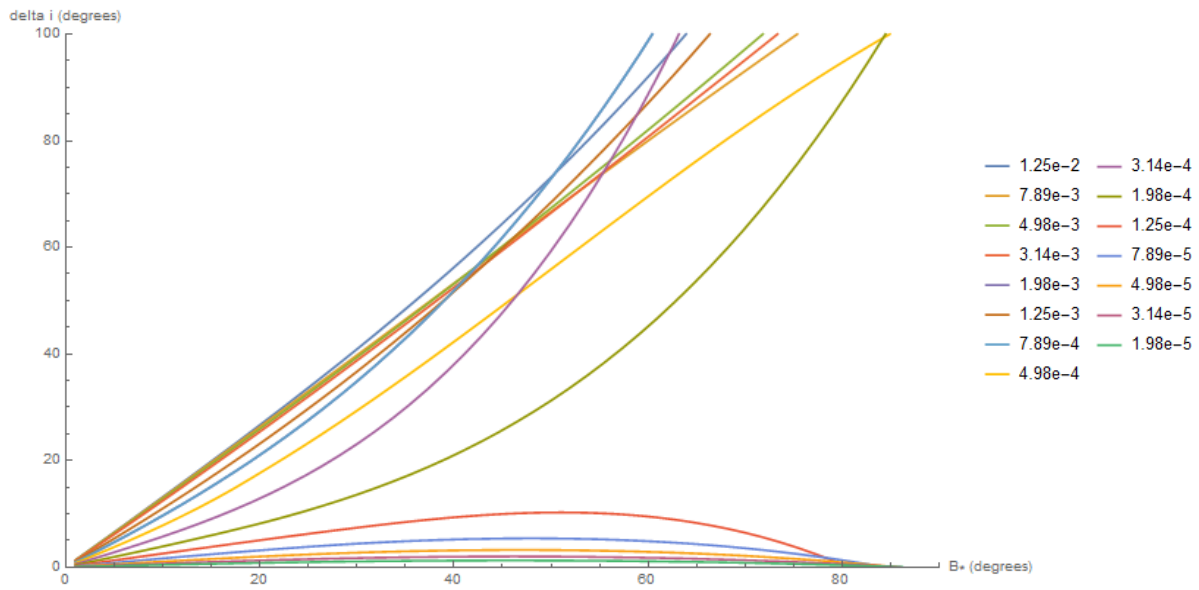
Figure 32. Interpolated Δi vs β_* curves for different $J_{2,0}$ at a_1=0.03 AU.
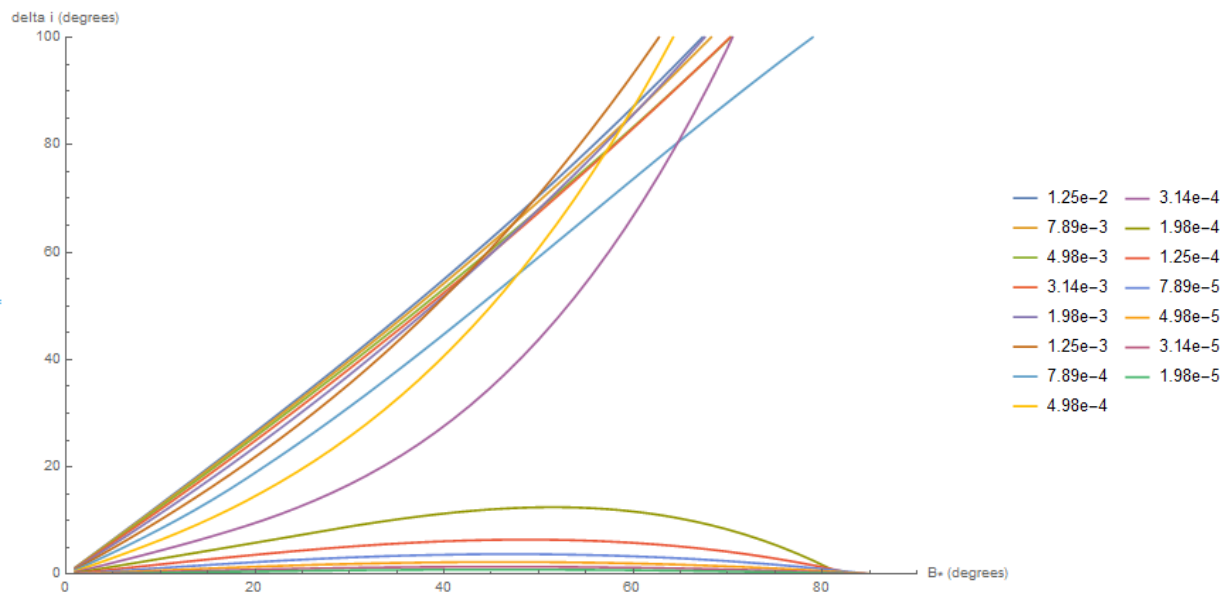
Figure 33. Interpolated Δi vs β_* curves for different $J_{2,0}$ at a_1=0.035 AU.
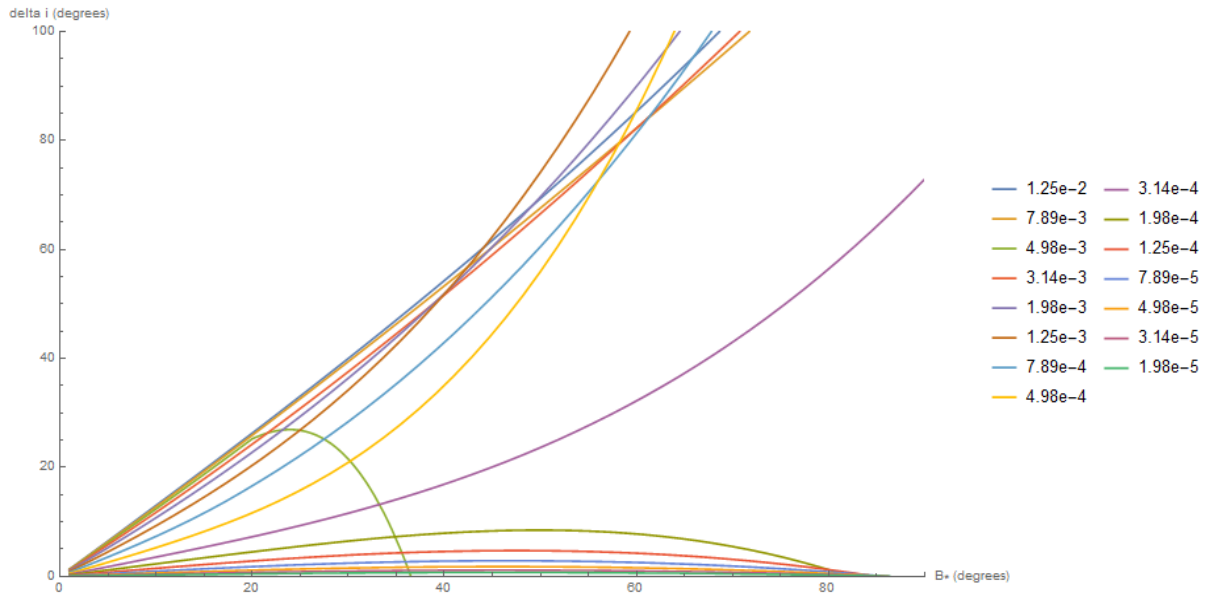
Figure 34. Interpolated Δi vs β_* curves for different $J_{2,0}$ at a_1=0.04 AU.
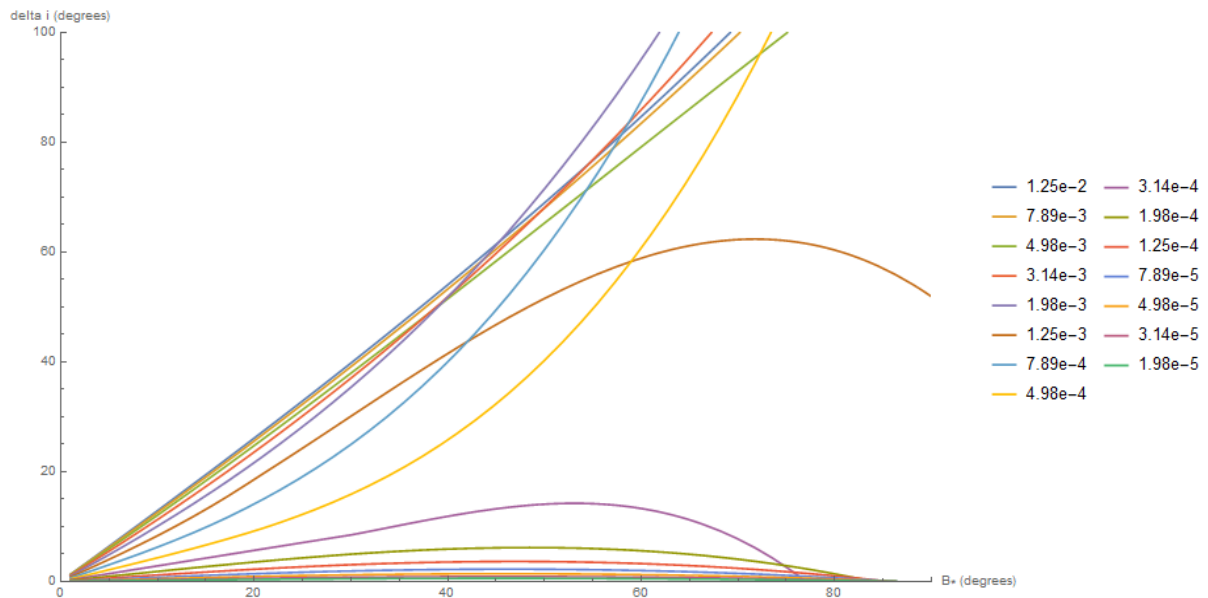
Figure 35. Interpolated Δi vs β_* curves for different $J_{2,0}$ at a_1=0.045 AU.
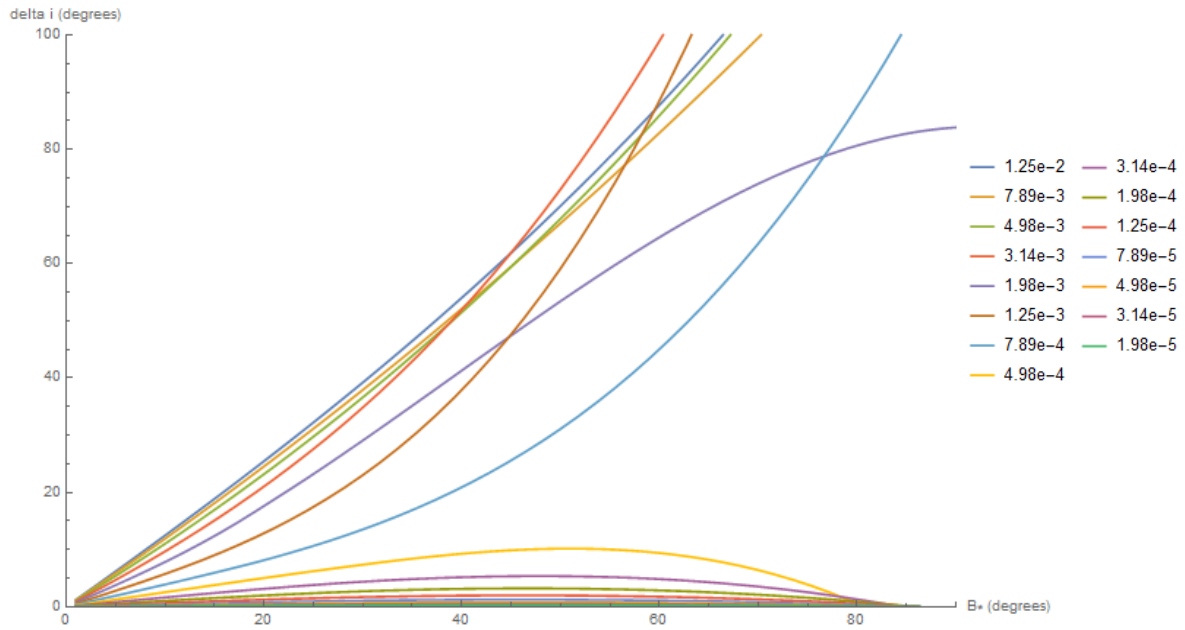
Figure 36. Interpolated Δi vs β_* curves for different $J_{2,0}$ at a_1=0.05 AU.
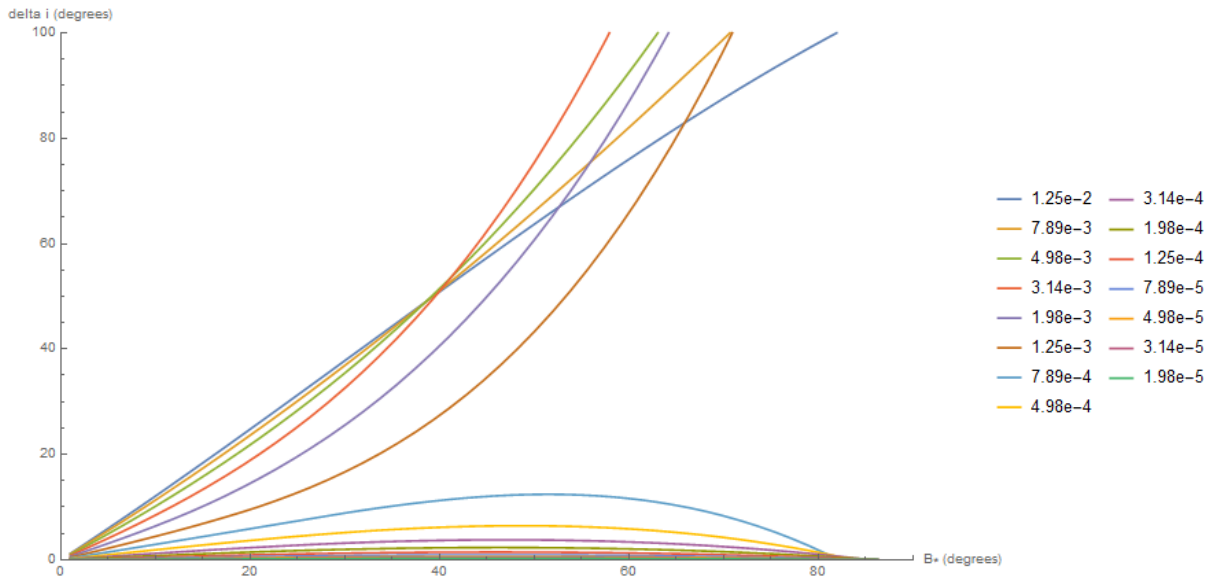
Figure 37. Interpolated Δi vs β_* curves for different $J_{2,0}$ at a_1=0.055 AU.
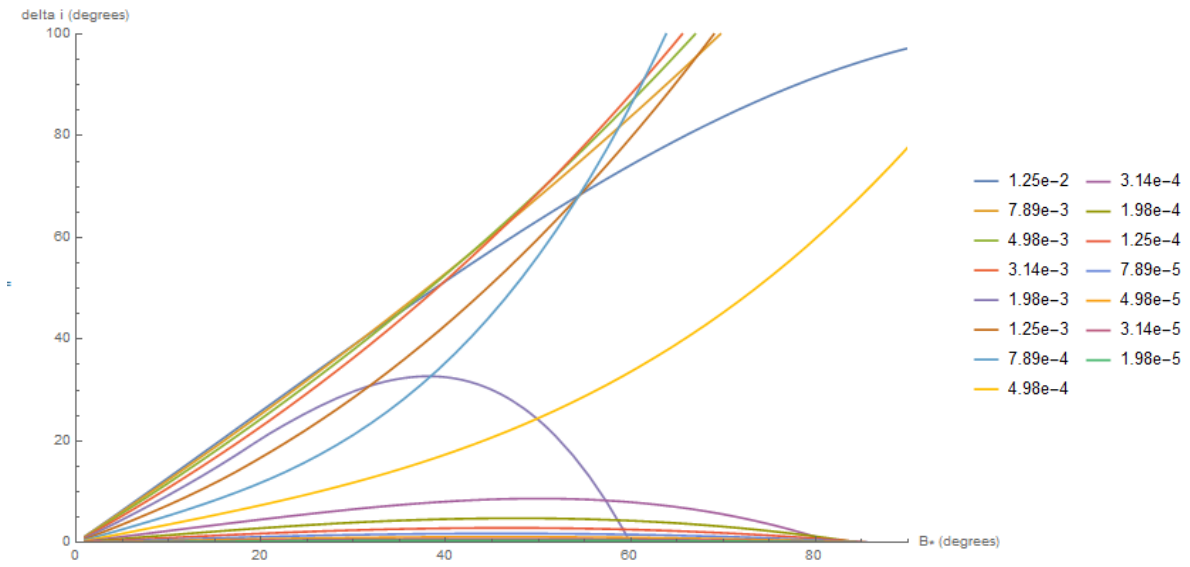
Figure 38. Interpolated Δi vs β_* curves for different $J_{2,0}$ at a_1=0.06 AU.
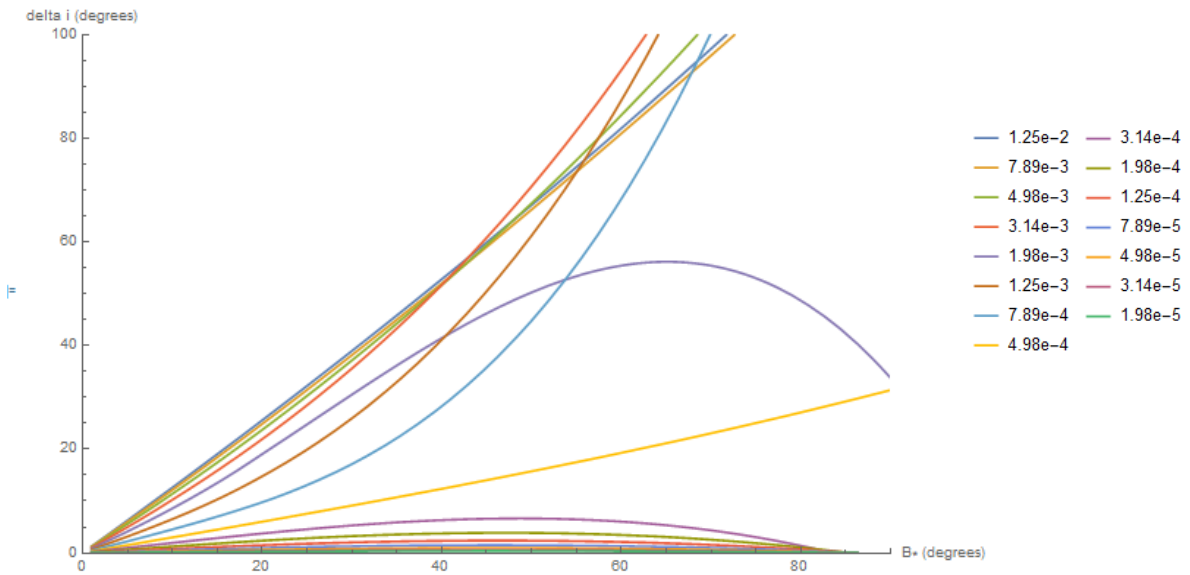
Figure 39. Interpolated Δi vs β_* curves for different $J_{2,0}$ at a_1=0.07 AU.
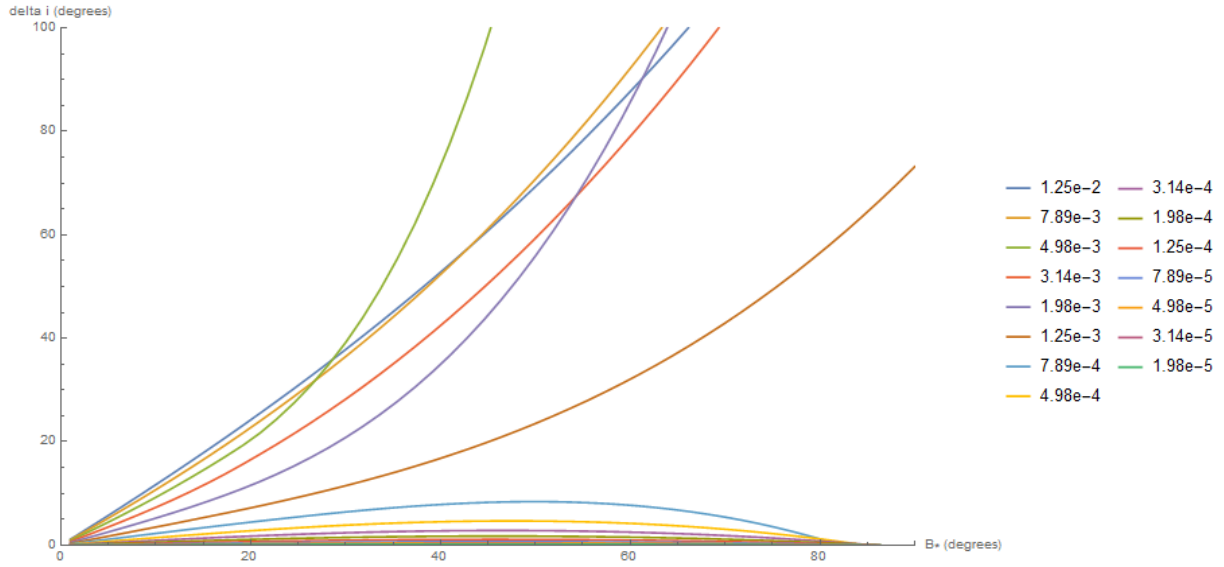
Figure 40. Interpolated Δi vs β_* curves for different $J_{2,0}$ at a_1=0.08 AU.
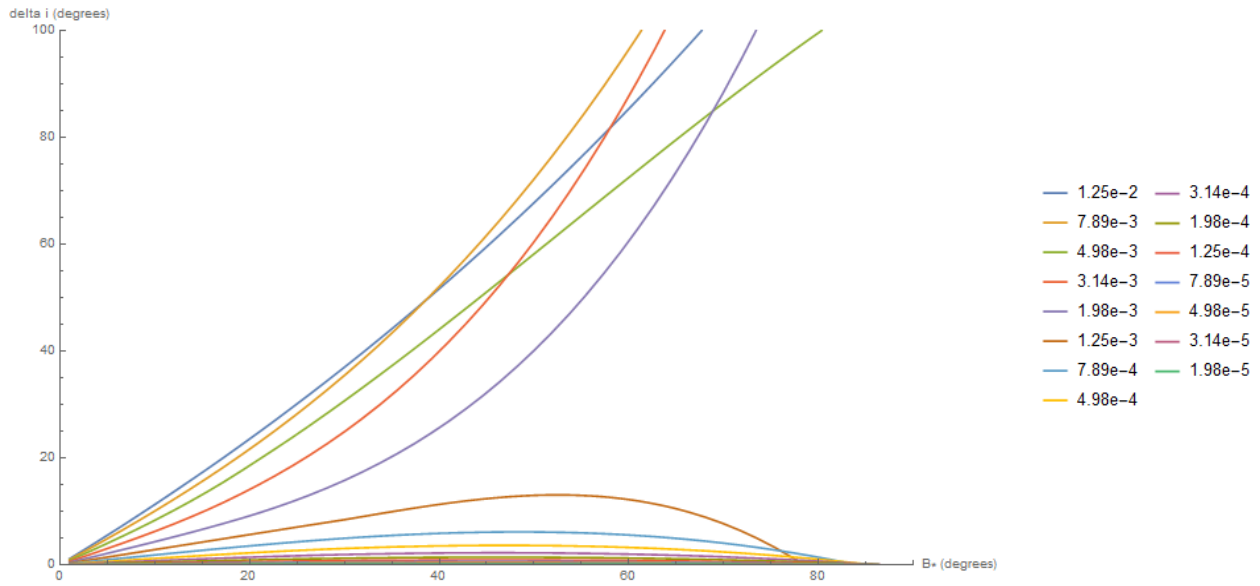
Figure 41. Interpolated Δi vs β_* curves for different $J_{2,0}$ at a_1=0.09 AU.
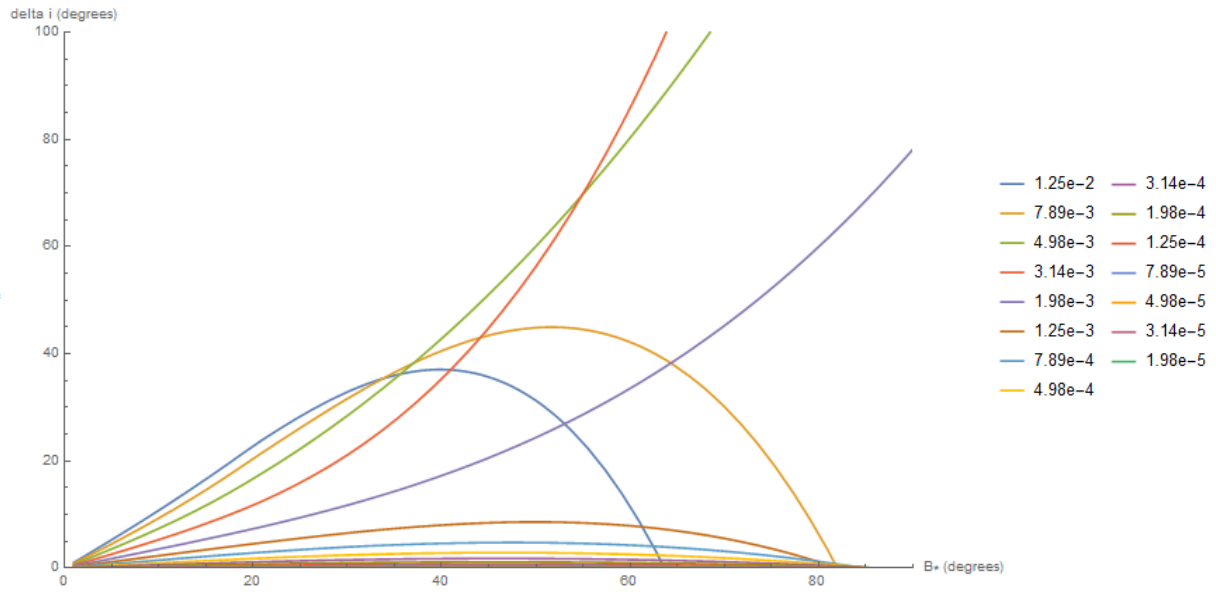
Figure 42. Interpolated Δi vs β_* curves for different $J_{2,0}$ at a_1=0.1 AU.

BIOGRAPHY OF THE AUTHOR

Katee Schultz was born in Bangor, Maine, and proceeded to hit most major milestones in places ending in "Maine". She attended Mt. View High School in Thorndike, where science was often her worst subject because the wording was too picky. Upon being exposed to topics in modern physics at the University of Maine at Farmington and discovering it a satisfying challenge, Katee took advantage of a unique degree program to learn as much physics as possible from a teaching school with two physics professors. In 2015, she earned a B.A. from UMF, double majoring in Applied Mathematics and Interdisciplinary Studies in Physics and Math, with a minor in Anthropology. She spent some time as a brewer's assistant before realizing that life without challenges is way boring. Katee then began graduate school at the University of Maine in 2017 and wasn't bored. She was recently awarded the UMaine College of Liberal Arts and Sciences Award for Outstanding Graduate Student 2020. Katee is a candidate for the Master of Science degree in Physics and Astronomy from the University of Maine in May 2020.